THE STATISTICAL ANALYSIS OF LIGHT SCATTERING DATA

FOR POLYMER CHARACTERIZATION

THE STATISTICAL ANALYSIS OF LIGHT SCATTERING DATA

FOR POLYMER CHARACTERIZATION

BY

NICHOLAS J. BURN, B.A.Sc.

A Thesis

Submitted to the School of Graduate Studies

in Partial Fulfillment of the Requirements

for the Degree

Master of Engineering

McMaster University

June 1986

MASTER OF ENGINEERING   McMASTER UNIVERSITY
(Chemical Engineering)   Hamilton, Ontario

TITLE: The Statistical Analysis of Light Scattering Data
                   For Polymer Characterization

AUTHOR: Nicholas J. Burn, B.A.Sc. (University of Ottawa)

SUPERVISOR: Dr. J.F. MacGregor

NUMBER OF PAGES: 211

ABSTRACT

The models derived from classical light scattering theory for predicting Rayleigh light scattering contain useful parameters such as polymer weight average molecular weight, z-average radius of gyration and virial coefficients. The methods used to estimate these model parameters have not been based on sound statistical principles. It is with improved statistical estimation methods for these parameters that this thesis is concerned with. The methods of linear least squares, non-linear least squares and error propogation were applied to the analysis of wide angle and low angle laser light scattering data and the results compared.

From the theory of dynamic light scattering, methods have been developed to reconstruct particle size distributions of unimodal, bimodal and polydisperse polymer solutions from the data accumulated in a single experiment. Some of these methods of reconstruction are based upon the estimation of the coefficients in a sum of exponentials. Estimating sums of exponentials is a highly ill-conditioned problem and the problems encountered thereof are examined in this thesis. Linear least squares, non-linear least squares and exponential sampling techniques were applied to experimental data from a number of simulated polymer distributions and the final results compared.

ACKNOWLEDGEMENT

I would like to dedicate this work to my wife, Karen, whose support, love and understanding has been undying during the course of this thesis.

TABLE OF CONTENTS

LIST OF FIGURES

LIST OF TABLES

INTRODUCTION

Proper applications of polymer materials depend upon such polymer properties as melt temperature and viscosity. These in turn are dependent upon fundamental properties such as the polymer's molecular weight averages, latex particle sizes, and their respective distributions. There are a number of analytical techniques available to characterize polymers in terms of these fundamental properties. These include gel permeation chromatography, membrane osmometry, ultracentrifugation and light scattering. The characterization of polymers from light scattering experiments, using sound statistical techniques, is the main thrust of this thesis.

Light scattering is a widely used and important technique and, for the purposes of this work, is classified into two groups; classical and dynamic light scattering experiments. Classical light scattering comprises wide angle and low angle laser light scattering techniques. From these types of experiments, estimates of the weight average molecular weight and radius of gyration may be obtained for a wide range of polymer molecules ranging in size from as low as 300 g/mol up to 10 g/mol. These upper and lower limits depend upon the choice of solvent and the amount of dissymmetry present (Billingham, 1977). Dynamic light scattering is the newest application of light scattering theory and provides estimates of a polymers particle size distribution and mean particle diameter. This technique is applicable to particles ranging in size from 20 to 3000 nanometres.

The methods for the analysis of light scattering data, however, have been lacking in their appreciation of some of the statistical problems inherent in the data. In evaluating a polymers suitability for the purpose for which it is inteded, it is important that sound statistical procedures are used to determine it's properties. The application of sound statistical data analysis techniques has been demonstrated to be quite effective in providing improved estimates of useful quantities such as the Wilson parameters (Sutton and MacGregor, 1977) and reactivity ratios (Patino-Leal et al, 1980).

This thesis examines the data analysis techniques of classical and dynamic light scattering experiments. In considering classical light scattering experiments, this work is primarily concerned with the improved statistical estimation of the weight average molecular weight, which appears as a parameter in the light scattering equations. In the case of dynamic light scattering, the primary concern is with the statistical problems encountered during the reconstruction of the particle size distribution.

Each of the following chapters is divided into presentations of the material pertaining to classical, and then dynamic light scattering. Chapter 2 gives a comprehensive development of the theory upon which the classical light scattering equations are based, and an introduction to the theory of dynamic light scattering. Chapter 3 describes some of the methods available for data analysis and their applications to light scattering experiments. In chapter 4, the

experimental data is described along with the FORTRAN programs that were used for parameter estimations. Finally, chapter 5 discusses the results obtained and gives the final conclusions and recommendations.

THEORY

2.1   Introduction

The theory of light scattered from particles in solution has it's foundation in physics. Workers such as Einstein, Rayleigh and Debye have all made important contributions. The classical light scattering theory presented below has been extracted from several general texts on light scattering and polymer molecules – Tanford (1961), Billingham (1977), Flory (1953), Huglin (1972), Stacey (1956). Citations referring to individual workers may be found in these references.

2.2   Classical Light Scattering Theory
2.2.1 Rayleigh's Theory

Lord Rayleigh first developed his theory for the scattering of light by particles small compared to their wavelength in 1871. This theory relates the intensity of scattered light as a function of angle for polarized and non-polarized light.

The dipole moment, p, induced in a particle when subjected to an electric field of strength, E, is directly proportional to E. The proportionality constant is the polarizability, α. A dipole moment is induced because the electrons and nucleus of a particle are subject to opposite forces in an electric field.

$$p = \alpha E \qquad\qquad (2.1)$$

Let an isotropically polarizable particle, small in size compared to the wavelength of the incident light, be in the path of a plane polarized beam of light travelling in the x-direction, see figure 2.1. Then, the electric field of such a light wave is

$$E = E_0 \cos(2\pi)(\nu t - x/\lambda) \qquad (2.2)$$

where E_0 is the maximum amplitude, ν is the frequency, λ is the wavelength of the incident light in the medium, t is time and x is the location along the line of propagation. Combining equations 2.1 and 2.2,

$$p = \alpha E_0 \cos(2\pi)(\nu t - x/\lambda) \qquad (2.3)$$

An oscillating dipole is itself a source of electromagnetic radiation. The radiation thus emitted is called the scattered radiation from the particle and has field strength proportional to the second derivative of the dipole moment, p, with respect to time. At a given distance, r, from the particle to the observer, the field strength is proportional to $\sin(\theta_1)$, where θ_1 is the angle between the direction of observation of the scattered radiation and the dipole axis, and is inversely proportional to the distance, r. Taking the second derivative of p with respect to t, we get

$$\frac{d^2p}{dt^2} = -4\pi^2 \nu^2 \alpha E_0 \cos(2\pi)(\nu t - x/\lambda) \qquad (2.4)$$

The scattered field strength is given by,

$$E_s = \frac{4\pi^2 \nu^2 \alpha E_0 \sin(\theta_1)}{c^2 r} \cos(2\pi)(\nu t - x/\lambda) \qquad (2.5)$$

where the proportionality $\sin(\theta_1)/r$ has been introduced, and the square

of the speed of light in the medium, $\tilde{c}$, is added to maintain correct dimensionality. Since $\lambda = \tilde{c}/\nu$, these terms can be eliminated from equation 5 to yield

$$E_s = \frac{4\pi^2\alpha E_0 \sin(\theta_1)}{\lambda^2 r} \cos(2\pi)(\nu t - x/\lambda) \qquad (2.6)$$

Note that the scattered radiation has the same frequency as the incident light. Cases where this is not so, such as the Raman effect, are not considered here.

The intensity of the incident and scattered light is proportional to the square of the field strength averaged over the period of vibration ($t=0$ to $t=1/\nu$).

$$I_0 \propto E_0^2 \cos^2(2\pi)(\nu t - x/\lambda) \qquad (2.7)$$

$$i_s \propto \frac{16\pi^4\alpha^2 E_0^2 \sin^2(\theta_1)}{r^2\lambda^4} \cos(2\pi)(\nu t - x/\lambda) \qquad (2.8)$$

We are interested in the intensity ratio of scattered light to incident light.

$$\frac{i_s}{I_0} = \frac{16\pi^4\alpha^2 \sin^2(\theta_1)}{r^2\lambda^4} \qquad (2.9)$$

Note that the dipole is always in the yz-plane, and parallel to the plane of polarization.

Suppose the incident light beam is now non-polarized instead of plane polarized. A non-polarized light beam is equivalent to the superposition of two plane polarized light beams whose planes of polarization are perpendicular to each other, and are of equal intensity and independent in phase, see figure 2.2. The intensity of
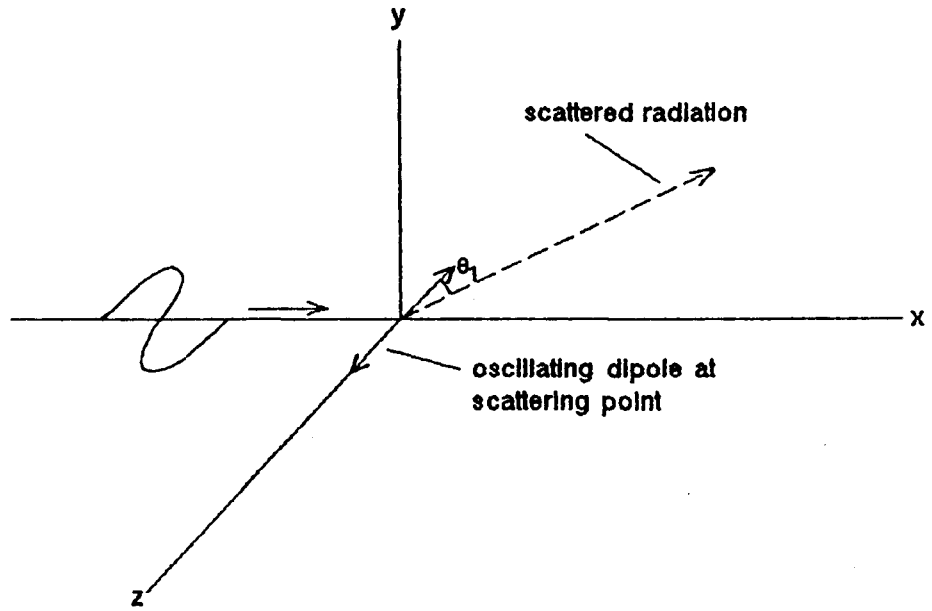
Figure 2.1 – Light scattered from plane polarized light
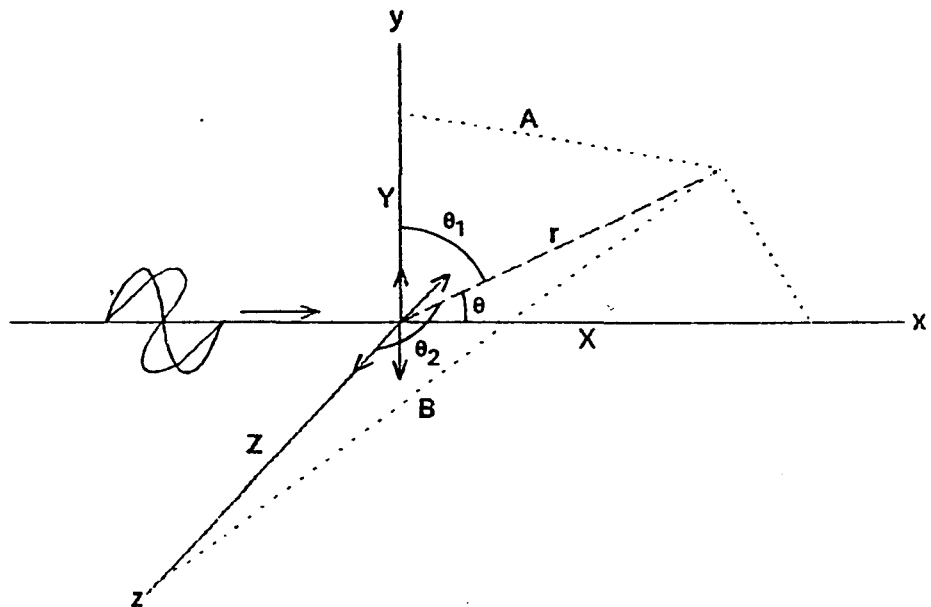
Figure 2.2 – Light scattered from un-polarized light

the scattered radiation is the sum of the two component intensities, each of which is half the original intensity of the non-polarized beam,

$$\frac{(i_s)_1}{\frac{1}{2}I_o} = \frac{16\pi^4\alpha^2\sin^2(\theta_1)}{r^2\lambda^4} \tag{2.10}$$

$$\frac{(i_s)_2}{\frac{1}{2}I_o} = \frac{16\pi^4\alpha^2\sin^2(\theta_2)}{r^2\lambda^4} \tag{2.11}$$

and the total scattered intensity is then

$$i_s = \frac{8\pi^4\alpha^2}{r^2\lambda^4}(\sin^2\theta_1 + \sin^2\theta_2)I_o \tag{2.12}$$

The quantities θ_1 and θ_2 are the angles between the direction of observation of the scattered light and the two dipole axes, y and z. For simplicity, let the two component planes of polarization be vertically and horizontally polarized — ie, the yx and zx planes.

Now, let θ be the angle between the line of observation of the scattering and the x-axis. The quantities X, Y and Z are the projections of the length, r, on the x, y and z axes respectively. From the geometry of figure 2.2, it can easily be shown that $\sin^2\theta_1 + \sin^2\theta_2 = 1 + \cos^2\theta$,(see appendix 1). Substituting this relation into 2.12

$$\frac{i_s}{I_o} = \frac{8\pi^4\alpha^2}{r^2\lambda^4}(1 + \cos^2\theta) \tag{2.13}$$

Particles whose scattering obeys equation 2.13 are said to exhibit Rayleigh scattering.

The angular dependence of the intensity of scattered light for polarized (equation 2.9) and non-polarized (equation 2.13) is displayed in figures 2.3 and 2.4 respectively.

An alternative derivation is based on the consideration of two special cases:

1. The scattering is in the xz plane, hence $\Theta_1 = 90°$, and the

   incident beam is perpendicularly polarized with respect to

   the scattering plane. Thus $\sin^2 \Theta_1 = 1$ and,

   $$\frac{(i_s)_1}{I_0} = \frac{16 \eta^4 \alpha^2}{r^2 \lambda^4} \qquad (2.14)$$

   Here, the scattered intensity is independent of angle.

2. The scattering is in the xy plane, hence $\Theta_2 = 90°$, and the

   incident beams polarization is parallel to the scattering

   plane. From trigonometric considerations, $\sin^2 \Theta_2 = \cos^2 \Theta$,

   and then,

   $$\frac{(i_s)_2}{I_0} = \frac{16 \eta^4 \alpha^2 \cos^2 \Theta}{r^2 \lambda^4} \qquad (2.15)$$

Since an unpolarized beam can be resolved into perpendicular and parallel components with respect to the scattering plane, then for an unpolarized beam,

$$i_s = \frac{(i_s)_1 + (i_s)_2}{2} = \frac{8 \eta^4 \alpha^2}{r^2 \lambda^4}(1 + \cos^2 \Theta) I_0 \qquad (2.16)$$
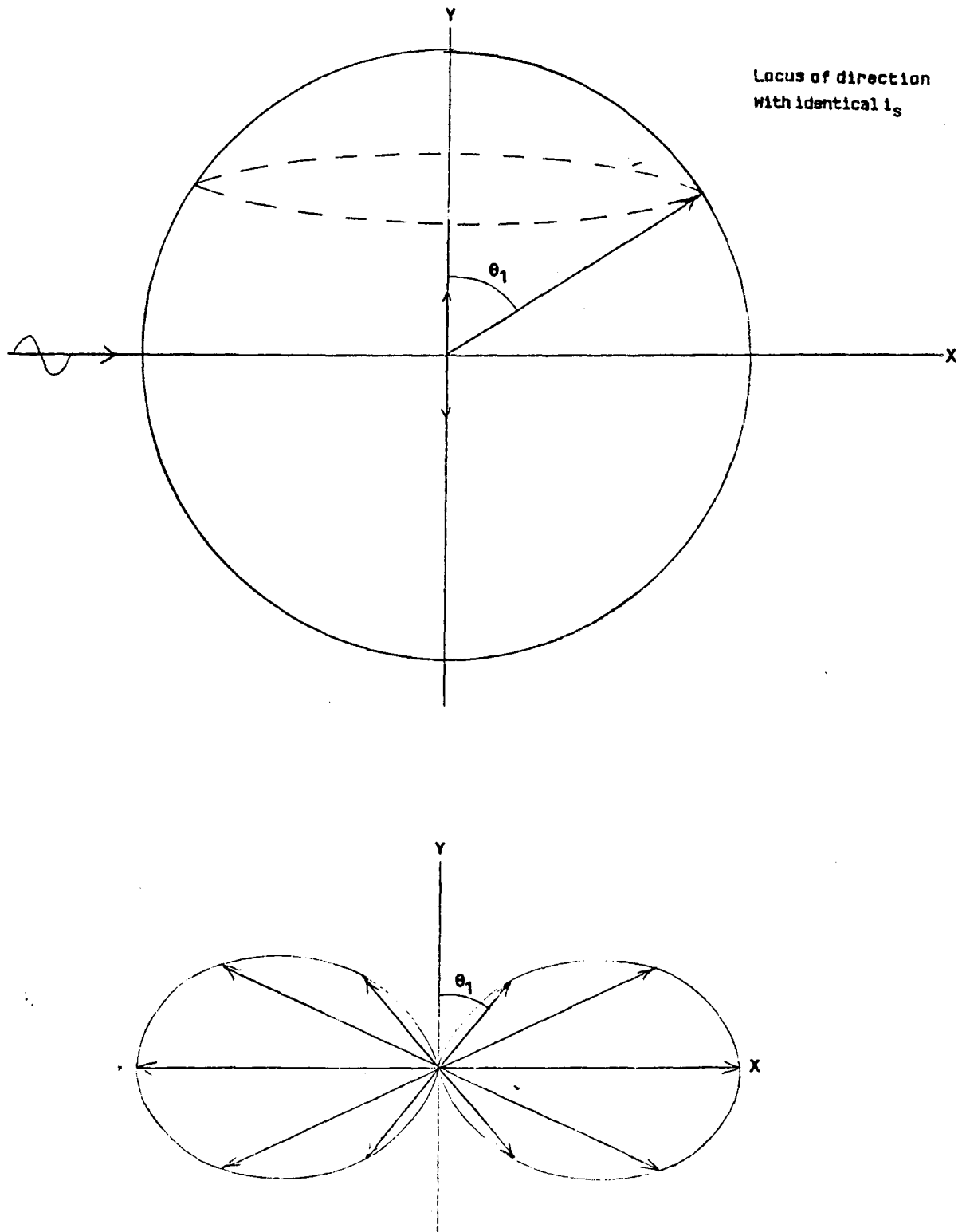
Figure 2.3 – Scattering envelope for plane polarized light
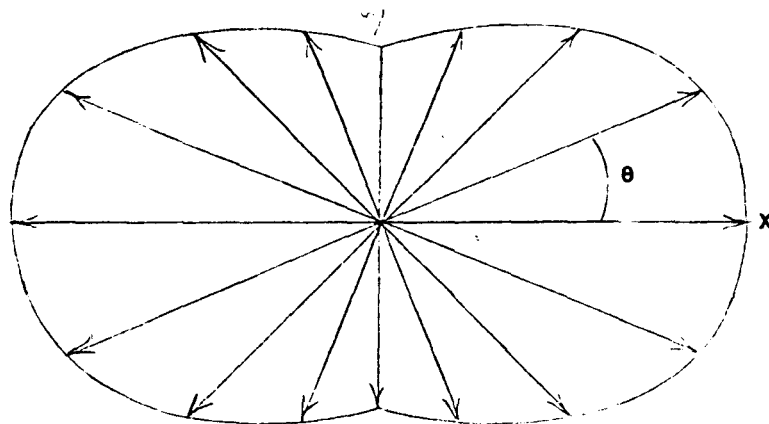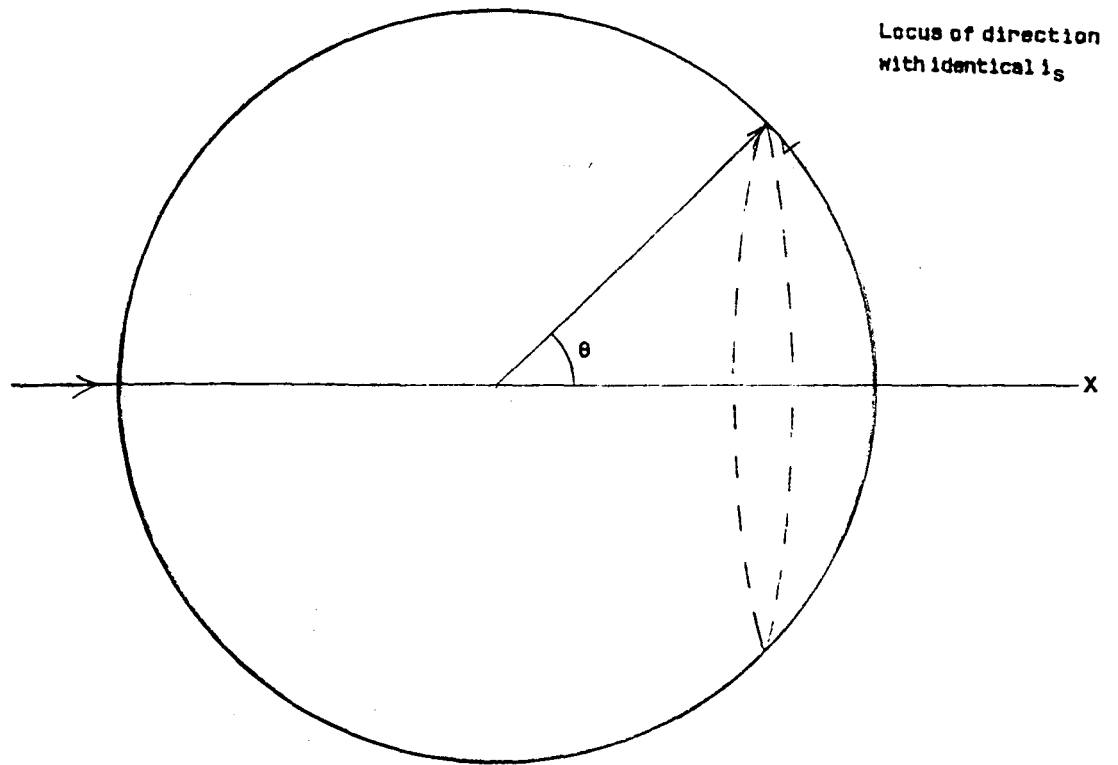
Figure 2.4 – Scattering envelope for un-polarized light

This is the same result as equation 2.13. Note that the sum is divided by two since each component has only half the intensity of the origonal polarized beam.

Equation 2.13 contains several parameters which relate to a particular experimental set-up. These parameters are eliminated by defining a reduced scattering intensity or Rayleigh ratio, R_θ. For a non-polarized light beam, define R_θ to be

$$R_\theta = \frac{i_\theta r^2}{I_o(1 + \cos^2\theta)} \tag{2.17}$$

Combining equations 2.13 and 2.17, we have

$$R_\theta = \frac{8\pi^4\alpha^2}{\lambda^4} \tag{2.18}$$

2.2.2 Ideal Gas Model

A simple model for the scattering of light from a solution of small molecules of size less than $\lambda/20$, which exhibit Rayleigh scattering may be derived if we consider the solution to be an ideal gas of solute molecules dispersed in the solvent. The total reduced scattering intensity from a solution containing n particles per unit volume is

$$R_\theta = \frac{8\pi^4 n\alpha^2}{\lambda^4} \tag{2.19}$$

For dilute polymer solution, the polarizability constant, α can be expressed in terms of electric (dielectric constant, D) or optical (refractive index, $\eta^2 = D$) properties.

$$\alpha = \frac{\eta^2 - \eta_o^2}{4\pi n \eta_o^2} = \frac{D - D_o}{4\pi n D_o} \tag{2.20}$$

where η and η_0 are the refractive indices of the solution and solvent respectively.

For infinitely dilute solutions, η can be expressed as a linear function of polymer concentration, c.

$$\eta = \eta_0 + c\,\frac{d\eta}{dc} \tag{2.21}$$

If we square both sides and assume that $c^2(d\eta/dc)^2 \ll 2\eta_0 c(d\eta/dc)$, then

$$\eta^2 - \eta_0^2 = 2\eta_0 c\,\frac{d\eta}{dc} \tag{2.22}$$

Substituting 2.22 into 2.20, we obtain for the polarizability

$$\alpha = \frac{c(d\eta/dc)}{2\pi n \eta_0} \tag{2.23}$$

Now we can substitute for the polarizability in equation 2.19 to get

$$R_\theta = \frac{2\pi^2 c^2}{\lambda^4 n \eta_0^2}\left(\frac{d\eta}{dc}\right)^2 \tag{2.24}$$

Making use of the relations $c = nM/N_{AV}$ and $\lambda = \lambda_0/\eta_0$ where M is the molecular weight, N_{AV} is Avogadro's number and λ_0 is the wavelength of the incident light, we now have for R_θ

$$R_\theta = \frac{2\pi^2 \eta_0^2}{\lambda_0^4 N_{AV}}\left(\frac{d\eta}{dc}\right)^2 cM \tag{2.25}$$

$$= K^* cM \tag{2.26}$$

where K^*, an optical constant has been defined as

$$K^* = \frac{2\pi^2 \eta_0^2}{\lambda_0^4 N_{AV}}\left(\frac{d\eta}{dc}\right)^2 \tag{2.27}$$

Equation 2.27 can be re-arranged into the more familiar form

$$\frac{K^*c}{R_\theta} = \frac{1}{M} \qquad (2.28)$$

The assumptions under which 2.28 are valid may be summarized,

1. Non-polarized light

2. Small molecules

3. Isotropic molecules

4. Polymer solution infinitely dilute; ie - molecules

   independent of one another

5. Equation (2.22) holds

6. The expressions for α and η arise as a consequence of

   dilute solutions

7. Monodisperse solute

The ideal gas representation of a dilute polymer solution which led to $R_\theta = K^*cM$ totally ignores different thermodynamic interactions. In the next sub-section, a derivation based on fluctuation theory relates the scattered intensity to the thermodynamic properties of the system. This is a more general treatment since it considers scattering from liquids and solutions instead of using an ideal gas representation.

2.2.3 Fluctuation Theory

As in the previous section, the equations are derived for small molecules subjected to non-polarized incident light.

Instead of representing the polymer molecules in solution as an ideal gas, consider a volume element, dV, small compared to the wavelength λ. At any given time, the properties (such as density, concentration, etc...) of an element will fluctuate from an average value within that element with respect to the neighbouring elements. The bulk property measured can be considered to be the average taken over all elements.

Fluctuations in the dielectric constant arise from two sources; fluctuations in density, and concentration caused by thermal agitation. The excess polarizability of a volume element due to its fluctuation from the average is given by

$$\Delta\alpha = \frac{\Delta D \, dV}{4\pi D_0} \qquad (2.29)$$

where $\Delta\alpha$ and ΔD are the fluctuations in the polarizability and dielectric constants respectively. In equation 2.29, the number of particles per unit volume, n, has been replaced by the number of volume elements per unit volume, $1/dV$.

The scattering intensity, i_θ, now depends on the average square of $\Delta\alpha$ for all volume elements, $(\overline{\Delta\alpha})^2$. This replaces α^2 so that

$$i_\theta = \frac{8\pi^4(\overline{\Delta\alpha})^2}{r^2\lambda^4 dV}(1 + \cos^2\theta)I_0 \qquad (2.30)$$

Squaring equation 2.29, substituting for $(\overline{\Delta\alpha})^2$ in 2.30, and recalling the definition for the Rayleigh ratio given in equation 2.17, we obtain

$$R_\theta = \frac{\eta^2 (\overline{\Delta D})^2 \, dV}{2 \, \lambda_0^4} \qquad (2.31)$$

For dilute polymer solutions, scattering of light results from fluctuations in the density and the concentration. The fluctuations in the dielectric constant can be expanded in terms of the fluctuations in these two properties as

$$(\overline{\Delta D})^2 = \left(\frac{\partial D}{\partial \rho}\right)^2 (\overline{\Delta \rho})^2 + \left(\frac{\partial D}{\partial c}\right)^2 (\overline{\Delta c})^2 \qquad (2.32)$$

Since the solution is dilute, the scattering due to density fluctuations is assumed to be the same as for the pure solvent, and is ignored. Therefore, consider only the scattering due to concentration fluctuations. Substituting for (ΔD),

$$R_\theta = \frac{\eta^2}{2\lambda_0^4} \left(\frac{\partial D}{\partial c}\right)^2 (\overline{\Delta c})^2 \, dV \qquad (2.33)$$

According to Einstein (1910), local variations in any fluctuating parameter, can be related to the thermodynamic properties of the system according to

$$(\overline{\Delta \xi})^2 = \frac{KT}{(\partial^2 A / \partial \xi^2)} \qquad (2.34)$$

where K is the Boltzmann constant, T is the absolute temperature, and A is the Helmholtz free energy. Also, according to Oster (1948)

$$\frac{\partial^2 A}{\partial c^2} = -\frac{\partial \mu_1}{\partial c} \frac{dV}{V_0 \, c} \qquad (2.35)$$

where μ_1 is the chemical potential of the solvent in solution and $\bar{V}_0$ is the molar volume of solvent in solution. Applying equation 2.34 to concentration, and substituting for $\partial^2 A / \partial c^2$, we arrive at

$$(\overline{\Delta c})^2 = -\frac{KT\bar{V}_0 \, c}{(\partial \mu_1 / \partial c)dV} \qquad (2.36)$$

The partial derivative in 2.36 can be expressed in terms of the osmotic pressure, Π. Since $\mu_1 - \mu_1^0 = -\Pi \bar{V}_0$, then

$$\frac{\partial \mu_1}{\partial c} = -\bar{V}_0 \frac{\partial \Pi}{\partial c} \qquad (2.37)$$

Since $D = \eta^2$, it can easily be shown that

$$\left(\frac{\partial D}{\partial c}\right)^2 = 4 \, \eta_0^2 \left(\frac{\partial \eta}{\partial c}\right)^2 \qquad (2.38)$$

Making the appropriate substitutions of equations 2.36, 2.37 and 2.38 into equaton 2.33, we have then, for Rayleigh's ratio,

$$R_\theta = \frac{2\Pi^2 \eta_0^4}{\lambda_0^4} \left(\frac{\partial \eta}{\partial c}\right)^2 \frac{KTc}{(\partial \Pi / \partial c)} \qquad (2.39)$$

The osmotic pressure is related to the solute molecular weight, M, through

$$\frac{\Pi}{c} = \frac{RT}{M} + Bc + Cc^2 + \ldots \qquad (2.40)$$

or

$$\Pi = cRT(1/M + A_2 c + A_3 c^2 + \ldots) \qquad (2.41)$$

where R is the gas constant.

Taking the first derivative of $\tilde{\eta}$ with respect to c, and substituting for ($\delta\tilde{\eta}/\delta$c) and K = R/$N_{AV}$ in equation 2.39, we have

$$R_\theta = \frac{K^* c}{1/M + 2A_2c + 3A_3c^2 + \ldots} \qquad (2.42)$$

or

$$\frac{K^* c}{R_\theta} = \frac{1}{M} + 2A_2c + 3A_3c^2 + \ldots \qquad (2.43)$$

This final result is identical to equation 2.28 with the exception that virial coefficients have been added. We can summarize the conditions and approximations under which equations 2.43 is valid below.

1. Non-polarized light

2. Small particles

3. Isotropic particles

4. Volume elements small compared to the wavelength of

the light

5. Dilute polymer solutions implying fluctuations in

dielectric constant dependent upon fluctuations in

polymer concentration only

6. Constant temperature and pressure

7. Monodisperse solute

Some of the above conditions are restrictive and prevent the use of equation 2.43 as a general model that can be applied to light scattering situations that we are interested in. In the next few sections, a more general model will be developed by taking into account polydispersity and large molecules.

2.2.4   Accounting for Polydispersity

Consider polydisperse systems in which the solute has a distribution of molecular weights. At infinite dilution, the total reduced Rayleigh ratio may be expressed as the sum of the ratios for each component, i, with molecular weight, M_i, in the distribution. Assuming the ideal gas representation, this is given by

$$(R_\theta)_{c=0} = \Sigma R_i = K^* \Sigma c_i M_i \tag{2.44}$$

Now, the concentration of each component, c_i, is given by w_i/V, where w_i is the weight of the polymer molecules with molecular weight M_i. The system concentration is given by the sum,

$$c = \Sigma c_i = \frac{\Sigma w_i}{V} \tag{2.45}$$

Combining 2.44 and 2.45,

$$\frac{K^*}{R_\theta} = \frac{V}{\Sigma w_i M_i} \tag{2.46}$$

Multiplying 2.46 by c and recalling the relation in 2.45,

$$\frac{K^*c}{R_\theta} = \frac{\Sigma w_i}{\Sigma w_i M_i} \qquad (2.47)$$

The right hand side of equation 2.47 is recognized as the weight average molecular weight, hence,

$$\frac{K^*c}{R_\theta} = \frac{1}{\overline{M}_w} \qquad (2.48)$$

Thus, we find that the M in the previous developments is the weight average molecular weight for polydisperse systems.

2.2.5 The Particle Scattering Function

When large molecules are present in the solution, the incident beam will be scattered at more than one point along the molecule. Thus, the path lengths of light scattered from different points to the detector will be different resulting in destructive interference and a reduced measurement of the scattered light intensity. The result is that the measured intensity at any angle in the forward direction is greater than that at the corresponding angle in the backward direction resulting in dyssymmetry of the scattered light intensity as shown in figure 2.5. The internal inteference reduces the scattered intensity at all angles except zero. Thus the previous developments are not applicable to molecules of large size.
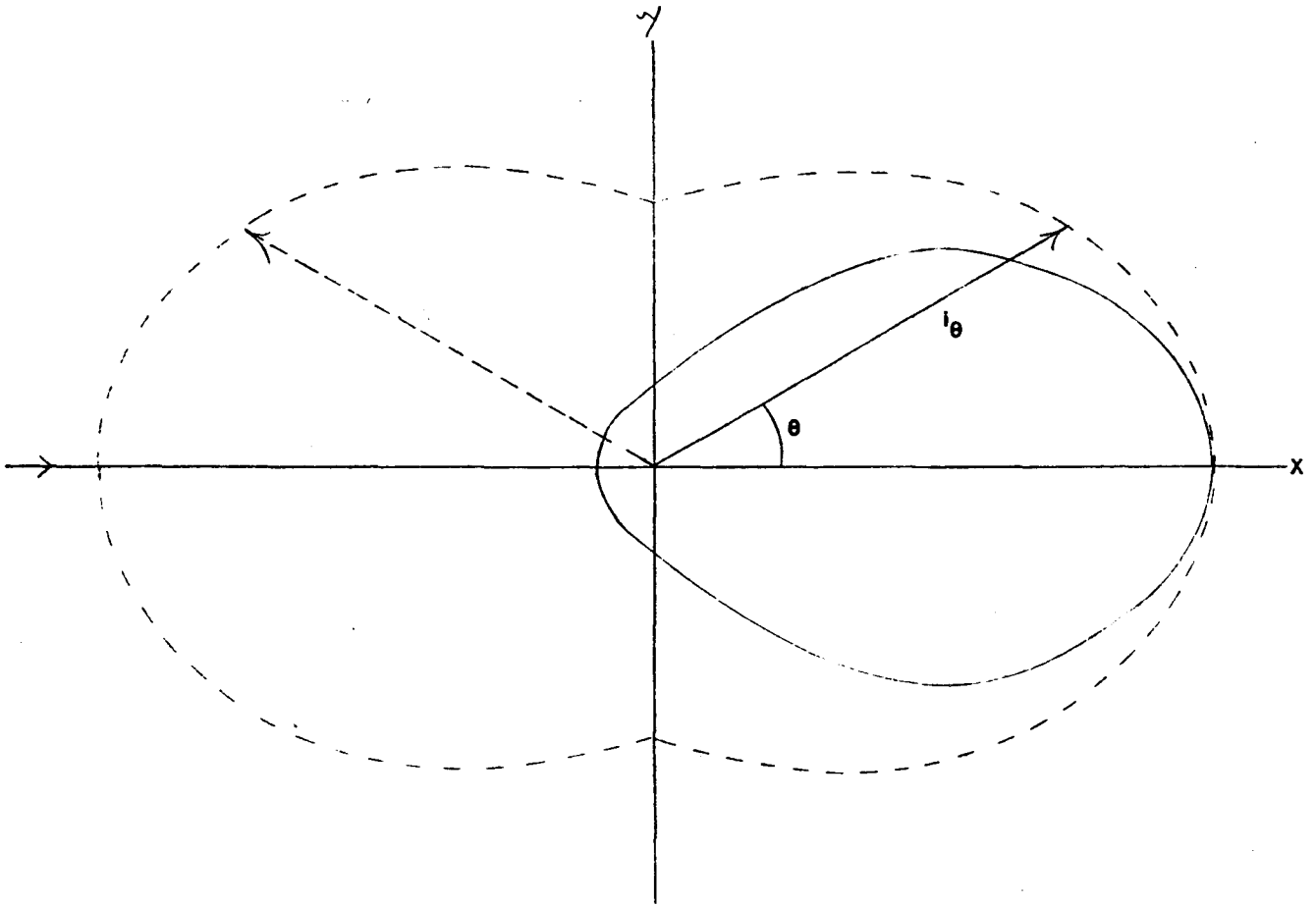
Figure 2.5 – Scattering envelope displaying the effect of large molecules

The effect of large size may be described by a function, $P(\theta)$, where

$$P(\theta) = \frac{\text{scattered intensity for large particles}}{\text{scattered intensity without interference}}$$

$$= \frac{R_\theta \text{ (large molecules)}}{R_\theta \text{ (no interference)}}$$

$$= \frac{R_\theta}{K^* cM} \qquad (2.49)$$

The expression for the ratio in 2.49 is called the particle scattering function and tries to account for the intramolecular interference of light scattered from large particles. Based on the random orientation of the scattering particle, the following relation was first obtained by Debye (1915)

$$P(\theta) = \frac{1}{\sigma^2} \sum_{i=1}^{\sigma} \sum_{j=1}^{\sigma} \frac{\sin(\mu r_{ij})}{\mu r_{ij}} \qquad (2.50)$$

where σ is the number of scattering elements, r_{ij} is the distance between a pair of elements, i and j, and μ is given by

$$\mu = \frac{4\beta}{\lambda} \sin(\theta/2) \qquad (2.51)$$

where λ is the wavelength of light in the medium.

It is well known that $\sin(x)$ can be re-expressed as an infinite sum,

$$\sin(x) = x - \frac{x^3}{3!} + \frac{x^5}{5!} - \ldots \qquad (2.52)$$

Hence

$$\frac{\sin(\mu r_{ij})}{\mu r_{ij}} = 1 - \frac{\mu^2 r_{ij}^2}{3!} + \frac{\mu^4 r_{ij}^4}{5!} - \ldots \qquad (2.53)$$

At low scattering angles, μ is small, and the third and remaining terms in the right side of 2.53 may be neglected, so that

$$\lim_{\theta \to 0} P(\theta) = \frac{1}{\sigma^2} \sum_{i=1}^{\sigma} \sum_{j=1}^{\sigma} \left[1 - \frac{\mu^2 r_{ij}^2}{3!} \right] \qquad (2.54)$$

$$= 1 - \frac{\mu^2 \, \Sigma \, \Sigma \, r_{ij}^2}{3! \, \sigma^2} \qquad (2.55)$$

since $\sum_{i}^{\sigma} \sum_{j}^{\sigma} 1 = \sigma^2$.

The mean square radius of gyration, $\langle s^2 \rangle$, may be defined as,

$$\langle s^2 \rangle = \frac{1}{2\sigma^2} \Sigma \, \Sigma \, r_{ij}^2 \qquad (2.56)$$

so that

$$\lim_{\theta \to 0} P(\theta) = 1 - \frac{\mu^2 \langle s^2 \rangle}{3} \qquad (2.57)$$

Or alternatively,

$$\frac{1}{\lim\limits_{\theta \to 0} P(\theta)} = \lim_{\theta \to 0} P^{-1}(\theta) = \left(1 - \frac{\mu^2 \langle s^2 \rangle}{3} \right)^{-1} \qquad (2.58)$$

For small values of x, $(1 - x)^{-1} \doteq 1 + x$, hence,

$$\lim_{\theta \to 0} P^{-1}(\theta) = 1 + \frac{\mu^2 \langle s^2 \rangle}{3} \qquad (2.59)$$

$$= 1 + \frac{16 \pi^2 \langle s^2 \rangle \, \sin^2(\theta/2)}{3 \lambda^2} \qquad (2.60)$$

Combining equations 2.43, 2.49 and 2.60, we have

$$\lim_{\substack{c \to 0 \\ \theta \to 0}} \frac{K^* c}{R_\theta} = \frac{1}{MP(\theta)} = \frac{1}{M} \left[1 + \frac{16 \pi^2 \langle s^2 \rangle \, \sin^2(\theta/2)}{3 \lambda^2} \right] \qquad (2.61)$$

The conditions and approximations under which 2.61 are valid are

1. Non-polarized light

2. Isotropic particles

3. Polymer solution infinitely dilute

4. Low angles

5. Monodisperse solute

6. Constant temperature and pressure

7. Assumption that fourth and higher order terms in 2.53

   are negligible

8. $(1 - x)^{-1} \doteq 1 + x$

2.2.6 Polydispersity of Large Molecules

To take into account the effect of polydispersity in macro-molecules, we note that

$$R_\theta = K^* \Sigma M_i P_i(\theta) c_i \qquad (2.62)$$

where i refers to each component of the mixture. Each $P_i(\theta)$ in 2.62 can be related to the corresponding radius of gyration, $<s_i^2>$,

$$P_i(\theta) = 1 - \frac{16\pi^2 <s_i^2> \sin^2(\theta/2)}{3\lambda^2} \qquad (2.63)$$

Thus,

$$\frac{K^*}{R_\theta} = \frac{1}{\Sigma M_i c_i - \frac{16\pi^2 \sin^2(\theta/2) \Sigma M_i c_i <s_i^2>}{3\lambda^2}} \qquad (2.64)$$

Since $c = \Sigma c_i$,

$$\frac{K^*c}{R_\theta} = \frac{\Sigma c_i}{\Sigma M_i c_i - \dfrac{16\pi^2\sin^2(\theta/2)}{3\lambda^2}\Sigma M_i c_i \langle s_i^2\rangle} \qquad (2.65)$$

$$\frac{K^*c}{R} = \frac{1}{\dfrac{\Sigma M_i c_i}{\Sigma c_i} - \dfrac{16\pi^2\sin^2(\theta/2)}{3\lambda^2}\dfrac{\Sigma M_i c_i \langle s_i^2\rangle}{\Sigma c_i}} \qquad (2.66)$$

Recalling that,

$$\frac{\Sigma M_i c_i}{\Sigma c_i} = \Sigma w_i M_i = \bar{M}_w \qquad (2.67)$$

then

$$\frac{K^*c}{R_\theta} = \frac{1}{\dfrac{\Sigma M_i c_i}{\Sigma c_i}\left\{1 - \dfrac{16\pi^2\sin^2(\theta/2)}{3\lambda^2}\dfrac{\Sigma c_i}{\Sigma M_i c_i}\dfrac{\Sigma M_i c_i \langle s_i^2\rangle}{\Sigma c_i}\right\}} \qquad (2.68)$$

$$= \frac{1}{\bar{M}_w\left\{1 - \dfrac{16\pi^2\sin^2(\theta/2)}{3\lambda^2}\dfrac{\Sigma M_i c_i \langle s_i^2\rangle}{\Sigma M_i c_i}\right\}} \qquad (2.69)$$

The z-average radius of gyration, $\langle s^2\rangle_z$, is given by

$$\langle s^2\rangle_z = \frac{\Sigma M_i c_i \langle s_i^2\rangle}{\Sigma M_i c_i} \qquad (2.70)$$

therefore, 2.69 can be written as,

$$\frac{K^*c}{R_\theta} = \frac{1}{\bar{M}_w\left\{1 - \dfrac{16\pi^2\langle s^2\rangle_z}{3\lambda^2}\sin^2(\theta/2)\right\}} \qquad (2.71)$$

Or, for low angles

$$\frac{K^*c}{R} = \frac{1}{\bar{M}_w}\left[1 + \frac{16\pi^2\langle s^2\rangle_z}{3\lambda^2}\sin^2(\theta/2)\right] \qquad (2.72)$$

2.2.7   The General Model

The light scattering equations, in their most general form, may be expressed as,

$$\frac{K^*c}{R_\theta} = \frac{1}{\bar{M}_w P(\theta)} + 2A_2c + 3A_3c^2 + \ldots \tag{2.73}$$

$$= \frac{1}{\bar{M}_w}\left[1 + \frac{16\pi^2\langle s^2\rangle_z}{3\lambda^2}\sin^2(\theta/2)\right] + 2A_2c + 3A_3c^2 + \ldots \tag{2.74}$$

In equation 2.73, note that 1) as particle size decreases, $P(\theta)$ approaches 1, 2) for monodisperse solutes, $\bar{M}_w = M$, and 3) in the limit that $\theta = c = 0$, 2.74 approaches equation 2.28.

All of the above light scattering equations were derived for non-polarized light, however it is easy to handle polarized light by replacing $(1 + \cos^2\theta)$ with 1 or $\cos^2\theta$ for vertically or horizontally polarized respectively in all of the developments, and noting that the optical constant K^* is multiplied by a factor of 2.

2.2.8   Turbidity

Instead of measuring the intensity of the light scattered by a solution containing particles, it is sometimes preferred to measure the energy loss of a light beam due to the scattering. A beam of initial intensity I_x decreases to intensity I_{x+dx} by the amount τIdx as a result of travelling a distance dx through a solution of turbidity, τ. Thus, the more turbid a solution is, the higher the energy loss of the beam. In travelling a distance x, an incident beam of intensity I_o will be reduced to an intensity I, and

$$\frac{I}{I_o} = \exp(-\tau x) \tag{2.75}$$

Since the decrease in intensity will be small, the above expression can be approximated by

$$\tau x = \frac{I_0 - I}{I_0} \qquad (2.76)$$

The derivations are not presented here, but it can be shown that the turbidity is directly obtainable from the Rayleigh ratio

$$\tau = \frac{16\pi}{3} R_\theta \qquad (2.77)$$

2.3   Experimental – Classical Light Scattering

In this section, the means of obtaining experimental light scattering measurements from wide and low angle instruments is presented.

2.3.1   Wide Angle Light Scattering

For the SOFICA wide angle light scattering instrument, the following relationship may be used,

$$R_\theta = \frac{\sin\theta}{1 + \cos^2\theta} \frac{R_b}{G_b} \frac{n_s^2}{n_v^2} \frac{1}{t_s^2(1 - 4f_s^2)} [i_\theta - 2f_s i_{180-\theta}] \qquad (2.78)$$

where R_b is the Rayleigh ratio for benzene at 90° and is a known constant, G_b is the relative scattered intensity for benzene at 90°, $i_{90^\circ b}/I_0$, n_s^2/n_v^2 is the correction for the refractive indices of the scattering solution and the solvent in the vat, $t_s = 1 - f_s$ is the Fresnel coefficient or transmission coefficient, f_s the fraction of incident light reflected at the glass/solvent interface, and i_θ, $i_{180-\theta}$

are the scattered intensities (the difference between galvanometer readings at θ^o for the solution and solvent; $G_\theta(sol'n) - G_\theta(solv.)$).

If the refractive indices of the solvent and glass are similar (as are those for benzene and glass), the above expression may be approximated by

$$R_\theta = \frac{R_b}{G_b} \frac{sin\theta}{1 + cos^2\theta} \, i_\theta \qquad (2.79)$$

$$= \frac{R_b}{G_b} \frac{sin\theta}{1 + cos^2\theta} [G_\theta(sol'n) - G_\theta(solv.)] \qquad (2.80)$$

where $sin\theta$ is a correction to account for the volume change when viewing the solution cell at different angles, and $1 + cos^2\theta$ is present to account for the state of polarization of the light; the current form is for non-polarized light and is replaced by 1 or $cos^2\theta$ for perpendicularly or parallel polarized light respectively.

Recall that the Rayleigh ratio may be defined as

$$R_\theta = \frac{i_\theta r^2}{I_0 (1 + cos^2\theta)} \qquad (2.81)$$

At $\theta = 90^o$, and using pure benzene as a solvent, it can be shown that the constant, r^2, (and any other constants that may need to be present) is equivalent to the term R_b/G_b,

$$\frac{R_{90^o|b|}}{i_{90^o|b|}/I_0} = r^2 \qquad (2.82)$$

But, $i_{90^o|b|}/I_0 = G_{90^o|b|}$, therefore

$$\frac{R_{90^o|b|}}{G_{90^o|b|}} = \frac{R_b}{G_b} = r^2 \qquad (2.83)$$

Recall that G is the actual measured quantity in the form of a galvanometer reading and R_b is a known constant. Thus,

$$R_\theta = \frac{R_b}{G_b} \frac{1}{1 + cos^2\theta} \frac{i_\theta}{I_o} \tag{2.84}$$

$$= \frac{R_b}{G_b} \frac{1}{1 + cos^2\theta} [G_\theta(sol'n) - G_\theta(solv.)] \tag{2.85}$$

The correction term, $sin\theta$, is introduced to give the final expression that is used to calculate the Rayleigh ratio from experimental measurements at different scattering angles,

$$R_\theta = \frac{R_b}{G_b} \frac{sin\theta}{1 + cos^2\theta} [G_\theta(sol'n) - G_\theta(solv.)] \tag{2.86}$$

2.3.2   Low Angle Laser Laser Light Scattering

Low angle laser light scattering (LALLS) is a special case of wide angle light scattering that simplifies the light scattering model equation by restricting the sample concentrations and angles of measurement to low values. As both θ and c approach zero in equation 2.74, we have

$$\frac{K^*c}{R_\theta} = \frac{1}{\bar{M}_w} + 2A_2c \tag{2.87}$$

The polymer Rayleigh ratio, R_θ, is the difference between the Rayleigh ratios for the polymer solution and the solvent

$$R_\theta = R_\theta(sol'n) - R_\theta(solv.) \tag{2.88}$$

where $R_\theta(solv.)$ is a known constant. For the Chromatrix KMX-6 laser light scattering instrument, $R_\theta(sol'n)$ is given by

$$R_\theta = \frac{G_\theta - bl}{G_o - bl} (\sigma'\lambda'j)^{-1}D \tag{2.89}$$

where G_θ and G_o are the galvanometer readings at angles θ and 0 degrees, bl is the base line measurement to account for base line drift, $(\sigma'\lambda'\gamma')^{-1}$ is a function of solid angle, field stop and refractive index and is a known constant, and D is a function of the attenuating filters.

2.4   Dynamic Light Scattering Theory

Dynamic light scattering (also known as photon correlation spectroscopy and quasi-elastic light scattering) is concerned with the time behaviour of the scattered light intensity measurements rather than the average intensity measurement as in the classical theory. The fluctuations in intensity arise from Brownian motion of the solute particles due to collisions with solvent molecules. Thus, the particles translate their position through the solution in a random walk fashion.

The probability, $P(r,t)$, of finding a particle a distance r from it's origin at time t is given by the diffusion equation

$$\frac{\delta P(r,t)}{\delta t} = D_t \nabla P(r,t) \qquad (2.90)$$

where D_t is the translational diffusion coefficient of the particles. From the solution of the above equation, the mean lifetime of a fluctuation in the measured intensity is equal to the average time required for the random walk diffusion of the scattering particle to change it's optical path lengths to a detector by one-half wavelength

of light and is given by

$$\frac{1}{\tau} = \Gamma = D_t K^2 \tag{2.91}$$

where τ is called the mean decay time and K is a geometric factor dependent upon the wavelength of the light source λ, the solvent index of refraction n_s, and the scattering angle θ,

$$K = \frac{4 \pi n_s \sin(\theta/2)}{\lambda} \tag{2.92}$$

For spherically symmetric scatterers, D_t, the translational diffusion coefficient, can then be related to the particles hydrodynamic radius by the Stokes-Einstein equation

$$R_h = \frac{K_B T}{6 \pi \eta \, D_t} \tag{2.93}$$

where K_B is Boltzmann's constant, T is the absolute temeperature and η is the solvent viscosity.

Other types of particle diffusion caused by solvent collisions, such as rotational and intramolecular diffusion, may also be evaluated, but will not be considered here since we are dealing with spherical particles.

The mean decay time of the fluctuations may be found by measuring experimentally the second-order, un-normalized autocorrelation function of the scattered intensity,

$$G^{(2)}(\tau) = \langle I(t) \, I(t + t') \rangle \tag{2.94}$$

where I(t) and I(t + t') are the scattered intensities at times t and (t + t') respectively. The < > symbol represents a running sum of

such products, taken for different values of t, so a reliable statistical average of $G^{(2)}(\tau)$ may be obtained for a given separation time t'. Obviously, as the separation time increases, the dependence of $I(t + t')$ on $I(t)$ is reduced and the correlation function decreases. Typically, an autocorrelator computes $G^{(2)}(\tau)$ for 64 different values of $t' = \Delta t, 2\Delta t, ..., 64\Delta t$, where Δt is the channel width. For a good description of how the autocorrelation function is computed digitally, see Pusey et al (1974).

The first-order, normalized autocorrelation function of the scattered intensity, $g^{(1)}(\tau)$ is related to $G^{(2)}(\tau)$ through

$$G^{(2)}(\tau) = A[1 + \beta g^{(1)}(\tau)^2] \qquad (2.95)$$

where A is the baseline measurement at infinite time (equivalent to the square of the average intensity, $\langle I \rangle$), β is a constant and $g^{(1)}(\tau)$ is an exponential function

$$g^{(1)}(\tau) = f[\exp(-\Gamma t)] \qquad (2.96)$$

For a monodisperse particle size distribution, $g(\tau)$ is a single exponential decay,

$$g^{(1)}(\tau) = \beta \exp(-\Gamma t) \qquad (2.97)$$

Thus, the particle size may be determined from an estimate of Γ and equations (2.91), (2.92) and (2.93). As the size of the particle increases, it will diffuse more slowly through the solution and have a longer delay time. Thus, small particles have a quick decay time while large particles have a slow decay time.

For polydisperse particle size distributions, $g^{(1)}(\tau)$ is an integral sum of exponentials, each particle size contributing to the total function according to it's relative amount in the distribution.

$$g^{(1)}(\tau) = \int_0^\infty f(\Gamma) \exp(-\Gamma t) d\Gamma \qquad (2.98)$$

where $f(\Gamma)$ is the intensity weighted distribution function of decay ratios or diffusion coefficients. Particles far away from the mean of the distribution have little contribution while those near the centre have the largest contribution. In this case, we are interested in obtaining estimates of $f(\Gamma)$ and Γ to define the particle size distribution.

2.5   Experimental – Dynamic Light Scattering

The objective of current dynamic light scattering instruments is to compute digitally the autocorrelation function of the scattered intensity from the photon counts stored in a number (usually 64) of channels. The means of recovering the distribution of particle sizes, $f(\Gamma)$, from equation (2.98) is better left for discussion in chapter three.

METHODS OF ANALYSIS

3.1   Introduction

The purpose of this chapter is to examine some of the different methods that are available for estimating the parameters in the light scattering models. Good estimates of parameters such as weight average molecular weight and radii of gyrations, and the associated confidence intervals for the parameters are useful for polymer characterization and quality control.

3.2   Classical Light Scattering

As can be seen in the development of the theory in the previous chapter, light scattering techniques are powerful and useful analytical tools since the weight average molecular weight of a polymer and in some cases, the z-average radius of gyration and virial coefficients, appear in the models as parameters that may be determined through fitting procedures. It is the improved statistical estimation methods for these parameters that is the primary consideration of this study.

3.2.1   Classical Forms of Data Analysis - WALS and LALLS

The classical interpretation of data from wide angle light scattering (WALS) and low angle laser light scattering (LALLS) experiments have largely been based on graphical methods.

The most common form of WALS data analysis has been the Zimm plot (1948). From the general light scattering model given in equation (2.74), it can be seen that a bilinear plot of $K^x c/R_\theta$ against $\sin(\theta/2) + \acute{K}c$ as a function of scattering angle and concentration can be used as a convenient way of presenting the data. k' is an arbitrary constant used to spread the plot along the x-axis. Thus, a grid is formed requiring measurements of R_θ at different levels of concentration and scattering angle. An example of a Zimm plot is shown in figure 3.1. Double extrapolation to the intercept on the y-axis at $\theta = c = 0$ provides an estimate of $1/\bar{M}_w$. The radius of gyration is given by the intercept at $\theta = c = 0$ and the initial slope of the line $c = 0$,

$$<s^2>_z = \frac{3\lambda^2}{16\pi^2} \frac{\text{initial slope of line c=0}}{\text{intercept } (K^x c/R_\theta)} \qquad (3.1)$$

Finally, an estimate of the second virial coefficient A_2 is obtained from the initial slope of the line $\theta = 0$. An estimate of A_3 may then be directly calculated from equation (2.74). For a good discussion on graphical treatments of WALS data, see chapter 5 of Huglin (1972).

The graphical treatment of LALLS data is less complicated owing to it's simpler model form given in equation (2.87). Here, a single linear plot of $K^x c/R_\theta$ against concentration should yield a straight line whose intercept is $1/\bar{M}_w$ and slope is A_2. Thus, only a few measurements (usually four of five) of R_θ, at a single low scattering angle, as a function of concentration are required. A typical plot of

LALLS data is shown in figure 3.2.

The major problems with these graphical methods are: (1) they require subjective extrapolations to zero concentration and/or zero angle which may be very difficult if there is any curvature in the plots; (2) they do not efficiently use all the data in estimating the parameters; (3) they do not properly account for all the sources of experimental error; (4) the graphs include the concentration variable on both axes, thus one is fitting an induced relationship of c against c; and, (5) they provide no estimate of the precision of the parameter estimates. While automating the graphical analysis with computers may eliminate the first problem, these techiques still suffer from the other problems mentioned. We propose eliminating these other problems with statistically sound methods of analysis.

3.2.2   Statistical Alternatives

One statistical approach that has been employed in the analysis of light scattering data has been to minimize

$$\sum_{i=1}^{n} \left[\left(\frac{K^* c_i}{R_{\theta i}}\right)_{obs} - \left(\frac{K^* c_i}{R_{\theta i}}\right)_{cal} \right]^2 \qquad (3.2)$$

with respect to the parameters in the model, where n is the number of observations. In the case of WALS data, this represents a non-linear least squares approach using $K^* c / R_\theta$ as the response variable, and has been attempted by Roberts et al (1977). In LALLS data analysis, this is simply fitting a straight line via linear least squares.

Figure 3.1 – Example Zimm Plot

$K'c/R_\theta$ vs $\sin^2(\theta/2)$ + k*c

$\sin^2(\theta/2)$ + k*c

+   Extrapolated Points   △   Data Points
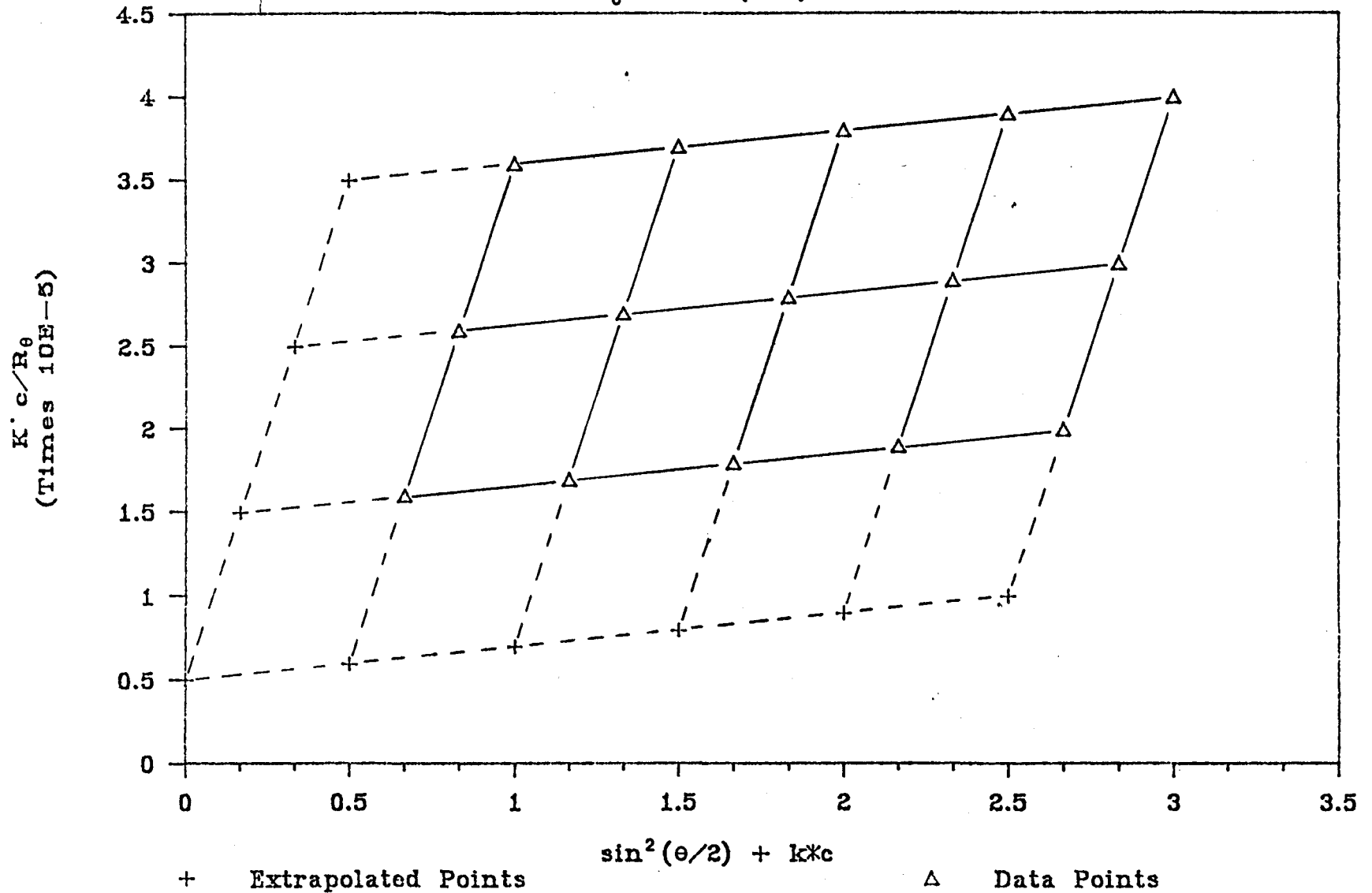
Figure 3.2 – Example LALLS Plot

$K^{\cdot} c/R_\theta$ vs Concentration

Concentration

| + Extrapolated Point | △ Data Points |
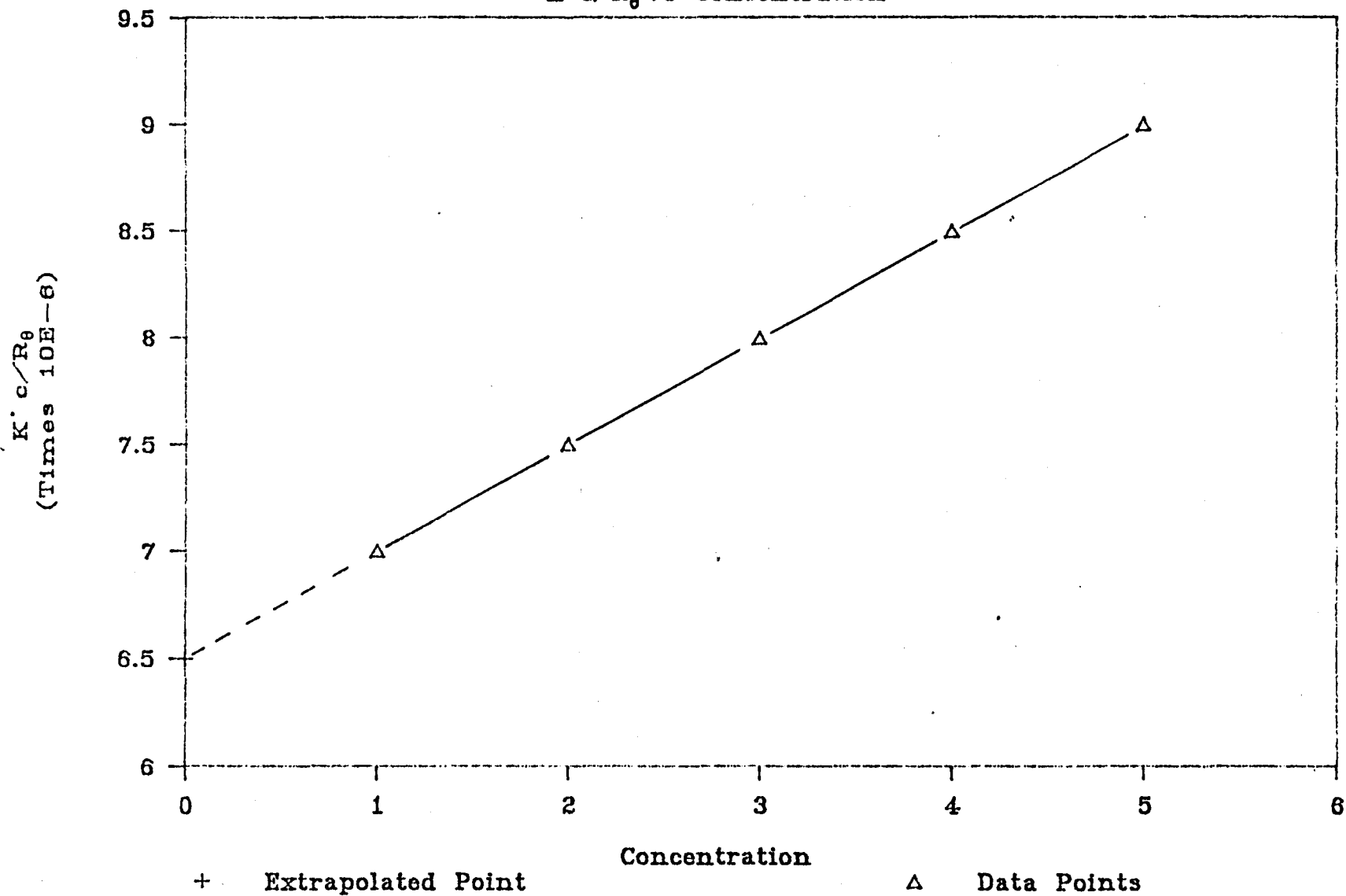
Problems arise with this approach however, since some of the assumptions, under which a least squares analysis is valid, are violated. Namely, (1) the values of the operating variables such as c and θ are assumed to be known exactly when in fact they are all measured and thus subject to error, and (2) the error variance of $K^* c/R_\theta$ is assumed to be constant over the region of operating variables thus leading to inappropriate relative weighting given to each observation.

An alternative approach to regression is to minimize

$$\sum_{i=1}^{n} [(R_{\theta_i})_{obs} - (R_{\theta_i})_{cal}]^2 \qquad \qquad (3.3)$$

where the light scattering models are re-expressed in terms of R_θ. This is preferrable over the original expression since R_θ is no longer introduced in a non-linear fashion. This is desirable since the major source of measurement error is in G_θ, the galvanometer reading at scattering angle θ. Under this fitting criterion, both WALS and LALLS data require using a non-linear least squares procedure. However, although an improvement, this approach does not entirely reconcile the two problems mentioned above.

A more approprite statistical analysis of light scattering data would be to use an error-in-variables approach for the case where the models are nonlinear in the variables, as described by Reilly and Patino-Leal (1981). Instead of expressing a relationship in terms of one unknown dependent variable equated to a function of known independent variables, we define

$$f(\underline{\xi}_i, \underline{\beta}) = 0 \qquad\qquad i=1,2,\ldots,v \qquad\qquad (3.4)$$

to be a function of v unknown independent variables $\underline{\xi}$ and p unknown parameters $\underline{\beta}$ where $\underline{\xi}$ and $\underline{\beta}$ are v x 1 and p x 1 vectors and there are n observations of $\underline{\xi}$. The $\underline{\xi}$ are the true but unknown values of the operating variables. These are measured with errors as

$$\underline{z}_i = \underline{\xi}_i + \underline{\epsilon}_i \qquad\qquad (3.5)$$

where $\underline{z}$ and $\underline{\epsilon}$ are v x 1 vectors of the experimentally measured values of the operating variables and the normally distributed random errors with mean vector zero and a known positive definite covariance matrix $\underline{V}$ respectively.

When equation (3.4) is nonlinear in the operating variables $\underline{\xi}_i$, it can be linearized by taking the linear terms of a Taylor series expansion around some value $\hat{\underline{\xi}}_i$ of $\underline{\xi}_i$

$$f(\hat{\underline{\xi}}_i, \underline{\beta}) + \underline{B}_i(\underline{\xi}_i - \hat{\underline{\xi}}_i) = \underline{0} \qquad\qquad (3.6)$$

where $\underline{B}_i$ is a 1 x v vector of partial derivatives with respect to each operating variable

$$\underline{B}_i = \left[\frac{\delta f(\underline{\xi}_i, \underline{\beta})}{\delta(\underline{\xi}_i)_j} \right]_{\underline{\xi}_i \cdot \hat{\underline{\xi}}_i} \qquad\qquad j=1,2,\ldots,v \qquad\qquad (3.7)$$

The second term in equation (3.6) can be defined as the error obtained by using $\hat{\underline{\xi}}_i$ instead of the true values $\underline{\xi}_i$. Then

$$f(\hat{\underline{\xi}}_i, \underline{\beta}) = \underline{e}_i \qquad\qquad (3.8)$$

The posterior probability density function for $\underline{\beta}$ can be shown to be (Reilly and Patino-Leal, 1981)

$$Df(\underline{\beta}/\underline{X}) \propto \exp\{-\tfrac{1}{2}\sum_{i=1}^{n} [f(\hat{\underline{\xi}}_i, \underline{\beta})]^T (\underline{B}_i \underline{V} \underline{B}_i^T)^{-1} f(\hat{\underline{\xi}}_i, \underline{\beta})\} \qquad (3.9)$$

where $\underline{X}$ is the matrix of known data.

Maximizing (3.9) requires estimating the $\hat{\xi}_i$ and β vectors through an interative procedure in the exact error-in-variables methods. A good approximation to this method may be obtained by always linearizing at the measured values of the operating variables z_i, and estimating only the unknown parameters β. This is known as the approximate error-in-variables method or the method of error propagation. Setting $\hat{\xi}_i = z_i$, the posterior probability density function is then

$$Df(\beta/\underline{X}) \propto \exp\{-\tfrac{1}{2}\sum_i [f(z_i, \beta)]^T (B_i \underline{VB}_i^T)^{-1} f(z_i, \beta)\} \qquad (3.10)$$

and the partial derivatives in $\underline{B}_i$ are now evaluated at $\xi_i = z_i$. Equation (3.8) is now

$$f(z_i, \beta) = \underline{e}_i \qquad (3.11)$$

If the covariance matrix $\underline{V}$ is diagonal, each element being the variance associated with each operating variable, then maximizing the probability density function in (3.10) is equivalent to minimizing

$$\sum_{i=1}^{n} \frac{e_i^2}{var(e_i)} \qquad (3.12)$$

with respect to the unknown parameters β, where $var(e_i)$ is estimated at each stage in the iteration from the error propagation expansion

$$var(e_i) = \sum_{j=1}^{v} \left[\frac{f(\xi_i, \beta)}{(\xi_i)_j} \right]^2_{\xi_i=z_i} var(\xi_i)_j \equiv B \underline{V}B^T \qquad (3.13)$$

This is merely minimizing a weighted sum of squares of the e_i's where the weights are the inverse of the variance in the e_i's. Reilly and Patino—Leal (1981) discuss applications of both the exact and approximate methods and compare the results. They conclude that an exact solution offers only a marginal improvement over the

approximate solution. Sutton and MacGregor (1977) applied the error propagation approach successfully to the analysis of vapour-liquid equilibrium data.

3.2.3 Application of Statistical Methods to WALS and LALLS Data Analysis

An estimation program employing a Marquardt compromise procedure called UWHAUSDD was used for all of the data analysis runs. This program allows for a user-supplied MODEL subroutine where the form of the objective function to be minimized is defined. Copies of UWHAUSDD and the WALS and LALLS analysis programs used are given in appendices 2-A, 2-B and 2-C.

It is straight-forward to apply all of the statistical methods discussed in the previous section. In the case of the arbitrary least squares criterion in (3.2), one minimizes

$$\sum_{i=1}^{n} \left[\left(\frac{K^* c_i}{R_{\theta_i}} \right)_{obs} - \frac{1}{\overline{M}_w} \left\{ 1 + \frac{16\pi^2 \langle s^2 \rangle_z \sin^2(\theta_i/2)}{3\lambda^2} \right\} - 2A_2 c_i - 3A_3 c_i^2 \right]^2 \quad (3.14)$$

with respect to the parameters $\overline{M}_w$, $\langle s^2 \rangle_z$, A_2, and A_3 for WALS data, and

$$\sum_{i=1}^{n} \left[\left(\frac{K^* c_i}{R_{\theta_i}} \right)_{obs} - \frac{1}{\overline{M}_w} - 2A_2 c_i \right]^2 \quad (3.15)$$

with respect to $\overline{M}_w$ and A_2 for LALLS data. In the case of the somewhat more acceptable least squares criterion in (3.3), we minimize

$$\sum_{i=1}^{n} \left[(R_{\theta_i})_{obs} - \frac{K^* c_i}{\frac{1}{\overline{M}_w} \left\{ 1 + \frac{16\pi^2 \langle s^2 \rangle_z \sin^2(\theta_i/2)}{3\lambda^2} \right\} - 2A_2 c_i - 3A_3 c_i^2} \right]^2 \quad (3.16)$$

for WALS data, and

$$\sum_{i=1}^{n} \left[(R_{\theta_i})_{obs} - \frac{K' c_i}{1/\bar{M}_w + 2A_2 c_i} \right]^2 \qquad (3.17)$$

for LALLS data.

The objective functions for error-propagation analysis are more complicated but still easy to program. For WALS data, we minimize (3.12) where e_i and var(e_i) are given by

$$e_i = f(R_{\theta_i}, c_i, \theta; \bar{M}_w, \langle s^2 \rangle_z, A_2, A_3) \qquad (3.18)$$

and

$$\text{var}(e_i) = \left(\frac{\partial f}{\partial R_{\theta_i}} \right)^2 \text{var}(R_{\theta_i}) + \left(\frac{\partial f}{\partial c_i} \right)^2 \text{var}(c_i) + \left(\frac{\partial f}{\partial \theta_i} \right)^2 \text{var}(\theta_i) \qquad (3.19)$$

Two different applications of the method of error propagation may be defined where f is given by the expressions within the square brackets in (3.14) and (3.16).

The experimental R_{θ_i} is given by equation 2.80

$$R_{\theta_i} = \frac{R_b}{G_b} \frac{\sin \theta_i}{1 + \cos^2 \theta_i} [G_{\theta_i}(\text{sol'n}) - G_{\theta_i}(\text{solv.})] \qquad (3.20)$$

where the primary source of error is in the measurement of $G_{\theta_i}(\text{sol'n})$.

Defining H_{θ_i} to be

$$H_{\theta_i} = G_{\theta_i}(\text{sol'n}) - G_{\theta_i}(\text{solv.}) \qquad (3.21)$$

the above expression for var(e_i) then becomes

$$\text{var}(e_i) = \left(\frac{\partial f}{\partial H_{\theta_i}} \right)^2 \text{var}(H_{\theta_i}) + \left(\frac{\partial f}{\partial c_i} \right)^2 \text{var}(c_i) + \left(\frac{\partial f}{\partial \theta_i} \right)^2 \text{var}(\theta_i) \qquad (3.22)$$

For LALLS data, we again minimize equation (3.12), except that e_i and var(e_i) are given by

$$e_i = f(R_{\theta_i}, c_i; \bar{M}_w, A_2) \qquad (3.23)$$

and

$$\text{var}(e_i) = \left(\frac{\partial f}{\partial R_{\theta_i}}\right)^2 \text{var}(R_{\theta_i}) + \left(\frac{\partial f}{\partial c_i}\right)^2 \text{var}(c_i) \tag{3.24}$$

Again, two different applications may be defined where f is given by the expressions within the square brackets in (3.15) and (3.17).

Recall that the experimentally determined R_{θ_i} is given by equation (2.88) and (2.89)

$$R_{\theta_i} = \frac{G_{\theta_i} - bl}{G_{0_i} - bl} (\sigma' \lambda')^{-1} D - R_{\theta}(\text{solv.}) \tag{3.25}$$

and both G_{θ_i} and G_{0_i} contain measurement error. So, (3.24) then becomes

$$\text{var}(e_i) = \left(\frac{\partial f}{\partial G_{\theta_i}}\right)^2 \text{var}(G_{\theta_i}) + \left(\frac{\partial f}{\partial G_{0_i}}\right)^2 \text{var}(G_{0_i}) + \left(\frac{\partial f}{\partial c_i}\right)^2 \text{var}(c_i) \tag{3.26}$$

Evaluations of the partial differentials in equations (3.22) and (3.26) for the two types of error propagation applications may be found in appendix 3.

3.3 Dynamic Light Scattering

For the case of monodisperse distributions, it is a simple matter to estimate both β and Γ in equation (2.97) with a non-linear least squares algorithm. First, compute $g^{(1)}(\tau)$ by dividing the measured $G^{(2)}(\tau)$ by the baseline, subtracting one and taking the square root,

$$g^{(1)}(\tau) = \left[\frac{G^{(2)}(\tau)}{A} - 1.0\right]^{1/2} \tag{3.27}$$

Using the straightforward least squares objective function of minimizing

$$\sum_{i=1}^{n} [g_i^{(1)}(\tau) - \beta \exp(-\Gamma t_i)]^2 \tag{3.28}$$

with respect to the parameters β and Γ would appear to be reasonable since the experimental error resides in the single measured quantity $g^{(1)}(\tau)$. Here, n is the number of discrete observations we have of the second-order, un-normalized autocorrelation function.

In the case of bimodal distributions comprised of two monodisperse samples, it is possible to obtain estimates of both particle sizes and their relative weight fractions by minimizing

$$\sum_{i=1}^{n} [g_i^{(1)}(\tau) - \{ \beta_1 \exp(-\Gamma_1 t_i) + \beta_2 \exp(-\Gamma_2 t_i) \}]^2 \tag{3.29}$$

with respect to the four parameters β_1, β_2, Γ_1, and Γ_2.

Extending (3.28) to estimate the β and Γ parameters for trimodal and higher multimodal distribution is not feasible because of the highly ill-conditioned nature of the problem which limits the number of parameters that can be estimated. However, if prior information concerning the size of particles in a multimodal distribution comprising monodisperse samples is available, the values of Γ that correspond to the known values of the particle diameters can be calculated and only the β's estimated. Then, the objective function to minimize with respect to the parameters β_j

$$\sum_{i=1}^{n} [g_i^{(1)}(\tau) - \sum_{j=1}^{p} \beta_j \exp(-\Gamma_j t_i)]^2 \tag{3.30}$$

which is linear in the parameters. The estimates of β_j would then be the relative weights of each particle size corresponding to the known particle diameters. Again, the ill-conditioned nature of the problem and high correlations between parameter estimates generally limits the

number of parameters, p, that can be estimated to five or six in an unconstrained minimization.

For the case of polydisperse distributions, the determination of the particle size distribution (PSD) is much more difficult as it centres on the inversion of the LaPlace integral in equation (2.98). It is this problem that has been the central subject in many papers in the literature and has brought forth many novel analysis techniques in recent years that are applicable not only to dynamic light scattering, but to other estimation problems. A good discussion and comparison of all of these techniques was carried out by Stock and Ray (1985).

This chapter is primarily concerned with the statistical problems encountered when trying to reconstruct the particle size distribution by a method known as exponential sampling applied to raw autocorrelation data obtained from analytical instruments. This method is an extension of model (3.30) to polydisperse instead of multimodal distributions.

Since the raw autocorrelation data resembles an exponential decay, the method of exponential sampling approximates the continuous integral sum of exponentials in equation (2.98) by a discrete sum of exponentials at assumed values of the exponent. Thus, the objective is to fit a sum of exponentials, linear in the parameters, to $g^{(1)}(\tau)$, the first-order, normalized autocorrelation function. We now minimize

$$\sum_{i=1}^{n} [g_i^{(1)}(\tau) - \sum_{j=1}^{m} \beta_j \exp(-\Gamma_j t_i)]^2 \qquad (3.31)$$

at assumed values of the particle diameter. The exponents Γ_j are

easily calculated directly from equations (2.91), (2.92) and (2.93). The estimates of the parameters β_j are then estimates of $f(r_j)$, the contribution to the measured autocorrelation function of the scattered light intensity by particles of size r_j in the distribution of particle sizes.

A paper by Ostrowsky et al (1981) which first introduced this method describes the application of this technique to dynamic light scattering data. He suggests that the sampling be made at equal intervals on a natural logarithmic scale of particle sizes. This enables the sampling to cover a wide range of practical particle sizes. The spacing on the scale between adjacent samplings is given by

$$\ln(r_{k+1}) = \frac{\omega_{max}}{\eta} \ln(r_k) \qquad\qquad k=1,2,\ldots,M \qquad (3.32)$$

where the variable ω_{max} defines the distance between adjacent samples on the logarithmic scale. Ostrowsky recommends that the value of M be no larger than five or six. This limits to five or six the number of exponentials that are fit to $g^{(1)}(\tau)$ in equation (3.31). Because of the ill-conditioned nature of fitting a sum of exponentials, Ostrowsky states that large negative estimates of β may be obtained when attempting to fit $g^{(1)}(\tau)$ to a larger number of exponentials functions. Ostrowsky also determined that because of experimental error, ω_{max} may practically take on values no lower than 3.0 or greater than approximately 10.0. This ensures that the resolution on the scale is reasonable, depending on the sample, and avoids undue negative

parameter estimates.

Since the resolution of a PSD reconstructed from only five or six samplings over a range of perhaps one or two thousand nanometers is extremely poor, Ostrowsky further recommended that the objective function in (3.31) be minimized five or six times over M parameters in a series of shifts. Thus, one may increase the resolution of the fit to up to 36 parameter estimates by combining all the estimates from each fit together. The length of the shift along the logarithmic scale for each of the M samplings is given by

$$\ln(\Gamma_{k,l+1}) = \ln(\Gamma_{k,l}) + \frac{\omega_{max}/\pi}{N_s} \qquad \begin{array}{l} k=1,2,\ldots,M \\ l=1,2,\ldots,N \end{array} \qquad (3.33)$$

where N_s is the number of shifts. The shifting procedure along the scale of particle sizes is illustrated graphically in figure 3.3.

The attractive feature of the exponential sampling method is that a linear least squares estimation algorithm may be used. It is apparent that it would be unreasonable to use a non-linear least squares procedure to obtain estimates of both the β_j and the Γ_j (as in the monodisperse and bimodal cases) in a sum of exponentials model because of the extremely ill-conditioned nature of this problem. Again, UWHAUSDD was used to estimate the parameters in this linear model since UWHAUSDD allows for models that are linear in the parameters, not just non-linear models.

$$\frac{\omega_{max}}{n}$$

$$\frac{\omega_{max}/n}{N_s}$$

0 1 2   0 1 2   0 1 2

log scale
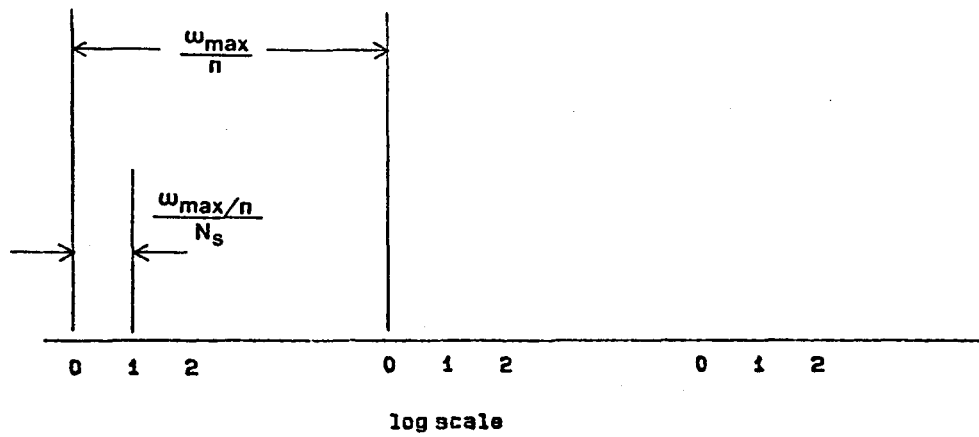
0 – initial Γ values
1 – Γ values after one shift
2 – Γ values after two shifts, etc...

Figure 3.3 –Shifting procedure used in DLS analysis programs

A more recent paper by Morrison (1985) suggested that the resolution of the fitted PSD may be greatly increased by constraining the parameter estimates to be non-negative. In this case, we minimize

$$\sum_{i=1}^{n}[g_i^{(1)}(\tau) - \sum_{j=1}^{m}\beta_j\exp(-\Gamma_j t_i)]^2 \quad \text{subject to} \quad \beta_j \geqslant 0 \quad (3.34)$$

Morrison claims that by including the non-negativety constraint, M may take on values of up to 20. Thus, by employing a non-negatively constrained linear least squares algorithm and applying the shifting procedure describe earlier, a very fine resolution of the logarithmic scale at which parameter estimates are obtained is possible with up to 120 estimates being used to reconstruct the particle size distribution. A constrained linear least squares algorithm developed by Lawson and Hanson (1974) which employs a QR decomposition technique was used to estimate the parameters in (3.34).

Morrison also noted that when $g_i^{(1)}(\tau)$ is known only at n data points (as in our case), the variance depends upon the measured light intensities. He suggested that minimizing the weighted sum of squares

$$\sum_{i=1}^{n}g_i^{(1)}(\tau)^2[g_i^{(1)}(\tau) - \sum_{j=1}^{m}\beta_j\exp(-\Gamma_j t_i)]^2 \quad \text{subject to} \quad \beta_j \geqslant 0 \quad (3.35)$$

Thus, smaller errors in the measurement of high light intensities at low lag times are assumed and more significance is attributed to these measurements.

<u>EXPERIMENTAL</u>

4.1   Introduction

This chapter outlines the experimental data that was used, how it was obtained, how it was used in the parameter estimation programs and the programs themselves.

4.2   Classical Light Scattering

4.2.1   Experimental Data

4.2.1.1 WALS

The experimental data used for WALS data analysis was obtained from a round-robin experiment conducted by RAPRA. Roberts et al (1977) used this data as one of the samples studied in their paper on the analysis of light scattering data. Table 4.1 displays a typical set of raw data obtained from a WALS instrument. The data shown in table 4.1 was collected from a RAPRA standard polystyrene sample with nominal weight-average molecular weight of 340,000 determined from extensive GPC analysis. The polymer was dissolved in a benzene solvent and subjected to vertically polarized blue light. The instrument used was a SOFICA photometer using a mercury lamp as the source of light. Since vertically polarized light was used, $(1 + \cos^2 \theta) = 1.0$ in equation (2.80). The instrument was also calibrated so that $G_b = 1.0$. Therefore, from equations (3.20) and (3.21), we have

$$R_\theta = R_b \sin\theta \, H_\theta \qquad (4.1)$$

The data shown in table 4.2 is specific to this polymer—solvent system and experimental arrangement just described. The raw data in table 4.1 and the system specific data in table 4.2 is all that is necessary to determine the measured value of R_θ in equation (2.80) and K' in equation (2.27). Thus, an experimentally determined value of $K^* c/R_\theta$ may be calculated. The feasibilty of performing a WALS data analysis on a specific polymer—solvent system is dependent upon the availability of the necessary data shown in table 4.2.

To apply the method of error propagation, estimates of the error variance in all of the measured variables are required. In a WALS experiment, these are H_θ, the difference between the measured galvanometer readings for the polymer solution and solvent; c, the polymer concentration in solution; and θ, the scattering angle at which measurement takes place. It is truly the variation in G_θ(sol'n) that we are interested in, but since G_θ(solv.) is a constant at each scattering angle, then the variation in G_θ(sol'n) is equivalent to the variation in H_θ as a function of scattering angle, but is not equivalent as a function of concentration.

Included with the data received from Roberts were two sets of eight replicate experiments on a polystyrene sample in toluene solvent subjected to blue and green incident light respectively. Each set was similar to the data given in table 4.1 in that galvanometer measurements were recorded from a grid of eleven scattering angles and five concentrations. There was one exception where a set contained

TABLE 4.1

Galvanometer Readings – G_θ(sol'n), G_θ(solv.)

Scattering Angle (degrees)	Polymer Concentration (g/ml)					
	0.01943	0.01295	0.00648	0.00486	0.00259	0.0
20	18.4	19.0	19.4	18.0	15.0	4.00
30	12.2	12.6	12.4	11.8	9.25	2.35
37.5	9.63	10.2	10.0	9.30	7.40	1.81
45	8.21	8.51	8.35	7.90	6.30	1.52
60	6.55	6.85	6.62	6.30	4.86	1.21
75	5.79	6.00	5.78	5.44	4.20	1.07
90	5.50	5.70	5.42	5.10	3.83	1.00
105	5.59	5.78	5.45	5.11	3.86	1.03
120	6.15	6.30	5.92	5.56	4.15	1.12
135	7.35	7.52	7.03	6.54	4.90	1.36
142.5	8.49	8.60	7.99	7.46	5.61	1.54
150	9.99	10.4	9.50	8.81	6.89	1.86

TABLE 4.2

Constants for Polystyrene/Benzene System

Symbol	Comments	Value
λ_o	wavelength of the incident light (polarized blue light)	4.358×10^{-5} cm
n_o	solvent refractive index	1.5196
$d\eta/dc$	refractive index increment	0.1110 cm^3/g
R_b	Rayleigh ratio for benzene at 90°	6.24×10^{-5} cm^{-1}
S_b	relative scattered intensity for benzene at 90°	1.0
$K^{\cdot}$	an optical constant given by $\dfrac{4 n^2 \eta_o^2}{\lambda_o^4 N_{AV}}\left(\dfrac{d\eta}{dc}\right)^2$	5.17×10^{-7}

measurements at only four concentrations. Thus it was possible to calculate an estimate of the variance in the galvanometer readings at each grid point; see table 4.3. Each variance has seven degrees of freedom. By pooling the estimated variances along the rows and columns in table 4.3 estimtes of the error variance as a function of scattering angle and concentration may be obtained. The error estimates as a function of angle each have 35 degrees of freedom, while those as a function of concentration each have 77 degrees of freedom. The overall variance estimate of 41.8 has 385 degrees of freedom. The analysis of this set of replicate experiments had been carried out by Howley (1981). Plots of the estimated variance of G_θ(sol'n) as a function of θ and c, and 95% confidence intervals are given in figures 4.1 and 4.2. It is apparent from these figures that the estimated variance in G_θ(sol'n) has a quadratic dependency on θ and is independent of c. Thus, the error in the galvanometer readings increases quadratically as the angle of observation moves away from 90 degrees. Therefore, appropriate weighting must be accounted for when calculating the contribution to the total error variance in equation (3.19) by the galvanometer measurements.

A quadratic function could be fit to the data points plotted in figure 4.1 and used in the error propagation model equations to calculate the variance to be used for weighting the galvanometer data. However, galvanometer readings are recorded at arbitrary magnitudes (within a grid of experiments) depending upon the scaling employed by the experimenter. For example, the data used in the analysis of

TABLE 4.3

Estimated Variance in G_θ (sol'n) from a set of Eight Replicate Experiments

Scattering Angle (degrees)	Polymer Concentration (g/ml)					Pooled Variance by Row
	0.0101	0.0067	0.0050	0.0034	0.0025	
30	145.7	70.6	140.6	85.6	126.9	113.9
37.5	87.9	52.5	101.4	53.7	63.4	71.9
45	58.1	33.7	53.1	31.4	43.7	44.2
60	21.1	22.7	33.1	13.9	19.6	22.1
75	9.4	11.4	15.6	8.6	11.8	11.3
90	7.1	7.1	9.6	6.6	6.0	7.3
105	12.1	10.9	16.0	7.6	5.7	10.5
120	23.6	14.4	32.3	18.5	12.6	20.3
135	49.0	28.5	72.3	27.8	19.4	39.5
142.5	79.7	34.2	82.1	28.4	23.9	49.7
150	134.2	48.0	67.9	51.4	47.7	69.8
Pooled Variance by Column	57.2	30.4	56.7	30.3	34.6	41.8

Figure 4.1 — WALS

Estimated var(G_θ) vs Scattering Angle

Estimated var(G_θ)

Scattering Angle (degrees)

□   Estimated Variance   +   95% Conf. Limit

57
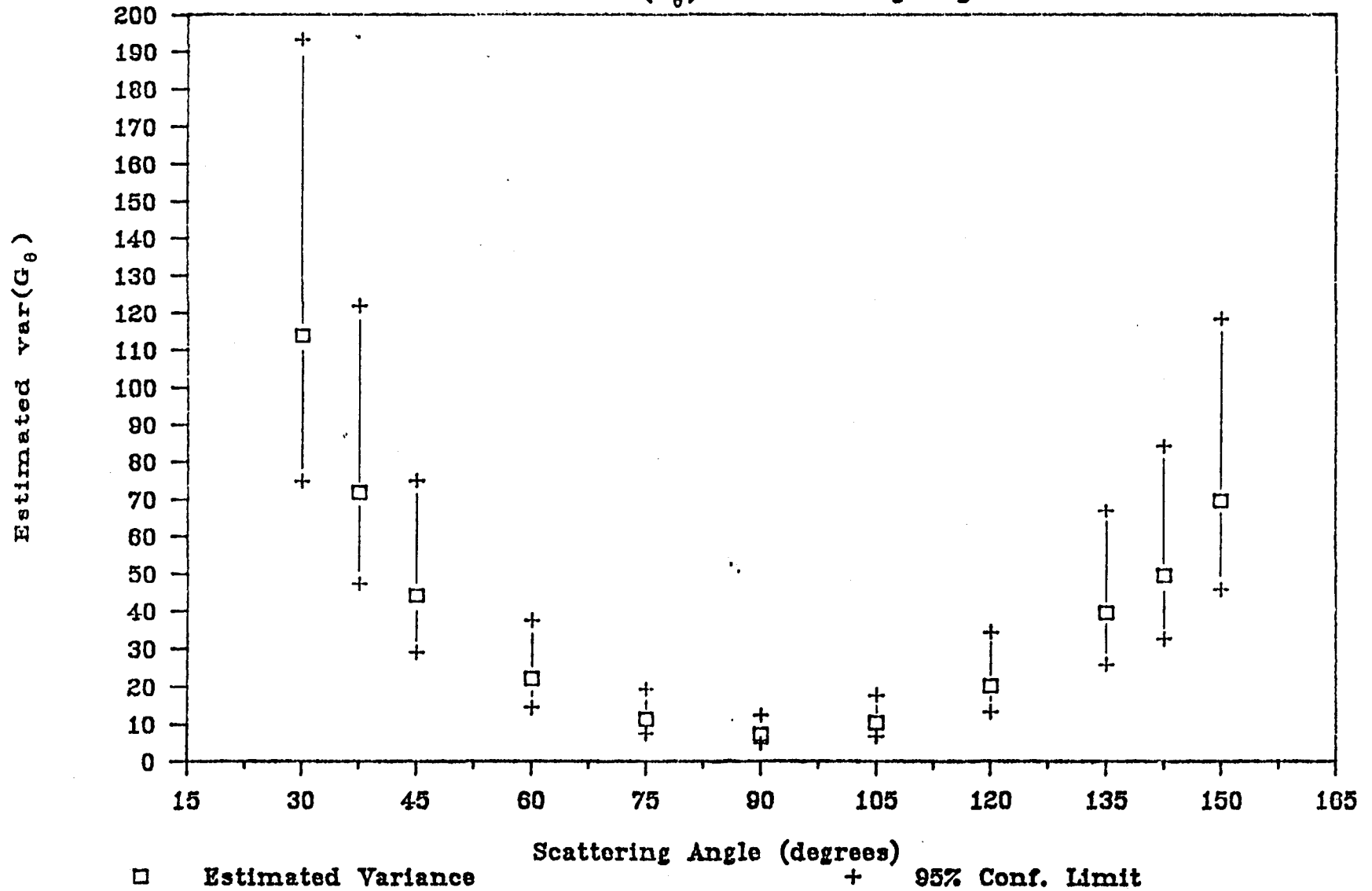
Figure 4.2 – WALS
Estimated var(G_θ) vs Polymer Conc.
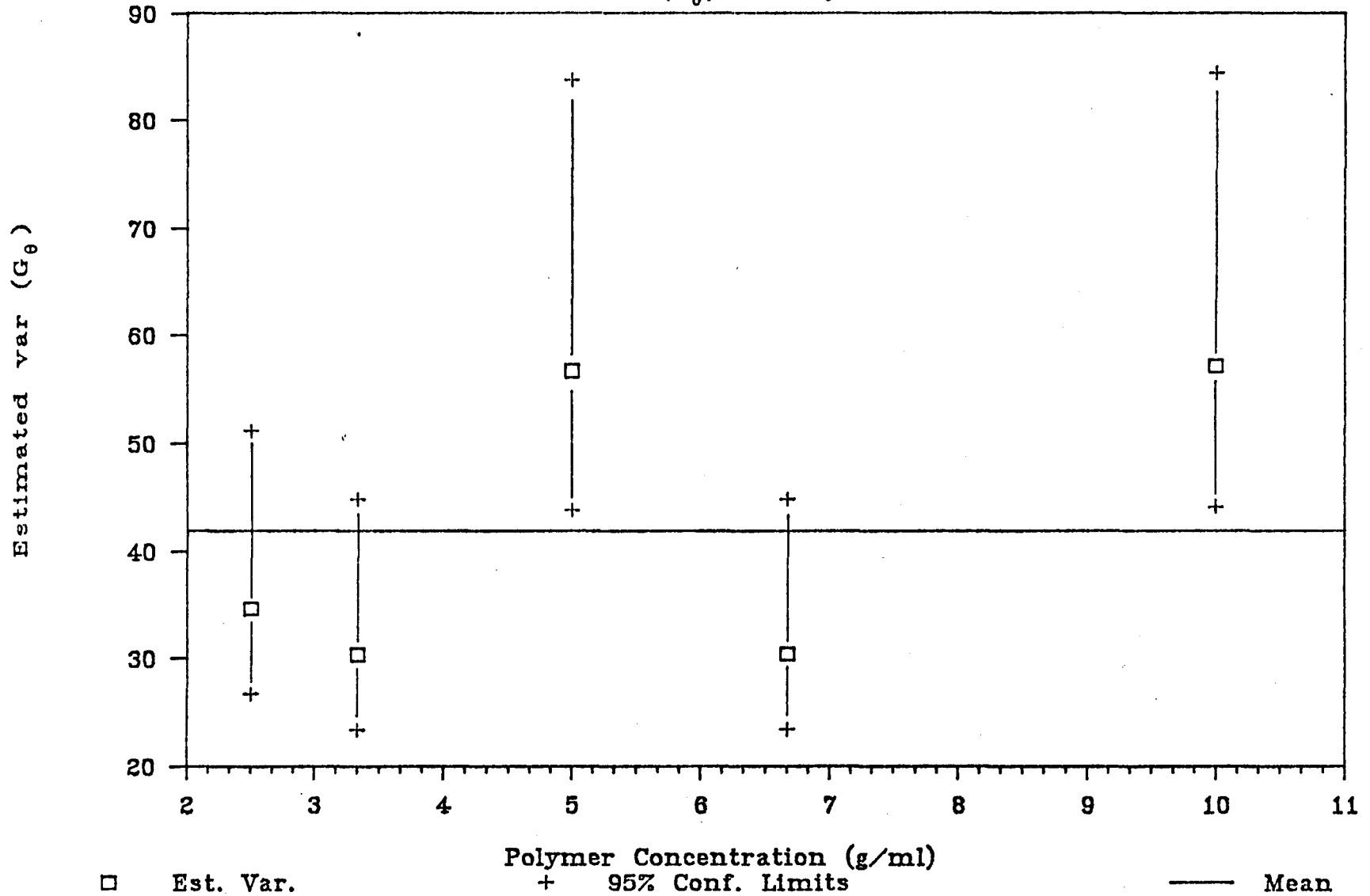
variance was one order of magnitude higher than the that given in table 4.1. Thus, any function fit to the data in figure 4.1 would be dependent upon the experimenter's arbitrary choice of scale. The magnitude of the estimated variances of the data in table 4.1 would therefore be too high if a fitted quadratic function was used.

Since only the relative weighting of galvanometer readings and the scattering angle are of interest, the data was transformed by taking the natural logarithm of each point and repeating the analysis of variance; see table 4.4. Use can be made of the approximate relationship

$$\text{var}(H_\theta) = \text{var}\{G_\theta(\text{sol'n})\} \doteq (\overline{G_\theta})^2_\theta \text{var}[\ln\{G_\theta(\text{sol'n})\}] \qquad (4.2)$$

where $(\overline{G_\theta})^2_\theta$ is the average measured galvanometer reading for the polymer solution at scattering angle θ. By using equation 4.2, appropriate estimates of $\text{var}(H_\theta)$ may be obtained independent of the scale used during data collection. The estimates of the variance in the logarithm of $G_\theta(\text{sol'n})$ and their 95% confidence intervals are plotted against scattering angle in figure 4.3. From this figure it can be seen that $\text{var}[\ln\{G_\theta(\text{sol'n})\}]$ is independent on scattering angle. The average value of $\text{var}[\ln\{G_\theta(\text{sol'n})\}]$ is 0.00586. Therefore, appropriate estimates of $\text{var}(H_\theta)$ may be calculated from

$$\text{var}(H_\theta) = 0.00586(\overline{G_\theta})^2_\theta \qquad (4.3)$$

Figure 4.4 shows that the calculated estimates of $\text{var}(H_\theta)$ agree reasonably well with the data in figure 4.1.

TABLE 4.4

Estimated Variance in ln $[G_\theta(\text{sol'n})]$ from a set of Eight Replicate Experiments
$(x\ 10^3)$

Scattering Angle (degrees)	Polymer Concentration (g/ml)					Pooled Variance by Row
	0.0101	0.0067	0.0050	0.0034	0.0025	
30	5.038	2.639	6.021	4.798	10.194	5.738
37.5	5.371	3.580	8.200	5.315	8.859	6.265
45	5.884	3.736	7.029	5.056	10.269	6.395
60	4.752	5.532	9.632	4.845	10.351	7.022
75	3.505	4.584	7.651	5.039	10.693	6.294
90	2.760	4.023	5.487	5.001	6.286	4.713
105	4.122	4.611	8.259	5.284	5.329	5.521
120	5.044	3.924	10.326	7.738	7.436	6.894
135	5.181	3.656	11.344	5.766	6.276	6.443
142.5	5.562	2.755	8.237	3.779	4.843	5.035
150	5.528	2.240	3.722	3.864	5.544	4.180
Pooled Variance by Column	4.759	3.753	7.809	5.136	7.825	5.864

Figure 4.3 – WALS

Est. var[ln(G_θ)] vs Scattering Angle

Estimated var[ln(G_θ)]

Scattering Angle (degrees)

□   Est. Var.   +   95% Conf. Limits   —— Mean
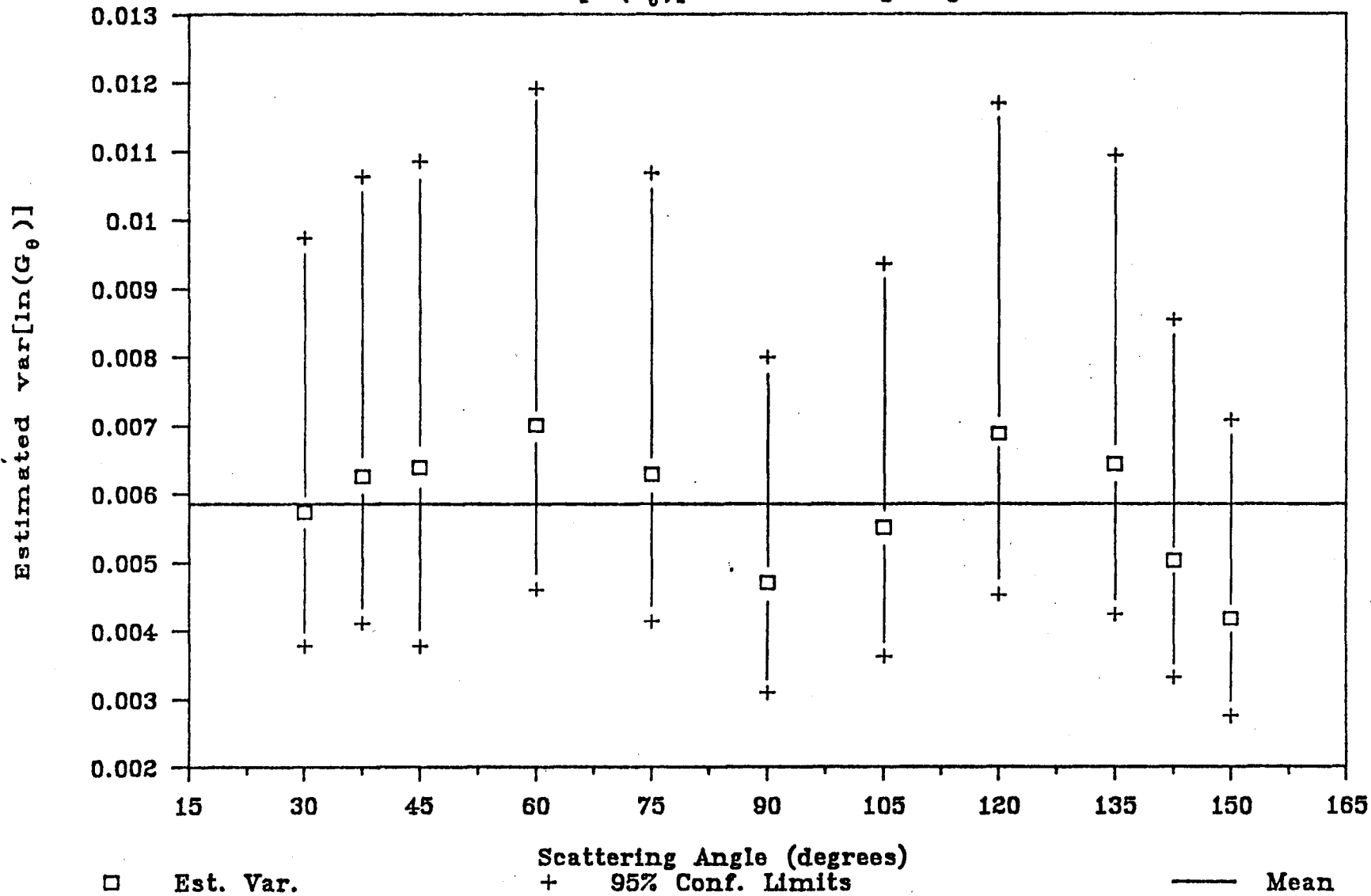
Figure 4.4 – WALS
Prod & Est var(G_θ) vs Scattering Angle

Estimated and Predicted var(G_θ)

Scattering Angle (degrees)

$\square$ $0.00586 \times \overline{(G_\theta)}_\theta^2$ $\triangle$ Estimated var(G_θ)
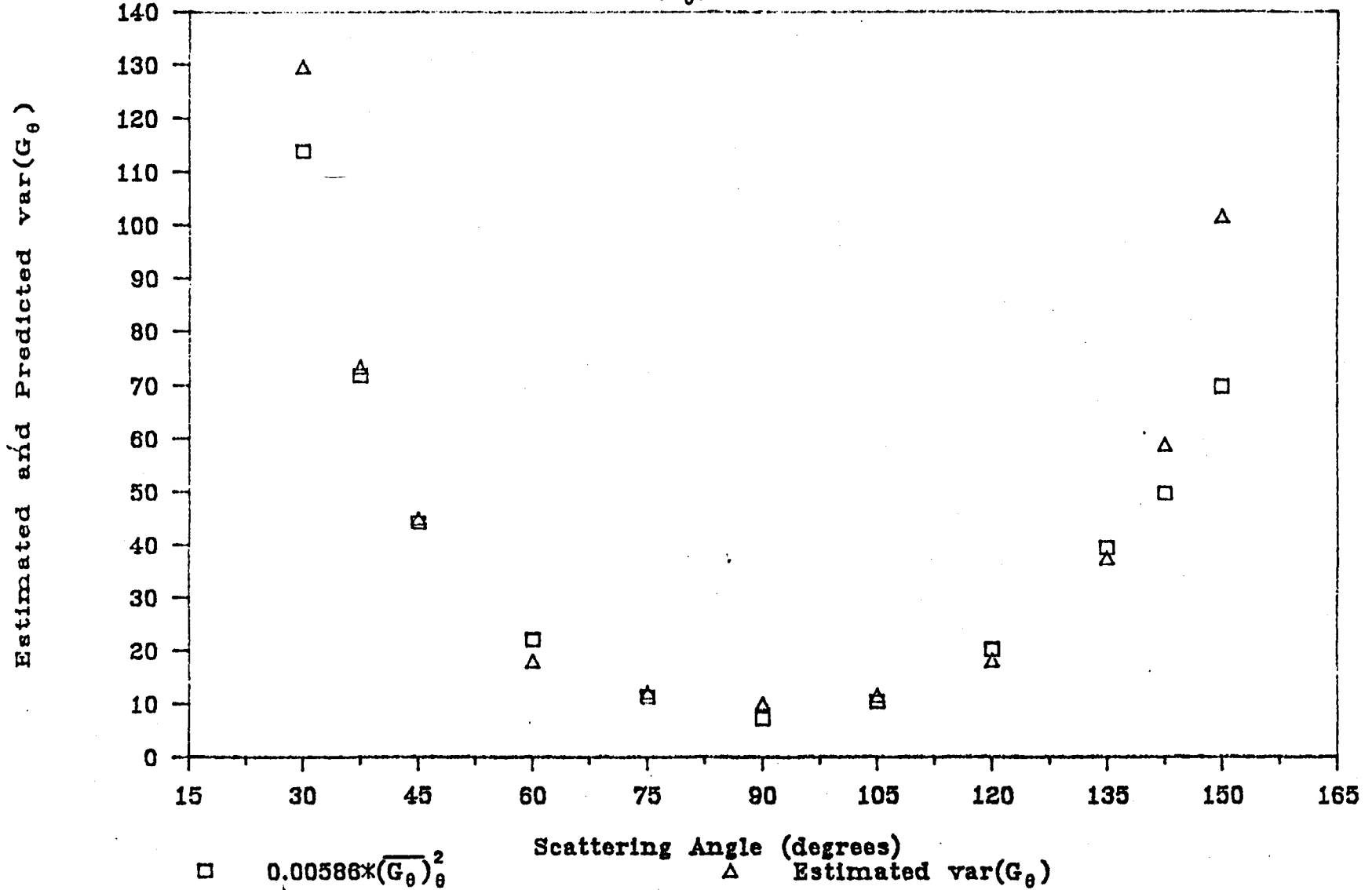
Estimates of the error variance in measuring the polymer concentration are dependent upon the way in which the solutions were prepared. The usual method is to dissolve a known amount of dry polymer in the solvent and prepare the samples through successive dilutions of the original sample. Thus, the error present in the concentration of the samples is dependent upon the errors in weighing out the dry polymer and the dilution volumes. The errors that may have occurred in preparing the samples that were studied are not known. However, Rubio (1984) has shown by the method of error propagation that the error associated with the dilution process decreases with increasing dilution. Therefore, the initial sample with the highest polymer concentration has the largest error variance in the concentration. To study the importance of the contributions of the concentration variance to the total error variance in equation (3.19), the standard deviation in the concentration measurement was arbitrarily set to three different values: 0.05%, 0.5% and 5.0% of the measured concentration.

Finally, an estimate of the error in measuring the scattering angle is required to complete equation (3.19). The scattering angle at which measurement takes place can be set manually or to pre-determined values automatically set by the manufacturer. Again, the means of angle setting was unknown for the experimental data used. Assuming that the scale of angle settings was graduated by degrees of one, a value of 0.5 degrees was used as an estimated of the standard deviation in the angle setting.

4.2.1.2 <u>LALLS</u>

The experimental data used for LALLS was obtained from two graduate students in the department of chemical engineering at McMaster University. In the course of their graduate work, Alexander Penlidis and Victor Stanislawczyk collected data from the departments Chromatix KMX-6 LALLS instrument for a number of polyvinylacetate and polyacrylamide polymer samples in ethylacetate and water solvents respectively. This instrument uses a He-Ne laser light. A typical set of data is given in table 4.5. All of the data sets chosen to be analyzed contained five measurements and had baseline measurements of zero, simplifying equation (3.25). The system specific data required to calculate K^* and R_θ for the two polymer systems is given in table 4.6.

The recorded values of G_θ and G_0 were taken from a chart recording, an example of which appears in figure 4.5. The scale of the chart paper is 1000 units. The attenuators on the instrument are manipulated in such a way as to obtain measurements of G_θ between 900 and 1000, and measurements of G_0 greater than 250 but less than G_θ. The G_θ and G_0 are then corrected for the different attenuators used the attenuating function in equation (2.89). For the KMX-6, D is given by

$$D = \prod_{i=1}^{4} (att)_i \qquad \text{where} \quad \begin{aligned} (att)_1 &= 0.248 \\ (att)_2 &= 6.448 \times 10^{-2} \\ (att)_3 &= 4.077 \times 10^{-3} \\ (att)_4 &= 1.6367 \times 10^{-5} \end{aligned} \qquad (4.4)$$

If an attenuator is not in for a given measurement, then $(att)_i = 1.0$

TABLE 4.5

Galvanometer Readings – G_o . G_θ

Polymer Concentration (g/ml x 10^4)	G_o	G_θ
3.589	492	895
7.691	317	880
10.254	275	890
14.356	230	900
17.945	220	890

TABLE 4.6

Constants for: (1) Polyvinalyacetate/Ethylacetate System and
(2) Polyacrylamide/Water System

Symbol	Comments	System 1	System 2	Units
λ_o	wavelength of the incident light	6.33×10^{-5}	6.33×10^{-5}	c m
n_o	solvent refractive index	1.3724	1.33	—
dn/dc	refractive index increment	0.111	0.185	cm^3/g
θ	scattering angle	4.73^o	4.73^o	degrees
$R_{\theta,solv}$	Rayleigh ratio for solvent	4.594×10^{-6}	—	—
$(\sigma'\lambda')^{-1}$	an optical function of solid angle, field stop and refractive index	652.95	477.42	—
K^*	an optical constant given by $\dfrac{4n^2 n_o^2}{\lambda_o^4 N_{AV}}\left(\dfrac{dn}{dc}\right)^2$	4.556×10^{-8}	1.185×10^{-7}	—

and attenuator 4 is always in.

Figure 4.5 shows that the measurement of G_θ is very noisy while it is very stable for G_o. The values recorded for G_θ represent an "eye-ball" average of the measurement. The usual way of recording G_θ is to take a lower envelope value. This method assumes that all of the higher fluctuations and peaks are attributable to dust and other impurities. An alternate method chosen ignored the gross peaks in the measurements and used the average of the main body of the measurment. The effect of these different methods on the parameter estimates will be examined later.

From equation (3.26), it can be seen that estimates of the error variance of the measured galvanometer readings at scattering angle θ and at zero angle, and of the concentration of the polymer samples are required.

The polyacrylamide data used included three sets of replicate pairs of experiments. Thus, an analysis of variance was performed on the measurements of G_θ and G_o. The data used and the details of this analysis are relegated to appendix 4. The standard deviation in G_θ and G_o was estimated to be 10 - 14, and 12 - 24 respectively, depending on whether the extreme values marked by asterisks in appendix 4 are included or neglected in the analysis. The fluctuations about the mean within a measurement are not a major contributor to the error since as the length of time over which the measurment of G_θ is recorded increases, the statistical uncertainty
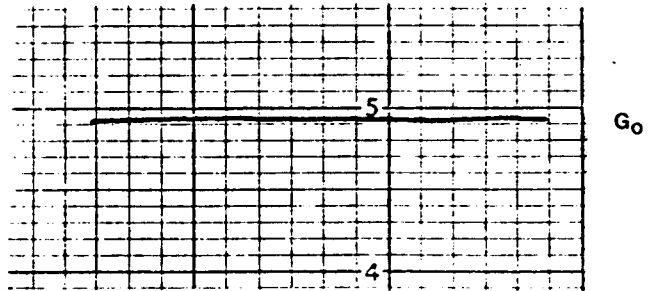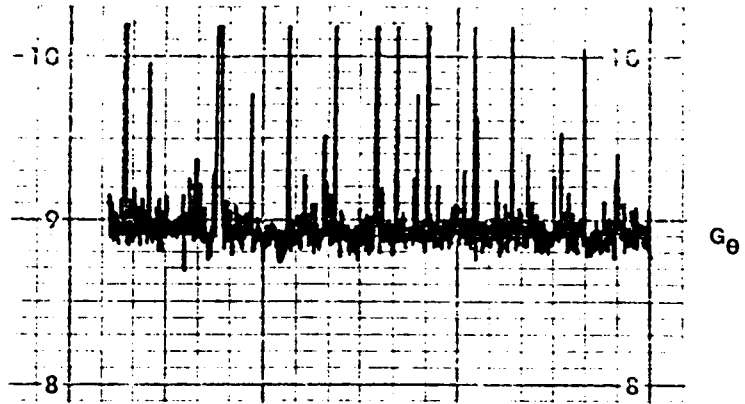
Figure 4.5 – Example of a LALLS chart recording

in the mean decreases. Thus, the deviation about the mean within an experiment is small compared to the deviation between the means of replicate experiments.

As in the case of WALS experiments, the error in the concentration of the polymer samples is dependent upon the errors in weighing the dry polymer and in the dilution volumes. However, the method of preparing samples is different from that previously described. Instead of successive dilutions, subsequent samples are prepared individually from the dilution of a fraction of the initially prepared solution. The initial sample is prepared by dissolving a known amount of dry polymer in 100 mL of solvent. Subsequent samples are prepared by diluting a portion of the initial solution according to the formula

$$c_i = \frac{c_1 v_{i1}}{v_{i1} + v_{i2}} \qquad ; \quad i=2,3,4,5 \qquad (4.5)$$

where v_{i1} and v_{i2} are the volumes of initial solution and solvent respectively that make up the i'th sample, and c_1 is the concentration of the first sample. The values of v_{i1} and v_{i2} that were used to prepare the samples studied are listed in table 4.7.

Applying the error propagation formula to equation (4.5) gives

$$\frac{var(c_i)}{c_i^2} = \frac{var(c_1)}{c_1^2} + \frac{v_{i2}^2}{v_{i1}^2 \, (v_{i1} + v_{i2})^2} var(v_{i1}) + \frac{1}{(v_{i1} + v_{i2})^2} var(v_i)$$

$$(4.6)$$

However, the error in measuring the volumes v_{i1} and v_{i2} is the same since the same type of pipette was used. Combining the last two terms and setting $var(v) = var(v_{i1}) = var(v_{i2})$, we obtain

TABLE 4.7

Dilution Volumes Used in Preparing Samples (ml)

Sample No.	PVac/EAc		Polyacrylamide/Water	
	V_{i1}	V_{i2}	V_{i1}	V_{i2}
2	20	5	15	15
3	20	15	10	10
4	15	20	5	10
5	10	40	5	25

$$\frac{\text{var}(c_i)}{c_i^2} = \frac{\text{var}(c_1)}{c_1^2} + \frac{v_{i1}^2 + v_{i2}^2}{v_{i1}^2 (v_{i1} + v_{i2})^2} \text{ var}(v) \qquad (4.7)$$

As mentioned earlier, $\text{var}(c_1)$ is dependent upon the weight of dry polymer and solvent volume

$$c_1 = \frac{w}{v_o} \qquad (4.8)$$

Applying the error propogation formula once again,

$$\frac{\text{var}(c_1)}{c_1^2} = \frac{\text{var}(w)}{w^2} + \frac{\text{var}(v)}{v_o^2} \qquad (4.9)$$

Estimates of $\text{var}(w)$ and $\text{var}(c)$ were determined to be $(5 \times 10^{-5} \text{g})^2$ and $(5 \times 10^{-2} \text{mL})^2$ respectively from the balance and pipettes used to prepare the samples. For every sample studied in both systems, v_o, the intial volume of solvent was 100 mL, however the amount of dry polymer added to make the initial solution was different; see table 4.8. Evaluation of $\text{var}(c_i)/c_i^2$ for all i showed this quantity to have little dependency on the initial concentration c_1. Therefore, the figures listed in table 4.9 represent the average value of $\text{var}(c_i)/c_i^2$ for each i for all the samples studied. So, the estimates of the error variance were calculated using

$$\text{var}(c_i) = c_i^2 \left[\frac{\overline{\text{var}(c_i)}}{c_i^2} \right] \qquad (4.10)$$

An example of the standard deviations calculated using equation (4.10) for one of the experiments is given in table 4.10. It is obvious that the error variance is not constant at different concentrations.

TABLE 4.8

Weight of Dry Polymer Added to 100 ml of Solvent to form Initial Solution

System	Sample ID	Weight of Dry Polymer (g)
PVAc/EAc	B 10 - 5	0.05960
	B 10 - 7	0.13585
	B 11 - 8	0.17945
	B 11 - 9	0.13630
Polyacrylamide/ Water	A - 9 E	0.05250
	A - 9 I	0.04870
	A - 10 C	0.05170
	A - 10 H	0.04850
	A - 11 D	0.05250
	A - 11 G	0.04770

TABLE 4.9

Average Estimates of $[var (c_i)/c_i^2]$ for PVAc/EAc and
Polyacrylamide/Water Systems

Sample No.	$\overline{[var (c_i)/c_i^2]} \times 10^7$	
	PVAc/EAc	Polyacrylamide/Water
1	4.88	12.44
2	47.38	81.89
3	36.77	137.44
4	61.57	568.00
5	174.88	734.66

TABLE 4.10

Estimated Variance in Concentration for Experiment B10-7

$$\text{var}(c_i) = c_i^2 \overline{[\text{var}(c_i)/c_i^2]}$$

Sample No.	c_i (g/ml)	var (c_i) (g/ml X 10^{13})
1	0.0013585	9.004
2	0.0010868	55.962
3	0.0007763	22.159
4	0.0005822	20.870
5	0.0002717	12.910

TABLE 4.11

Summary of Estimated Error Variances

Experiment	Variable	Estimated Error Variance	
WALS	G_θ	$0.00588\,(\overline{\overline{G_\theta}})^2_\theta$	
	c	$(0.005 \times c)^2$	$(g/ml)^2$
		$(0.05 \times c)^2$	"
		$(0.5 \times c)^2$	"
	θ	$(0.5)^2$	
LALLS	G_θ	$(10)^2 - (14)^2$	
	G_0	$(12)^2 - (24)^2$	
	c	$c_i^2\,\overline{[var\,(c_i)\,/c_i^2]}$	$(g/ml)^2$

A summary of all of the estimated error variances used in the parameter estimation programs for both WALS and LALLS data analysis appears in table 4.11.

4.2.2 Analysis Programs

For both the WALS and LALLS data, parameter estimates were obtained for four different objective functions for the purposes of comparison. These estimates were obtained from non-linear least squares and error propagation methods applied to K^*c/R_θ and R_θ. For the case of regression on K^*c/R_θ for LALLS data, ordinary linear least squares was used. A general algorithm for the WALS and LALLS parameter estimation programs is given in figure 4.6. The objective functions that were minimized for each of the four cases were presented in chapter 3. The main program prompts the user to 'ENTER ITYPE - 1,2,3,4' where the value of ITYPE determines the objective function according to table 4.12. Copies of these programs may be found in appendices 2-B and 2-C.

The estimation subroutine UWHAUSDD was used to estimate the model parameters (see appendix 2-A). This routine employs a Marquardt Compromise procedure which is basically an algorithm that compromises between the steepest descent method (for linear models) and the linearization method (for non-linear models) to find the minimum of an objective function. The parameters required in the UWHAUSDD argument list are described briefly below.

ITYPE   - problem number
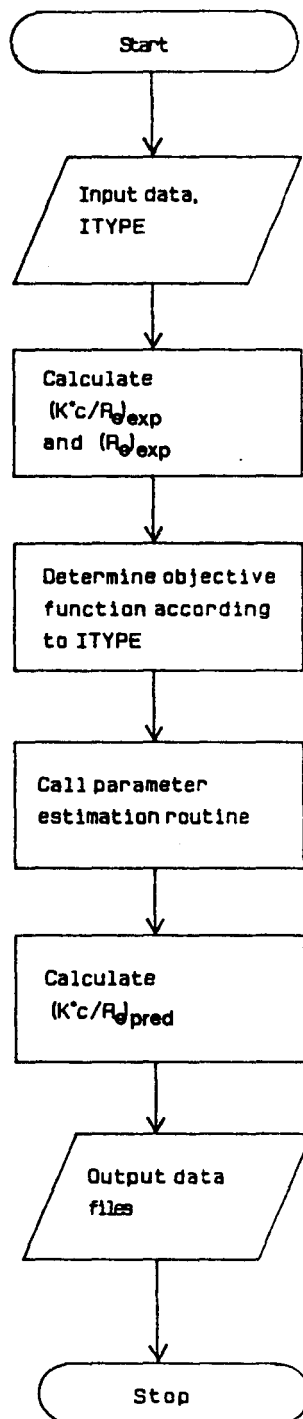
Figure 4.6 — General algorithm of WALS and LALLS programs

TABLE 4.12

Relation Between ITYPE and WALS/LALLS Objective Function

ITYPE	Objective Function: $f(z_i, \beta)$	Method of Estimation
1	$K^\bullet c / R_\theta$	error propogation
2	R_θ	error propogation
3	$K^\bullet c / R_\theta$	non-linear least squares (WALS), linear least squares (LALLS)
4	R_θ	non-linear least squares

MODEL   – external user supplied subroutine

NOB   – number of observations

OBJEC   – vector of objective function values to be met (0.0, $K^{*}c/R_\theta$, R_θ for method of error propogation, non–linear regression on $K^{*}c/R_\theta$ and R_θ respectively)

NP   – number of model parameters

BETA   – vector of model parameter estimates

DIFF   – vector defining parameter difference gradient at which objective function is evaluated

SIGNS   – vector allowing for non–negativety of parameter estimates; 0 for $-\infty < \beta < +\infty$; 1 for $\beta > 0$

EPS1 = 1×10^{-6} – convergence criterion for change in subsequent sums of squares of residuals

EPS2 = 1×10^{-9} – convergence criterion for change in subsequent values of each parameter estimate

MIT = 15   – maximum number of iterations allowed

FLAM = 1.0   – determine the step size taken by the

FNU = 10.0   estimation routine (values changed within routine); setting FLAM = 0.0 is equivalent to ordinary linear least squares estimation via steepest descent method

The external MODEL subroutine is supplied by the user and defines the

objective function(s) to be minimized; see appendices 2-B and 2-C.

The input data files for WALS and LALLS, although similar, are sufficiently different to warrant separate discussion.

4.2.2.1 WALS

An example of a WALS input data file is given in figure 4.7. Each input item is described below.

KPRIME — an arbitrary constant used in the absissa to construct a Zimm plot; see figure 3.1

CVAR, DTVAR — values of the variance estimates in measuring polymer concentration (0.05%, 0.5%, or 5%) and scattering angle (0.5 degrees)

UWHAUSDD parameters NOB, NP, EPS1, EPS2, MIT, FLAM, FNU as discussed previously

BETA — initial guess of model parameters $\bar{M}_w$, $\langle s^2 \rangle_z$, A_2, and A_3

C,DTHETA — polymer concentrations (5 values) and scattering angles (12 values) at which measurements were recorded

GSOLV — measured galvanometer readings for the solvent at each angle of measurement (12 values); independent of concentration

GSOLN — measured galvanometer readings for the polymer solutions (60 values); a function of

```
100                                                                                    !KPRIME
0.00 0.50                                                                              !CVAR,DTVAR
1 60 4 1.E-6 1.E-9 15 1. 10.                                                           !UWHAUSDD
330000 1.0 0.0004 0.01                                                                 !BETA
0.01943 0.01295 0.00648 0.00486 0.00259                                                !C
20. 30. 37.5 45. 60. 75. 90. 105. 120. 135. 142.5 150.                                 !DTHETA
4.00 2.35 1.81 1.52 1.21 1.07 1.00 1.03 1.12 1.36 1.54 1.86                            !GSOLV
18.4 19.0 19.4 18.0 15.0                                                                !GSOLN
12.2 12.6 12.4 11.8 9.25
9.63 10.2 10.0 9.3 7.4
8.21 8.51 8.35 7.9 6.3
6.55 6.85 6.62 6.3 4.86
5.79 6.00 5.78 5.44 4.20
5.50 5.70 5.42 5.10 3.88
5.59 5.78 5.45 5.11 3.86
6.15 6.30 5.92 5.56 4.15
7.35 7.52 7.03 6.54 4.90
8.48 8.60 7.99 7.46 5.61
9.99 10.4 9.50 8.81 6.89
5.17E-7 6.24E-5 1.0                                                                    !KSTAR,RB,GB
```

Figure 4.7 – WALS input data file

angle and concentration

KSTAR,RB,GB   – the values of K^*, R_b and G_b (refer to equation (2.78)

4.2.2.2 LALLS

An example of a LALLS input data file is given in figure 4.8 and a description of each item is given below.

GVAR,G0VAR   – values of the variance estiamtes in measuring G_θ and G_0 from chart recordings (10.0 and 12.0 respectively)

CVAR   – values of $[\overline{\mathrm{var}(c_i)/c_i^2}]$ used to estimate the variance in concentration measurement in equation (4.10) (5 values)

UWHAUSDD parameters NOB, NP, EPS1, EPS2, MIT, FLAM, FNU as discussed previously

BETA   – initial guess of model parameters $\overline{M}_w$ and A_2

C   – polymer concentrations at which measurements were recorded

GSOLN,GSOLN0   – measured galvanometer readings of G_θ and G_0 at each polymer concentration (5 values each)

DCODE   – a coded integer value between 1 and 5 corresponding to a specific attenuation function as given by equation 4.4; corresponding values of D are given in table 4.13

```
10.0 12.0                                              !GVAR,G0VAR
174.88D-7 61.57D-7 36.77D-7 47.38D-7 4.879D-7          !CVAR
1 5 2 1.E-6 1.E-9 15 1. 10.                            !UWHAUSDD
1000000 0.0002                                         !BETA
3.589D-4 7.6907D-4 10.2543D-4 14.356D-4 17.945D-4      !C
885 875 885 890 882                                    !GSOLN
492 317 275 230 220                                    !GSOLN0
3 3 3 3 3                                              !DCODE
4.5562D-8 4.5936D-6 652.952                            !KSTAR,RSOLV,
                                                        DISGMA
```

Figure 4.8 – LALLS input data file

TABLE 4.13

Relation Between DCODE and Value of Attenuating Function, D

DCODE	Attenuators In	$D = \prod_{i=1}^{4} (att)_i$
1	2, 4	1.0553×10^{-6}
2	3, 4	6.6728×10^{-8}
3	1, 3, 4	1.6549×10^{-8}
4	2, 3, 4	4.3026×10^{-9}
5	1, 2, 4	2.6173×10^{-7}

$$KSTAR, RSOLV, \quad - \text{ the values of } K^* , R_\theta \text{ for the solvent, and}$$

$$DSIGMA \qquad (\sigma'\chi)^1 \text{particular to a set of data}$$

4.2.2.3 WALS and LALLS Output Data Files

The output data files generated by the WALS and LALLS programs are now described.

ZIMMPROP.DAT   – stores the absissa and ordinate data
                required to construct a Zimm plot in the
                case of WALS and a K^*c/R_θ plot for LALLS

VARPROP.DAT   – contains the relative contributions of each
                error variance term accounted for in the
                error propagation model to the total error
                variance

STATPROP.DAT   – stores the complete UWHAUSDD screen output
                for later viewing if desired

SUMPROP.DAT   – contains a summary of UWHAUSDD results such
                as parameter estimates, confidence intervals
                and correlation matrix

RESIDS.DAT   – contains the residuals from the fit

Obviously, the file VARPROP.DAT is relevant only when the method of error prop gation is applied.

4.3   Dynamic Light Scattering

4.3.1   Experimental Data

To reconstruct particle size distributions through the application of the models given in equations (3.28) to (3.31), (3.34) and (3.35), raw autocorrelation data is needed. Such data was obtained from a NICOMP Model TC-200 computing autocorrelator at the C-I-L research laboratories in Toronto. All of the polymer samples studied were monodisperse, bimodal and polydisperse distributions prepared from Dow polystyrene latex particle standards. In addition to these samples a broad polyvinlyacetate distribution sample produced in an experimental continuous stirred tank emulsion polymerization reactor (Penlidis, 1985) was studied.

The Model TC-200 computes the second-order autocorrelation function over 64 channels, each channel corresponding to one unit of time delay, t. The last eight channels are used to determine the baseline A in equation (3.27) at infinite time delay. An example of the autocorrelation function $G^{(2)}(\tau)$ that the Model TC-200 displays is shown in figure 4.9. The raw autocorrelation data, is easily obtained from the Model TC-200 and displayed in the format given in figure 4.10.

In addition to the 64 channel contents, the total number of photopulses processed by the autocorrelator, the number of prescaled pulses and the elapsed time of the correlation in milli-seconds is
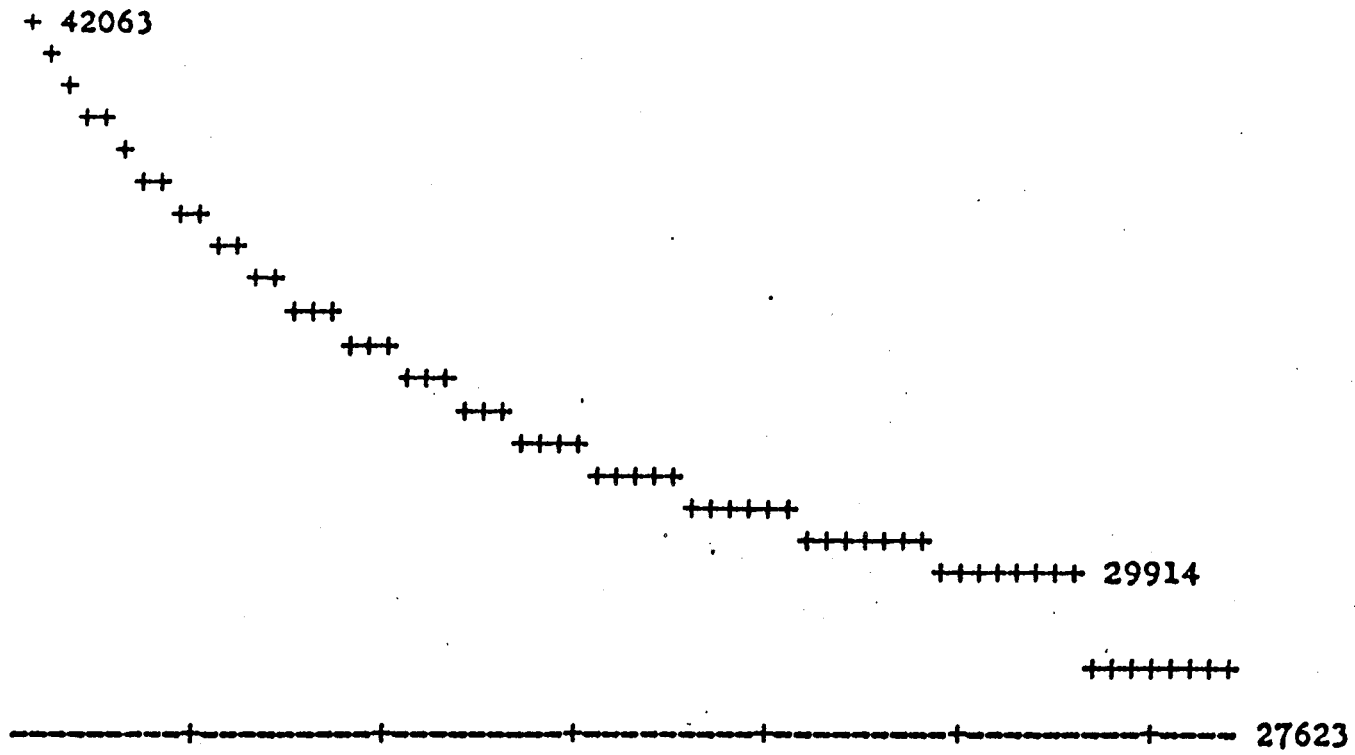
Figure 4.9 – Raw autocorrelation function display from NICOMP
Model TC-200; G ( )

```
TOTAL COUNTS       = 137088926
PRESCALED COUNTS   = 137105426
RUN TIME(MSEC)     = 732172
     CHANNEL CONTENTS
111397     110314     109234     108193
107207     106233     105315     104428
103568     102724     101919     101161
100420      99702      99024      98352
 97696      97098      96506      95919
 95372      94845      94327      93837
 93360      92889      92447      92028
 91628      91220      90831      90467
 90100      89763      89430      89104
 88803      88498      88218      87948
 87678      87419      87179      86928
 86708      86476      86270      86055
 85856      85661      85479      85284
 85105      84935      84760      84622
 79833      79847      79839      79841
 79848      79839      79845      79838
```

Figure 4.10 – Channel content display from NICOMP Model TC-200

displayed. These figures may be used to calculate the total number of counts and the baseline as a check on the displayed figures using the following relations

$$\text{total counts} = \text{prescaled counts} \times \text{prescale factor} \qquad (4.11)$$

$$\text{baseline} = \frac{\text{channel width} \times \text{total counts} \times \text{prescaled counts}}{\text{run time} \times 1000 \times 2048} \qquad (4.12)$$

The channel width and prescale factor are determined by the instrument during the initial stages of the run. The channel width is measured in micro-seconds. The factors of 1000 and 2048 account for the discrepancy in time units between channel width (μs) and run time (ms), and the fact that the displayed correlator channel contents have all been predivided by 2048. Thus, the actual value of $G^{(2)}(\tau)$ for the first channel is $111397 \times 2048 = 2.2814 \times 10^8$.

The values of the variables listed in table 4.14 were the same for each sample studied. The photon pulses were measured at a scattering angle of 90 degrees. With this information it can be determined that $K = 0.018673 \text{ nm}^{-1}$ for equation (2.92). The following relationships between D_t, the translational diffusion coefficient, and Γ, with the particle diameter D, may be derived.

$$D_t = \frac{214.174}{D/2} \quad \frac{\text{nm}^2}{\mu\text{s}} \qquad (4.13)$$

$$\Gamma = \frac{0.074679}{D/2} \quad \mu\text{s} \qquad (4.14)$$

from equations (2.91), (2.92) and (2.93). The particle diameter is equivalent to twice the hydraulic radius, R_h, for spherical particles, hence the denominators in equations (4.13) and (4.14) are D/2.

TABLE 4. 14

Constants Used in Dynamic Light Scattering Experiments

Symbol	Comments	Value
T	temperature of the experiment	293 K
η_s	solvent refractive index	1.330
sin (θ/2)	scattering angle where the measurement occurred	0.707
λ_o	laser wavelength	633×10^{-5} cm
K	an optical constant given by $\dfrac{4\pi\eta_s \sin(\theta/2)}{\lambda_o}$	0.018673 nm^{-1}

If prior information about the type of distribution being studied
is available, the Model TC-200 has the capability of allowing the user
to select a fit number to capitalize on this information. The fit
numbers range from 0 to 6, where 0 would be selected when the
distribution is known to be monodisperse or bimodal, and 6 for a broad
distribution. The default fit number of 2, which appears to assume a
slight bias towards bimodal distributions in the fitting procedure,
was employed for most of the sample runs in this study.

4.3.2   Analysis Program

The program used to estimate the model parameters in equations
(3.28) to (3.31), (3.34) and (3.35) is listed in appendix 2-D. Eight
model choices are available to the user depending on the value of
ITYPE. Table 4.15 details the correspondance between ITYPE and the
form of the objective function. The flowchart depicted in figure 4.6
is equally applicable to this program.

The estimation subroutines UWHAUSDD and NNLS (non-negative least
squares) were used to estimate the model parameters. UWHAUSDD was
discussed in section 4.2.2. The NNLS estimation routine employed was
developed by Lawson and Hanson (1974) at Pasadena's Jet Propulsion
Laboratory; see appendix 2-E. Their algorithm does not require an
external MODEL subroutine, but solves the set of linear equations

$$A_{n \times p} X_{p \times 1} = B_{n \times 1}, \qquad \text{subject to } X \geqslant 0 \qquad (4.15)$$

where the matrix A contains a set of n linear equation coefficients, X
is a vector of p parameters and B is a vector of response values. The

TABLE 4.15

Relation Between ITYPE and DLS Models

ITYPE	Equation	Model: $f(\beta_j)$	Method of Estimation
1	(3.31)	$\sum\limits_{j=1}^{m} \beta_j \exp(-\Gamma_j t_i)$ $\beta_j \ge 0$	NNLS – non-negative linear least squares
2	(3.31)		transformed NNLS
3	(3.27)	$\sum\limits_{j=1}^{m} \beta_j \exp(-\Gamma_j t_i)$	UWHAUSDD – linear least squares
4	(3.24)	$\beta \exp(-\Gamma t_i)$	UWHAUSDD – non-linear least squares
5	(3.25)	$\beta_1 \exp(-\Gamma_1 t_i) + \beta_2 \exp(-\Gamma_2 t_i)$	UWHAUSDD – non-linear least squares
6	(3.26)	$\beta_1 \exp(-\Gamma_1 t_i) + \beta_2 \exp(-\Gamma_2 t_i)$	UWHAUSDD – linear least squares
7	(3.26)	$\beta_1 \exp(-\Gamma_1 t_i) + \beta_2 \exp(-\Gamma_2 t_i)$ $+ \beta_3 \exp(-\Gamma_3 t_i)$	UWHAUSDD – linear least squares
8	(3.26)	$\beta_1 \exp(-\Gamma_1 t_i) + \beta_2 \exp(-\Gamma_2 t_i)$ $+ \beta_3 \exp(-\Gamma_3 t_i) + \beta_4 \exp(-\Gamma_4 t_i)$	UWHAUSDD – linear least squares

NNLS routine solves (4.15) through a QR matrix decomposition method. For this DLS application, the linear model has the following form.

$$\begin{bmatrix} \exp(-r_1 t_1) & \exp(-r_2 t_1) & \cdots & \exp(-r_m t_1) \\ \exp(-r_1 t_2) & \exp(-r_2 t_2) & \cdots & \exp(-r_m t_2) \\ \cdot & \cdot & & \cdot \\ \cdot & \cdot & & \cdot \\ \cdot & \cdot & & \cdot \\ \exp(-r_1 t_{56}) & \exp(-r_2 t_{56}) & \cdots & \exp(-r_m t_{56}) \end{bmatrix} \begin{bmatrix} \beta_1 \\ \beta_2 \\ \\ \\ \beta_m \end{bmatrix} = \begin{bmatrix} g_1^{(1)}(\tau) \\ g_2^{(1)}(\tau) \\ \cdot \\ \cdot \\ g_{56}^{(1)}(\tau) \end{bmatrix} \quad (4.16)$$

With this model form, it is simple to estimate anywhere from one up to twenty parameters at a time.

The parameters required by NNLS in the argument list are described below.

A   — n x p design matrix of measured or calculated quantities

MDA   — row dimension of A (equivalent to number of observations)

M   — number of observations

N   — number of parameters (equivalent to p)

B   — vector of observations or responses

X   — vector of parameter estimates

RNORM   — contains euclidean norm of the residual vector

W,ZZ   — vectors of working space of length N and M respectively

INDEX   — an integer vector of working space of length at least N

MODE   — an NNLS success/failure flag

The data that is read and used by the main program from the data input file is dependent upon the value of ITYPE entered interactively by the user. An example input data file is given in figure 4.11.

DELTAT   - channel width (micro-seconds)

TCOUNT   - total number of photopulses counted

PCOUNT   - number of prescaled counts

RUNT   - run time (milli-seconds)

PFAC   - prescale factor

COUNTS   - channel contents (64 values)

UWHAUSDD parameters NOB, NP, EPS1, EPS2, MIT, FLAM, FNU as

      discussed previously

SPN   - determines whether or not negative

          parameter estimates are allowed (yes, if

          SPN = -1; no, if SPN = 1)

BETAI   - initual guess of p   parameters (only for

          ITYPE > 3)

DL   - lower diameter value (in nanometers) at

          which parameter estimates start at

OMEGAMAX   - determines logarithmic spacing between

          parameter estimates on diameter scale

SHIFTS   - number of times a set of p parameters

          are estimated in each shift

NEX   - determines whether a weighted NNLS fit is

          performed (see equation (3.35)) where we

```
150 186178374 18616715 1055671 10      !DELTAT,TCOUNT,PCOUNT,RUNT,PFAC
311691 309025 306523 304122            !COUNTS
301799 299587 297448 295392
293417 291525 289688 287925
286243 284608 283035 281519
280067 278654 277296 275973
274720 273510 272337 271211
270125 269087 268074 267111
266173 265283 264431 263587
262781 262014 261269 260540
259849 259179 258535 257919
257333 256748 256185 255642
255114 254625 254161 253694
253256 252812 252390 251980
251586 251200 250834 250480
240799 240811 240813 240814
240837 240828 240826 240828
1 56 5 1.E-6 1.E-9 15 0. 10. -1        !UWHAUSDD
0.01 0.1 0.2 0.1 0.02                  !BETAI (IF ITYPE > 2)
3.0 5.0 6 1 1                          !DL,OMEGAMAX,SHIFTS,NEX1,NEX2
```

Figure 4.11 — DLS input data file

minimize

$$\sum_{i=1}^{n} [\, g_i^{(1)}(\tau)^{\text{NEX}} \;-\; \sum_{j=1}^{m} g_i^{(1)}(\tau)^{\text{NEX}-1} \, \beta_j \exp(-r_j \, t_i\,) \,]^2$$

(4.17)

− (4.17) is equivalent to (3.35) when

NEX = **2**; NEX = 1 is the unweighted case

Finally, several output data files are created by the main program.

DLSOUT.DAT   − contains $g^{(1)}(\tau)$ vs t data

DIS.DAT   − contains the parameter estimates of distribution fit

PREDICT.DAT   − contains the predicted values of $g^{1}(\tau)$

RESLIM.DAT   − contains the residuals of the fits

RESULTS AND DISCUSSION

5.1   Introduction

Some of the results from the computer parameter estimation runs are presented with accompanying discussions and conclusions.

5.2   Classical Light Scattering

5.2.1   Wide Angle Light Scattering

5.2.1.1 Experimental Results

The results presented in this section were obtained from the analysis of the data given in tables 4.1 and 4.2. A Zimm plot of this data ($K^{\ast}c/R_\theta$ vs sin $(\theta/2)$ + 100*c) is given in figure 5.1. From this figure, one can easily see the difficulty in obtaining results from a manual double extrapolation to zero polymer concentration and zero scattering angle. This alone justifies the use of computerized parameter estimation procedures.

The following initial guesses for the parameters in equation (2.74) were obtained from the results reported by Roberts et al (1977).

$$\overline{M}_w = 340\ 000$$
$$\frac{16\eta^2\langle s^2\rangle_z}{3\lambda^2} = 1.0 \qquad (\langle s^2\rangle_z \doteq 4.0\ \ 10^{-6}\ \text{cm})$$
$$A_2 = 0.0004$$
$$A_3 = 0.01$$

The results of the parameter estimation routines are presented in table 5.1. With these results, the contributions to the total error

Figure 5.1 — WALS

Zimm Plot of Robert's Data
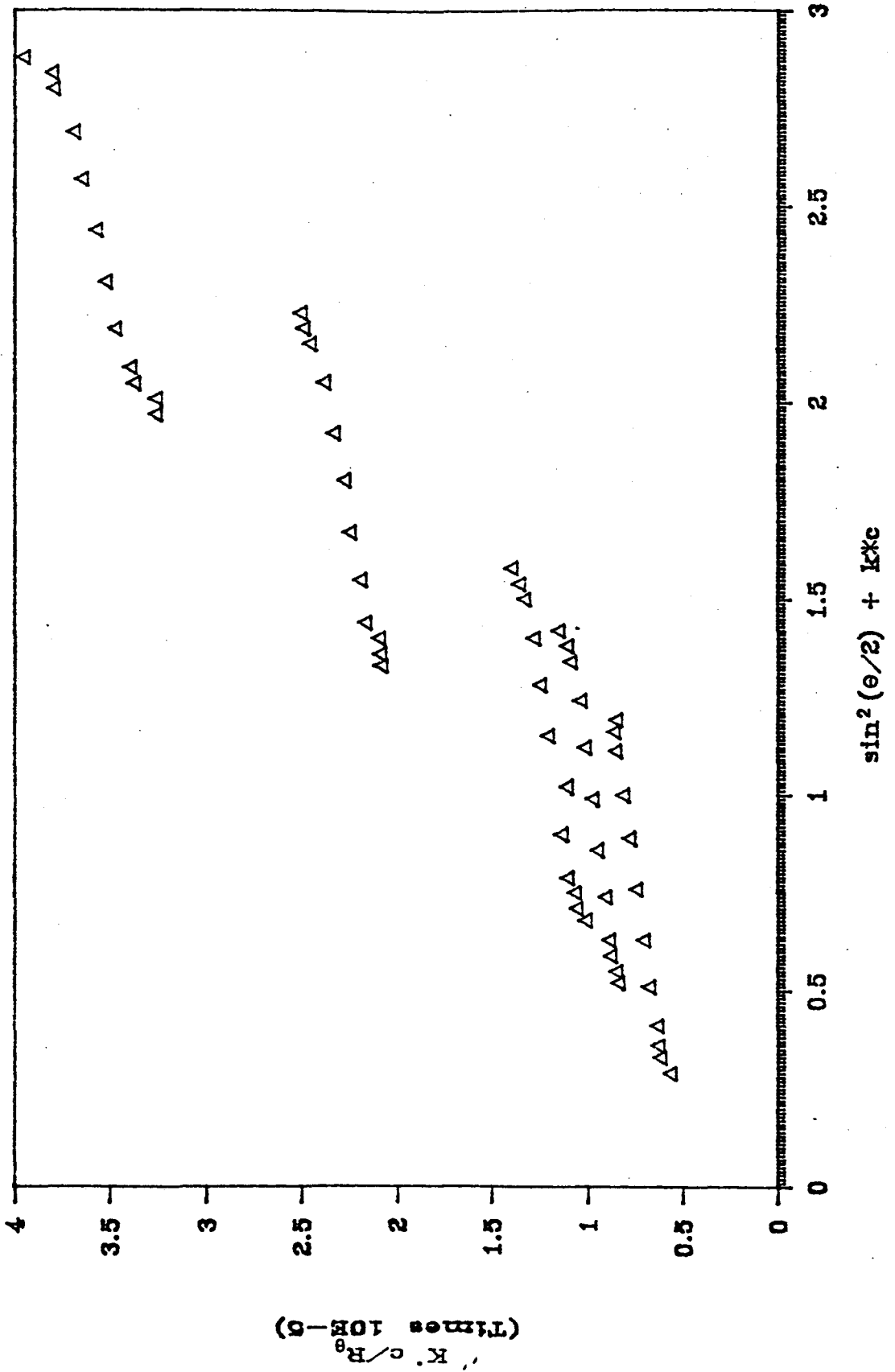
variance by concentration and scattering angle errors can be made as well as the effect of their presence or absence on the parameter estimates.

An important statistic to look at before discussing the results is the variance of the residuals given in the last column of table 5.1. This is given by

$$\sum_{i=1}^{n} \left[\frac{e_i}{\sqrt{var(e_i)}} - \left(\overline{\frac{e_i}{\sqrt{var(e_i)}}} \right) \right]^2 \Big/ \nu_e \qquad (5.1)$$

where the first term is the actual residual for point i, the second term is the mean of all of the residuals and ν_e is the associated degrees of freedom. For the linear case, and approximately for the non-linear case, the expected value of the mean of the residuals is zero, and equation (5.1) becomes

$$\sum_{i=1}^{n} \frac{e_i^2}{var(e_i)} \Big/ \nu_e \qquad (5.2)$$

and should have an expected value of one. However, all of the values of the variance of the residuals in table 5.1 are less that 0.1, one order of magnitude too small. This suggests that the assumed error structure is not correct, the magnitude of the estimated errors being too high. Since the effect on the parameter estimates and the variance of the residuals by the errors in scattering angle and concentration is small (with the exception of $var(c) = (0.05 \times c)^2$), it may be that too great a contribution is being attributed to the measurement of the galvanometer readings as predicted through equation (4.3). An examination of VARPROP.DAT revealed that the error variance calculated for the galvanometer readings accounted for greater than

90% of the total estimated error for most of the runs with the exception again being when var(c) = $(0.05 \times c)^2$. Even in this case, more than 80% of the estimated error was contributed by the galvanometer errors. This confirms that the errors in c and θ have the least significance and the error propagation runs (ITYPE = 1,2) were therefore repeated with equation (4.3) modified to

$$\text{var}(H_\theta) = 0.0005(\overline{G_\theta})_\theta^2 \tag{5.3}$$

The results of these runs are presented in table 5.2. A comparison of tables 5.1 and 5.2 shows that the point estimates of the parameters have not been significantly affected by using equation (5.3). However the variance of the residuals are now of the appropriate magnitude, approaching a value of one.

The discussion for the results in table 5.2 is divided into two categories; a study of the effects of the type of estimation routine employed and of the error structure assumed in the method of error propogation.

5.2.1.2 Effect of Estimation Routine

Table 4.12 contains a summary of the four estimation routines that were used from which the results in table 5.2 were obtained. Only the error propagation runs where var(c) = var(θ) = 0 are discussed here since these results are the only ones that are comparable with those obtained from the non-linear least squares method. In all of these cases, only the error in the measurement of G_θ(sol'n) is considered.

TABLE 5.1

Summary of Results from WALS Parameter Estimation

ITYPE	Standard Deviation c	θ	$\hat{\bar{M}}_w$	$\left(\dfrac{16\pi^2\langle s^2\rangle_2}{3\lambda^2}\right)$	$\hat{A}_2\ (\times10^4)$	$\hat{A}_3\ (\times10^4)$	Variance of the Residuals $\sum\limits_{i=1}^{n}\dfrac{e_i^2}{\mathrm{var}(e_i)}\Big/\nu_e$
1	0.0	0.0	326,000 ± 30,820	1.121 ± 0.149	4.567 ± 0.387	1.193 ± 0.132	0.0646
	0.005 × c	0.0	326,000 ± 30,820	1.121 ± 0.149	4.567 ± 0.387	1.193 ± 0.132	0.0646
	0.05 × c	0.0	326,000 ± 30,820	1.121 ± 0.149	4.567 ± 0.387	1.193 ± 0.132	0.0646
	0.5 × c	0.0	325,900 ± 30,960	1.123 ± 0.150	4.559 ± 0.388	1.197 ± 0.132	0.0630
	0.0	0.5	325,700 ± 30,610	1.118 ± 0.148	4.567 ± 0.385	1.193 ± 0.131	0.0631
	0.005 × c	0.5	325,700 ± 30,610	1.118 ± 0.148	4.567 ± 0.385	1.193 ± 0.131	0.0631
	0.05 × c	0.5	325,700 ± 30,620	1.118 ± 0.148	4.567 ± 0.385	1.193 ± 0.131	0.0631
	0.5 × c	0.5	325,600 ± 30,760	1.120 ± 0.149	4.560 ± 0.386	1.197 ± 0.131	0.0616
2	0.0	0.0	322,800 ± 29,420	1.113 ± 0.143	4.531 ± 0.384	1.211 ± 0.132	0.0644
	0.005 × c	0.0	322,800 ± 29,400	1.113 ± 0.143	4.531 ± 0.384	1.211 ± 0.132	0.0643
	0.05 × c	0.0	322,100 ± 28,170	1.103 ± 0.137	4.522 ± 0.373	1.220 ± 0.130	0.0585
	0.5 × c	0.0	301,300 ± 17,790	0.967 ± 0.083	4.272 ± 0.326	1.341 ± 0.147	0.0135
	0.0	0.5	322,900 ± 28,870	1.111 ± 0.140	4.527 ± 0.378	1.218 ± 0.130	0.0611
	0.005 × c	0.5	322,900 ± 28,850	1.111 ± 0.140	4.527 ± 0.378	1.218 ± 0.130	0.0610
	0.05 × c	0.5	321,900 ± 27,770	1.100 ± 0.135	4.517 ± 0.370	1.226 ± 0.129	0.0560
	0.5 × c	0.5	301,200 ± 17,770	0.966 ± 0.083	4.271 ± 0.325	1.342 ± 0.147	0.0134
3	–	–	417,000 ± 86,410	1.723 ± 0.444	5.075 ± 0.548	1.035 ± 0.161	–
4	–	–	320,300 ± 27,940	1.111 ± 0.139	4.512 ± 0.374	1.200 ± 0.129	–

TABLE 5.2

Summary of Results from WALS Parameter Estimation [modified var (H)]

ITYPE	Standard Deviation		Parameter Estimates ± 95% Confidence Intervals				Variance of the Residuals
	c	θ	$\widehat{M}_w$	$\left(\dfrac{16\pi^2(\widehat{s^2})_z}{3\lambda^2}\right)$	$\widehat{A}_2$ $(\times 10^4)$	$\widehat{A}_3$ $(\times 10^4)$	$\sum_{i=1}^{n} \dfrac{e_i^2}{var|e_i|} \Big/ v_e$
1	0.0	0.0	326,000 ± 30,820	1.121 ± 0.149	4.567 ± 0.387	1.193 ± 0.132	0.7570
	0.005 x c	0.0	326,000 ± 30,820	1.121 ± 0.149	4.567 ± 0.387	1.193 ± 0.132	0.7570
	0.05 x c	0.0	326,000 ± 30,840	1.121 ± 0.149	4.566 ± 0.387	1.193 ± 0.132	0.7547
	0.5 x c	0.0	324,700 ± 32,180	1.141 ± 0.157	4.493 ± 0.397	1.231 ± 0.136	0.5888
	0.0	0.5	323,200 ± 28,980	1.091 ± 0.141	4.563 ± 0.370	1.198 ± 0.126	0.6078
	0.005 x c	0.5	323,200 ± 28,980	1.091 ± 0.141	4.563 ± 0.370	1.198 ± 0.126	0.6078
	0.05 x c	0.5	323,200 ± 29,000	1.091 ± 0.141	4.563 ± 0.371	1.198 ± 0.126	0.6062
	0.5 x c	0.5	324,300 ± 30,720	1.119 ± 0.150	4.526 ± 0.382	1.220 ± 0.131	0.4896
2	0.0	0.0	322,800 ± 29,420	1.113 ± 0.143	4.531 ± 0.384	1.211 ± 0.132	0.7548
	0.005 x c	0.0	322,800 ± 29,250	1.112 ± 0.142	4.530 ± 0.382	1.212 ± 0.131	0.7453
	0.05 x c	0.0	313,300 ± 22,850	1.042 ± 0.109	4.413 ± 0.340	1.278 ± 0.130	0.4180
	0.5 x c	0.0	298,200 ± 16,540	0.935 ± 0.074	4.271 ± 0.345	1.340 ± 0.174	0.0249
	0.0	0.5	319,400 ± 25,940	1.080 ± 0.126	4.473 ± 0.357	1.266 ± 0.125	0.5143
	0.005 x c	0.5	319,300 ± 25,880	1.079 ± 0.126	4.472 ± 0.357	1.266 ± 0.125	0.5112
	0.05 x c	0.5	311,800 ± 22,270	1.026 ± 0.107	4.402 ± 0.337	1.293 ± 0.129	0.3483
	0.5 x c	0.5	297,600 ± 16,430	0.933 ± 0.074	4.263 ± 0.343	1.344 ± 0.173	0.0243
3	–	–	417,000 ± 86,410	1.723 ± 0.444	5.075 ± 0.548	1.035 ± 0.161	–
4	–	–	320,300 ± 27,940	1.111 ± 0.139	4.512 ± 0.374	1.200 ± 0.129	–

A glance at the four sets of parameter estimates clearly shows the results from a least squares analysis on K^*c/R_θ (ITYPE = 3) to be the least accurate (with respect to the estimate of the weight average molecular weight) and the least precise. The poor results may be attributed to the violation of an assumption under which least squares analysis is valid, that being that K^*c/R_θ has constant error variance. Recall that a strong quadratic relationship between the error variance of $G_\theta(sol'n)$ and the scattering angle was demonstrated in figure 4.1. Since R_θ appears in the denominator of K^*c/R_θ, the error variance of this latter variable would be far from constant.

The parameter estimates from the other three routines all agree favourably with each other and with results obtained by Roberts et al (1977). All of the point estimates are well within the 95% confidence intervals of the other point estimates.

The point estimates from the two error propagation applications are similar because the minimization of (3.12) is equivalent to minimizing

$$\sum_{i=1}^{n}\left\{\frac{H_{\theta i}}{var(H_{\theta i})}\left[1 - \left(\frac{K^*c_i}{R_{\theta i}}\right)_{pred}\left(\frac{K^*c_i}{R_{\theta i}}\right)_{obs}^{-1}\right]\right\}^2 \tag{5.4}$$

for ITYPE = 1, and

$$\sum_{i=1}^{n}\left\{\frac{H_{\theta i}}{var(H_{\theta i})}\left[1 - \left(\frac{K^*c_i}{R_{\theta i}}\right)_{obs}\left(\frac{K^*c_i}{R_{\theta i}}\right)_{pred}^{-1}\right]\right\}^2 \tag{5.5}$$

for ITYPE = 2, when $var(c) = var(\theta) = 0$. The only difference between (5.4) and (5.5) is the inversion of the ratio of predicted K^*c/R_θ values to observed. Thus, there are only small differences in the

results from the error propagation applications.

It is certain that accounting for the error structure exhibited in the measurement of $G_\theta(\text{sol'n})$ (figure 4.1) has yielded improved parameter estimates over simple non-linear regression of $K^* c/R_\theta$. Note, however that non-linear regression of R_θ yields results similar to those from error propagation. This was to be expected since R_θ contains the major source of error. However, the following analysis helps to explain the closeness of these results.

It can easily be shown that (3.3) is equivalent to minimizing

$$R_b^2 \sum_{i=1}^{n} \sin^2\theta_i [(H_{\theta_i})_{obs} - (H_{\theta_i})_{pred}]^2 \qquad (5.6)$$

which is a weighted sum of squares where the weights are given by $\sin^2\theta_i$. The variation in $1/\sin^2\theta$ with θ is quite similar to that of $\text{var}[G_\theta(\text{sol'n})]$ as given in equation (5.3). Figure 5.2 compares $1/\sin^2\theta$ with $0.0005(\overline{G_\theta})_\theta^2$, normalized to 1.0 at 90°, as a function of θ for the data used in this experiment. It is apparent from this figure that results obtained from a non-linear least squares application on R_θ are valid since appropriate relative weighting has been applied to the data points. Thus, these results compare favourably with those from the method of error propagation.

Figure 5.2 – WALS
Relative Weighting vs Scattering Angle

Relative Weighting

Scattering Angle (degrees)

□ $0.0005 \times (\overline{G_\theta})^2_\theta$ △ $1/\sin^2\theta$
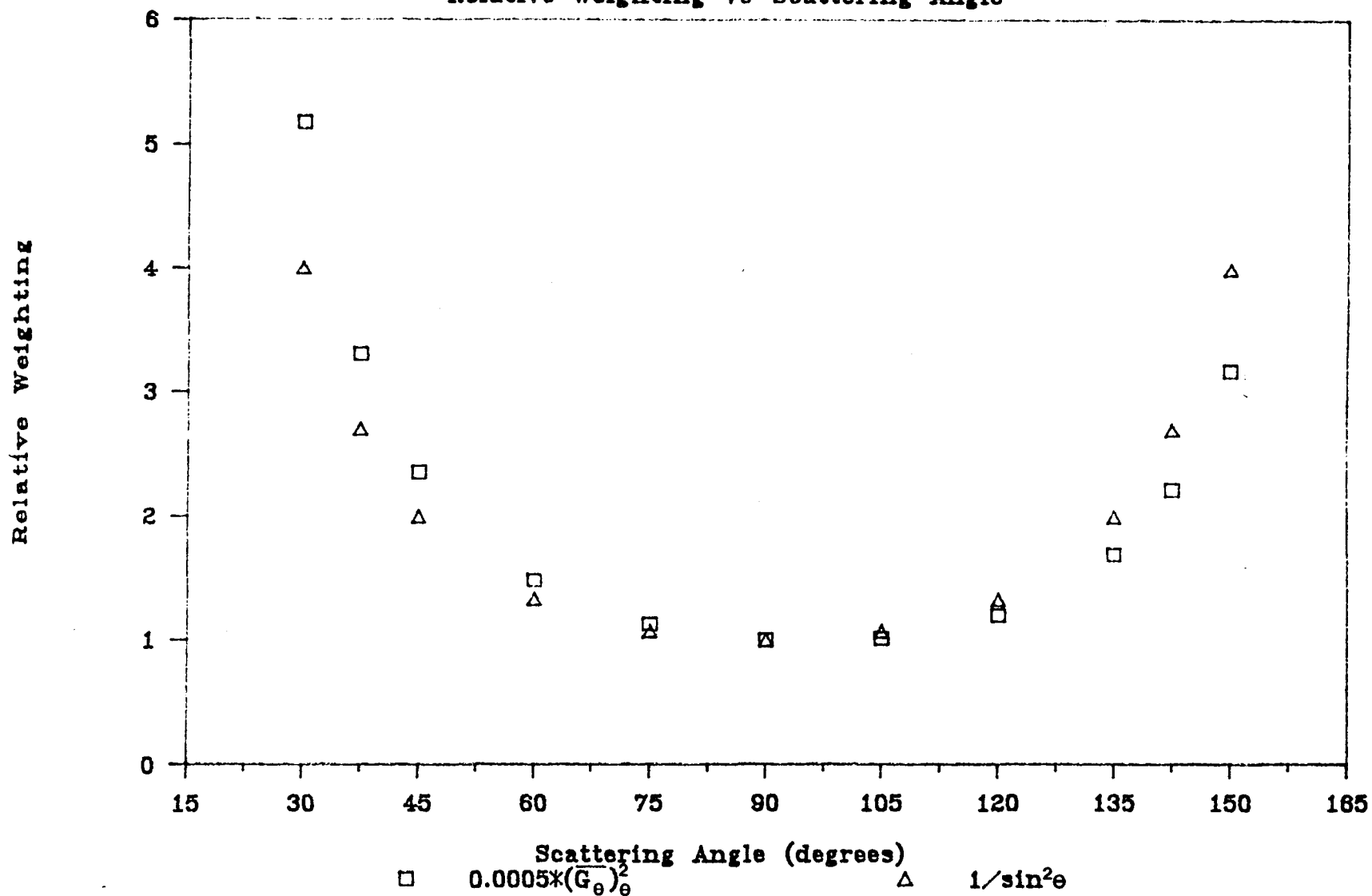
5.2.1.3 <u>Effect</u> <u>of</u> <u>Error</u> <u>Structure</u> <u>on</u> <u>Error</u> <u>Propagation</u>
<u>Errors</u> <u>in</u> <u>Polymer</u> <u>Concentration</u>

For ITYPE=1, increasing the relative error in polymer concentration from zero to 0.5% had little effect on the parameters listed in table 5.2. When the error is increased to 5.0% however, the point estimates of the parameters changed slightly and were less precise. The variance of the residuals also decreased from 0.75 to 0.59 suggesting that a 5.0% relative error in the polymer concentration is too high, causing $var(e_i)$ to be over- estimated. An examination of VARPROP.DAT showed the contribution of the error in concentration to be as high as 40% of the total error.

Similar conclusions may be drawn for the results obtained with ITYPE=2, although these results are more sensitive to changes in the relative error in the polymer concentration. That is, increasing the error in concentration effects a noticeable change in the point estimates and their precision at lower relative errors than with ITYPE=1. In fact, the contribution to the total error by the error in polymer concentration is as high as 76% with an 0.5% relative error and effectively 100% with a 5.0% relative error. Clearly, the error in measuring concentration has a greater effect on the results when the light scattering model in equation (2.74) is re-expressed in terms of R_θ and the method of error propagation is applied. This is because the concentration is more prominent in the partial derivative equations that comprise the calculation of the error variance, see

appendix 3.

Note that the estimated confidence limits for the parameter estimates decrease with increasing concentration error for ITYPE=2. One would normally expect the precision of the parameter estimates to decrease if larger or more errors are accounted for. The formula used to estimate the 95% confidence limits was

$$(C.L.)_j = \beta_j \pm 2\sqrt{V(\beta_j)} \qquad j=1,2,\ldots,p \qquad (5.7)$$

where $\sqrt{V(\beta_j)}$ is the j'th diagonal element of the parameter covariance matrix, given by

$$V(\underline{\beta}) = (\underline{\underline{X}}^T\underline{\underline{X}})^{-1}\sigma_e^2 \qquad (5.8)$$

where σ_e^2 is an estimate of the error variance, and in this case is given by

$$\sigma_e^2 = \sum_{i=1}^{n} \frac{e_i^2}{var(e_i)} \bigg/ \nu_e = \text{variance of the residuals} \qquad (5.9)$$

The value of the variance of the residuals decreases at a greater rate with increasing concentration errors than it did when ITYPE=1. It is actually two orders of magnitude too small when the relative error in polymer concentration was 5.0% suggesting that the assumed error structure is not correct. Thus, the resulting confidence limits estimated from equation (5.7) were too small. Therefore, incorrect error structures can yield misleading results.

Errors in Scattering Angle

The runs discussed in the previous section were repeated with an error in the measurement of the scattering angle of 0.5 degrees included. The results in table 5.2 show that accounting for this error had little effect on the point estimates but reduced the estimates of the confidence limits. Again, this is probably due to over-estimating the error in measuring the scattering angle. In general though, the error in the scattering angle had little effect on the final results, even though it contributed up to 67% to the total error.

It is interesting to comment on a trend that was observed in the magnitudes of the percent contribution that the error in the scattering angle makes to the total error when the percent contribution by the error in the polymer concentration is not dominant. The contribution to the total error is the greatest at low and high scattering angles, and the smallest at 90°, the trend being quadratic in nature. This corresponds to the lowest error contribution by the galvanometer readings at low and high angles where the least weighting is applied, and the greatest contribution at 90° where the most weighting is applied. This demonstrates that the quadratic weighting function determined in equation (5.3) is being applied correctly. This trend is masked when the error contribution by the polymer concentration becomes dominant at 5.0% relative error.

5.2.1.4 Residuals

It is worthwhile to comment here on some observations made of the residuals from the parameter estimations routines. A typical residual plot is given in figure 5.3. The order of the residuals is with descending values of polymer concentration nested within ascending values of scattering angle; ie - (20 ; 0.01943, 0.01295, 0.00648, 0.00486, 0.00254 g/ml), etc...

From figure 5.3, it is apparent that most of the residuals lie within ± 0.5, but there is a definite upward trend in the residuals from left to right. It turns out that the residuals below and above the main body each correspond to a measurement at 0.01943 g/ml polymer concentration - the highest value. This is much more evident in figure 5.4 where the relative error in polymer concentration is 5.0%. This clearly demonstrates the breakdown of the light scattering model (equation 2.74) that would be expected at high polymer concentrations (recall the assumptions listed in section 2.2.5). It is also evident from figure 5.4 that the main body of residuals broadens at the higher scattering angles. This too, is a result of model breakdown.

5.2.1.5 Summary

From the discussion presented above, it was concluded that when analyzing wide angle light scattering data, the primary concern should be to weight the galvanometer readings appropriately. In this study, a quadratic function of scattering angle was used to weight the data. It was shown that this function is easily incorporated into the method of error propagation and that non-linear regression of R_θ

Figure 5.3 – WALS Residuals

Typical Residual Plot
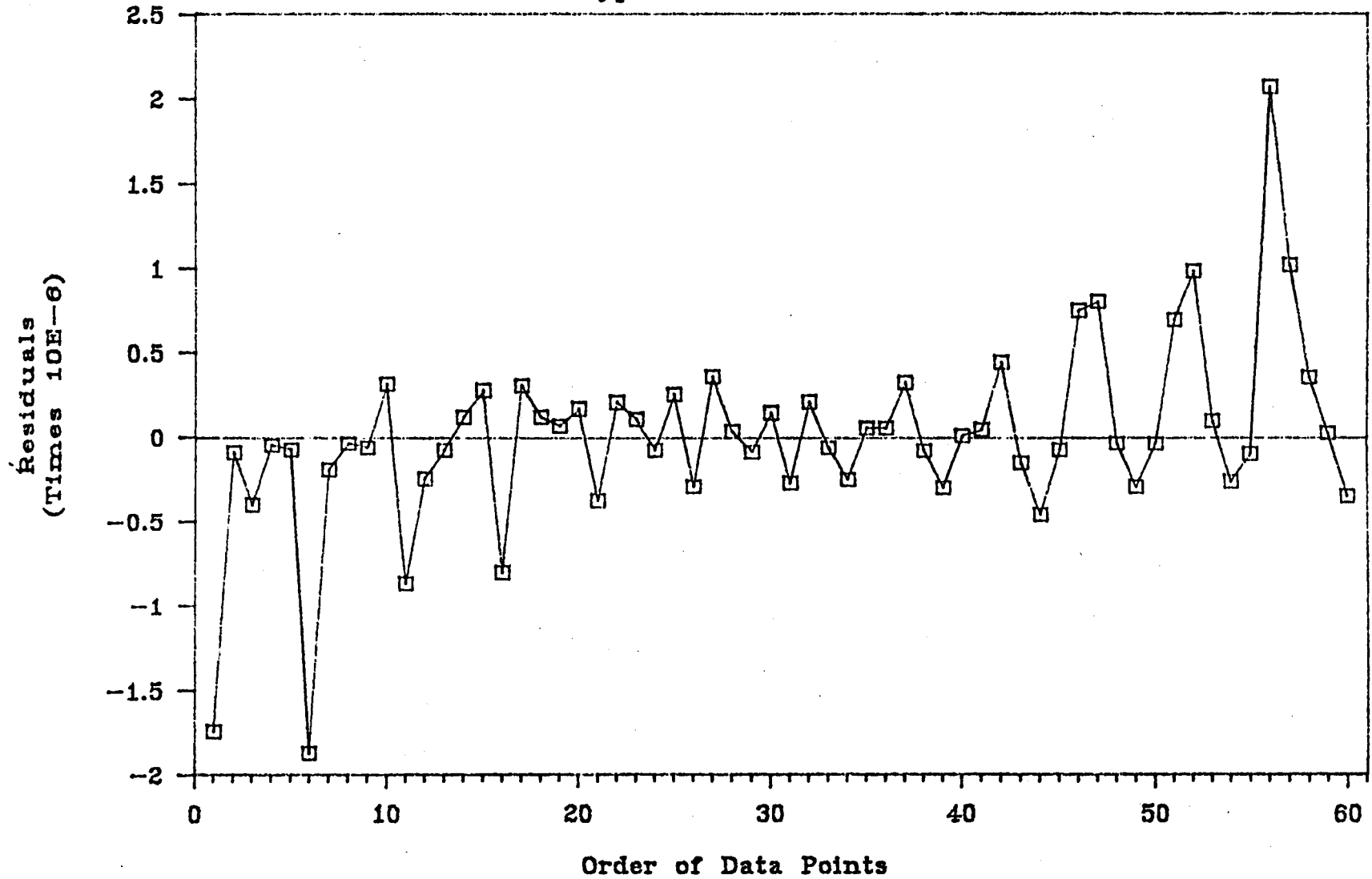
Figure 5.4 — WALS Residuals

St. Dev. of Conc. = 0.5%c
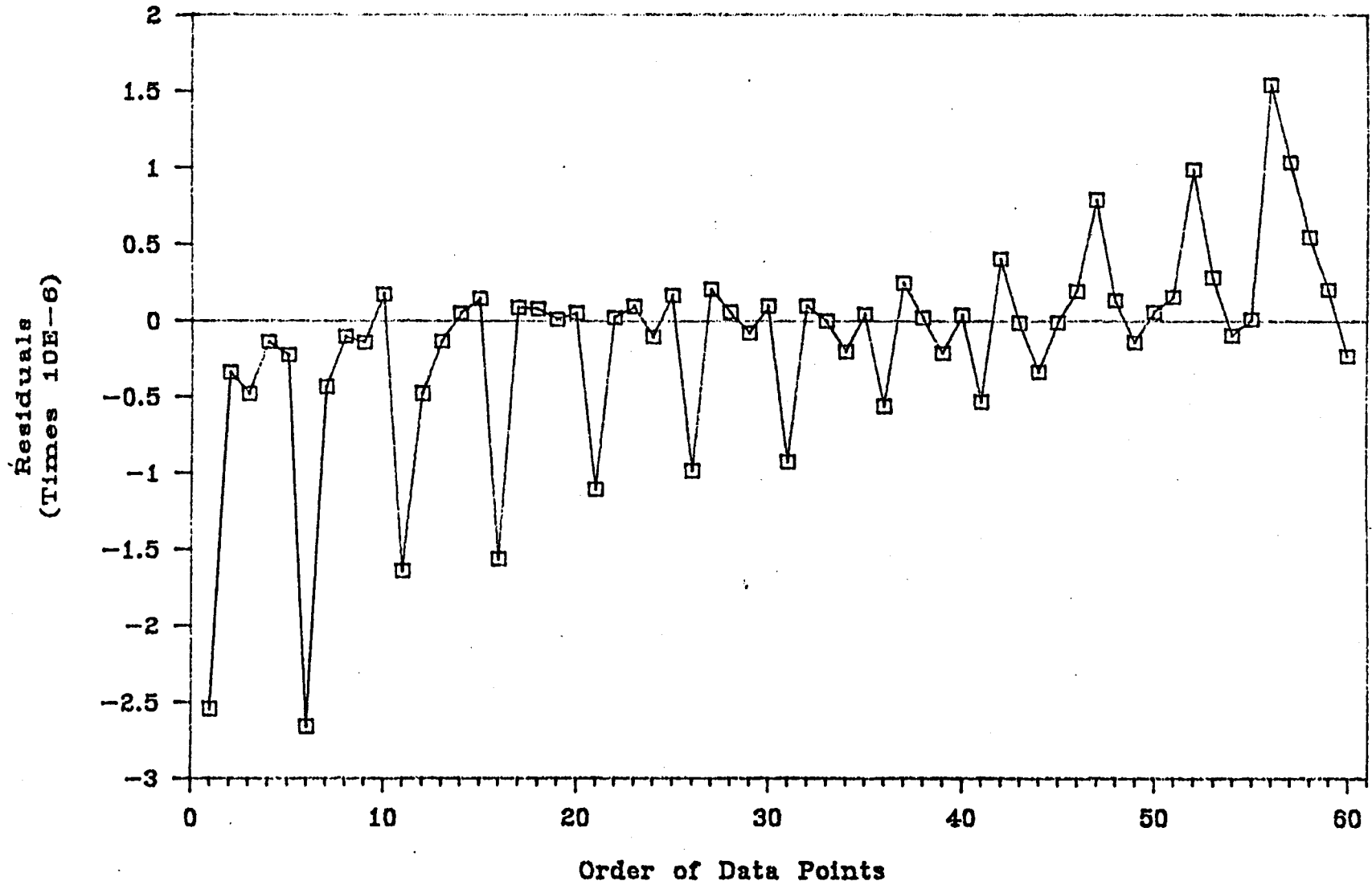
automatically weighs the data according to a similar function –
$1/\sin^2\theta$ A comparison of tables 5.1 and 5.2 shows that the form of
the function is more important than the magnitude as the point
estimates of the parameters were not greatly affected by a reduction
in the function of one order of magnitude.   Applications of these
methods yielded the best results.   However, care must be taken to
account for the proper error structure if the method of error
propagation is used.   Poor estimates of the error variance in the
measured variables may give misleading results.

On the basis of these results, it is recommended that non–linear
regression of R_θ be used to obtain estimates of the model parameters
and their associated confidence intervals.   If good estimates of the
error variance in polymer concentration and scattering angle are
available, the method of error propagation used for ITYPE=1 may be
applied.   The application for ITYPE=2 was too sensitive to changes in
the level of the error assumed in the polymer concentration.

5.2.2   Low Angle Laser Light Scattering
5.2.2.1 Experimental Results

The results discussed in this section were obtained from the
analysis of four sets of polyvinyl–acetate/ethyl–acetate (PVAc/EAc)
data and three sets of replicate pairs of polyacrylamide/water data,
making ten sets in total.   A typical plot of $K''c/R_\theta$ vs c is given in
figure 5.5.   The parameters $\bar{M}_w$ and A_2 in equation (2.87) are usually

Figure 5.5 – LALLS

K'c/R$_\theta$ vs Conc. for Sample B11-8

Concentration (g/ml)
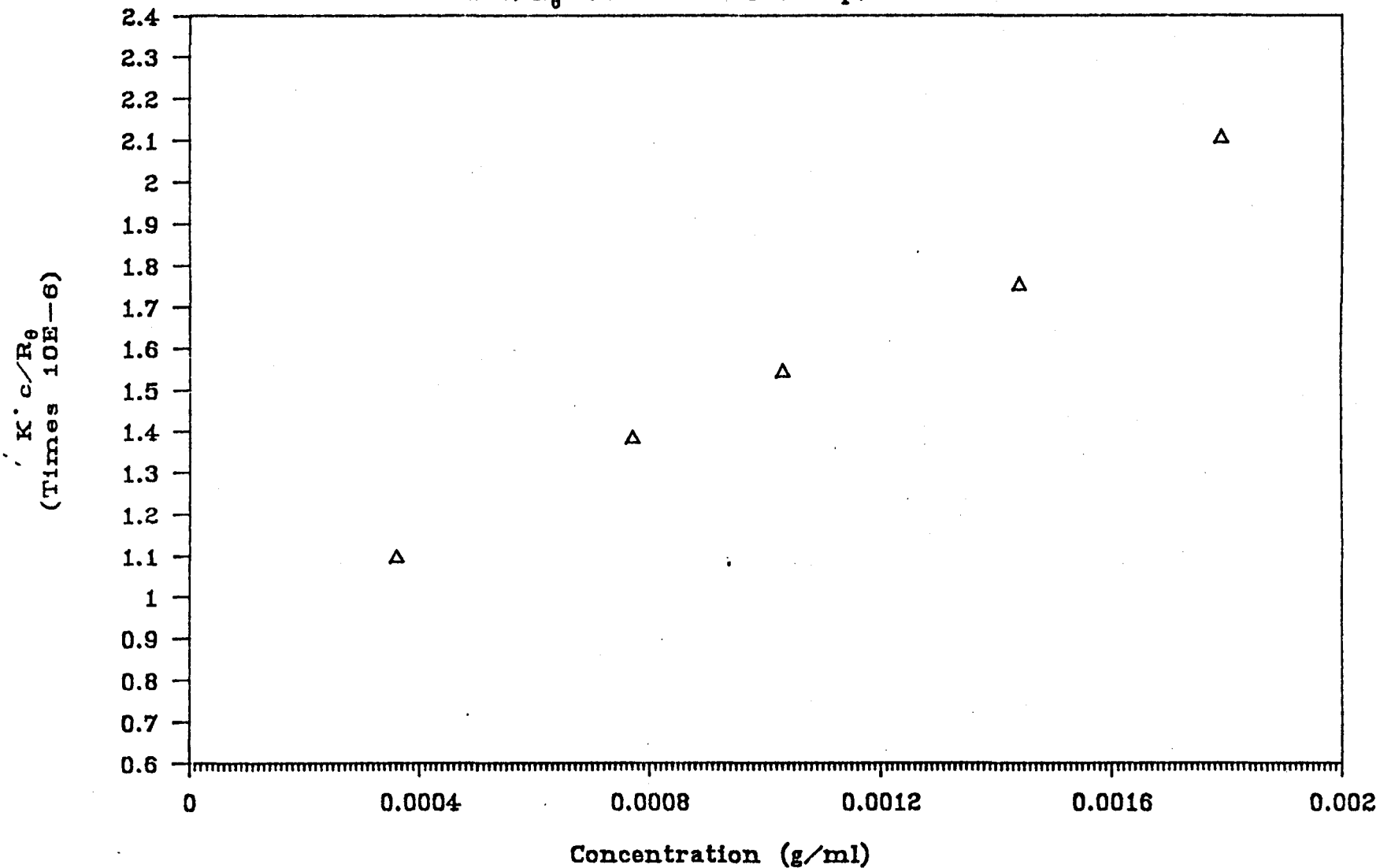
estimated by an "eye-ball" fit of the data in figure 5.5, or from a linear least squares fit.

A number of items that may affect the results of the LALLS data analysis are discussed below. Note that the analyses of sample B10-7 is based on only four data points instead of five. This is because it was found that one of the data points in the set was a severe outlier and the results from the parameter estimation routines were worthless.

5.2.2.2 Effect of Error Structure on Error Propagation

Recall that the estimated standard in G_θ and G_o were 10 - 12 and 12 - 24 units respecitvely. Estimates of the parameters $\bar{M}_w$ and A_2 were obtained for all four possible combinations of G_θ and G_o errors while applying the estimated concentration errors from equation 4.10 to all cases.

Changing levels of the standard deviation in G_θ and G_o had little effect on the point estimates of the parameters. However, increasing the standard deviation in G_o from 12 to 24 units decreased the values of the variance of the residuals by a factor of between three and four. In most samples studied, this decrease was away from the expected value of 1.0, thus suggesting that an estimated error variance of (24) is too high. An increase of the standard deviation in G_θ from 10 to 12 units, while also decreasing the variance of the residuals, had a much smaller effect on them than the change in G_o.

Since the standarad deviations of 12 and 24, for G_θ and G_0 respectively, were based on including extreme values in the analysis of variance (see appendix 4), it is now evident that the lower values of 10 and 12 are more appropriate. Indeed, the variance of the residuals is close the expected value of 1.0 for more of the samples studied under this case than any of the other three. It is also encouraging that consistent results were obtained for two independantly performed sets of experiments on two different polymer systems. Table 5.3 summarizes the results for ITYPE = 1,2 for standard deviations in G_θ and G_0 of 10 and 12 respectively.

The contribution to the total error variance by the error in the measurement of G_0 was by far the greatest at an average of 81% and 94% when the estimated standard deviations in G_0 was 12 and 24 units respectively. Most of the remaining error in the total error variance came from the measurement of G_θ. The contribution of the error in the measurement of the polymer concentration was rarely greater than 1% and was usually insignificant, accounting for an average of 0.3% of the total error variance. Since this contribution is so small, the runs were repeated with $var(c_i) = 0$ for all i, and using the values of 10 and 12 for the standard deviations of G_θ and G_0. These results appear in table 5.4.

Comparing table 5.4 with the results in table 5.3, it is apparent that neglecting the errors in measuring polymer concentration has not had much of an effect on the final results. However, neglecting the

errors in G_θ does have an adverse effect on the results. Both the values of the variance of the residuals and the confidence limits increase, suggesting that the total error variance has been under-estimated. Thus, the error in measuring G_θ should be included in the analysis.

5.2.2.3 Effect of Estimation Routine

The results for ITYPE = 3,4 are given in table 5.5. Comparing tables 5.4 and 5.5, it can be seen that, for each sample, the parameter estimates for the four different cases are not significantly different from each other.

Applying the same type of analysis on the two error propagation techniques as in the WALS case, the minimization of (3.12) can be shown to be equivalent to minimizing

$$\sum_{i=1}^{n} \left(\frac{R_{\theta i} G_{oi}}{(\sigma^2 \lambda^2)^{\frac{1}{2}} D_i}\right)^2 \left[1.0 - \left(\frac{K^* c_i}{R_{\theta i}}\right)_{pred} \left(\frac{K^* c_i}{R_{\theta i}}\right)_{obs}^{-1}\right]^2 \left[var(G_\theta) + \frac{G_\theta^2}{G_o^2} var(G_o)\right]^{-1} (5.10)$$

for ITYPE = 1, and

$$\sum_{i=1}^{n} \left(\frac{R_{\theta i} G_{oi}}{(\sigma^2 \lambda^2)^{\frac{1}{2}} D_i}\right)^2 \left[1.0 - \left(\frac{K^* c_i}{R_{\theta i}}\right)_{obs} \left(\frac{K^* c_i}{R_{\theta i}}\right)_{pred}^{-1}\right]^2 \left[var(G_\theta) + \frac{G_\theta^2}{G_o^2} var(G_o)\right]^{-1} (5.11)$$

for ITYPE = 2, when var(c) = 0.0. Once again, the only difference between these two formulas is the inversion of the ratio of predicted $K^* c / R_\theta$ values to observed. Thus, only small differences in the results between the two error propagation applications were to be expected.

While applying the method of error propagation to LALLS data is more desireable since it employs a more appropriate error structure in its analysis, the simpler methods of linear and non-linear regression of $K^* c/R_\theta$ and R_θ cannot abe discounted since these methods often offered comparable results.

5.2.2.4 Effect of Recorded Value for G_θ

Recall that in section 4.2.1, two different methods of recording the value for the measurement of G_θ from chart recordings was discussed. One method recorded a lower envelope value while the other recorded an average value from the main body of the chart recording while ignoring gross peaks. The first method is the one commonly used by experimenters. Employing the second technique effected an average increase of 10 units in the G_θ values. Values from both methods were recorded only for the PVAc/EAc samples. The results from using the latter method are presented in table 5.6.

Comparing tables 5.5 and 5.6, it can be seen that no significant difference exists other than a trend towards higher point estimates of $\bar{M}_w$. Certainly, as the values of G_θ increase, $K^* c/R_\theta$ decreases and the estimate of $\bar{M}_w$ would be expected to increase (since the intercept, $1/\bar{M}_w$ decreases). Since recording an average value from the main body of a chart recording can be less certain than recording a lower envelope value, and quite subjective regarding what constitutes a gross peak, this slight increase in $\hat{\bar{M}}_w$ may be considered somewhat arbitrary and variable. Therefore, use of the

TABLE 5.3

Summary of LALLS Results – Error Propogation (concentration error included)

Sample	ITYPE	Parameter Estimates $\pm$ 95% Confidence Intervals		Variance of the Residuals
		$\widehat{\overline{M}}_w$	$\hat{\lambda}_2 \, (\times 10^4)$	$\sum_{i=1}^{n} \frac{e_i^2}{\text{var}(e_i)} \Big/ v_e$
B 10-5	1	1, 278, 000 $\pm$ 160, 200	1.261 $\pm$ 1.287	1.005
	2	1, 267, 000 $\pm$ 155, 800	1.209 $\pm$ 1.270	0.996
B 10-7	1	2, 167, 000 $\pm$ 389, 400	1.431 $\pm$ 0.484	2.142
	2	2, 149, 000 $\pm$ 381, 600	1.422 $\pm$ 0.481	2.290
B 11-8	1	1, 157, 000 $\pm$ 63, 630	3.323 $\pm$ 0.294	0.183
	2	1, 159, 000 $\pm$ 61, 880	3.339 $\pm$ 0.290	0.178
B 11-9	1	2, 021, 000 $\pm$ 255, 900	0.844 $\pm$ 0.336	1.513
	2	2, 009, 000 $\pm$ 266, 100	0.876 $\pm$ 0.356	1.458
R - 9 E	1	181, 000 $\pm$ 11, 680	4.327 $\pm$ 0.576	0.640
	2	180, 400 $\pm$ 11, 980	4.306 $\pm$ 0.596	0.644
R-9I	1	205, 800 $\pm$ 15, 950	3.904 $\pm$ 0.756	1.333
	2	204, 600 $\pm$ 15, 810	3.862 $\pm$ 0.762	1.275
R - 10 C	1	799, 300 $\pm$ 34, 290	3.241 $\pm$ 0.158	0.150
	2	800, 100 $\pm$ 34, 230	3.248 $\pm$ 0.157	0.152
R - 10 H	1	982, 600 $\pm$ 102, 800	3.723 $\pm$ 0.195	0.984
	2	979, 900 $\pm$ 96, 100	3.729 $\pm$ 0.184	0.902
R - 11 D	1	1, 616, 000 $\pm$ 379, 300	3.524 $\pm$ 0.256	1.967
	2	1, 591, 000 $\pm$ 345, 000	3.516 $\pm$ 0.242	1.915
R - 11 G	1	1, 432, 000 $\pm$ 189, 000	3.388 $\pm$ 0.170	0.853
	2	1, 430, 000 $\pm$ 184, 600	3.391 $\pm$ 0.167	0.847

TABLE 5.4

Summary of LALLS Results - Error Propgation (no error in concentration)

Sample	ITYPE	Parameter Estimates $\pm$ 95% Confidence Interval		Variance of the Residuals $\sum_{i=1}^{n} e_i^2 / v_e$
		$\widehat{M}_w$	$\widehat{A}_2$ (x 10^4)	
B 1 0 - 5	1	1,278,000 $\pm$ 160,200	1.260 $\pm$ 1.288	1.008
	2	1,267,000 $\pm$ 155,800	1.207 $\pm$ 1.271	0.999
B 1 0 - 7	1	2,161,000 $\pm$ 385,800	1.427 $\pm$ 0.484	2.017
	2	2,143,000 $\pm$ 378,500	1.419 $\pm$ 0.481	2.151
B 1 1 - 8	1	1,157,000 $\pm$ 62,440	3.323 $\pm$ 0.294	0.183
	2	1,159,000 $\pm$ 61,690	3.339 $\pm$ 0.290	0.178
B 1 1 - 9	1	2,022,000 $\pm$ 255,900	0.885 $\pm$ 0.336	1.518
	2	2,009,000 $\pm$ 266,200	0.877 $\pm$ 0.356	1.462
R - 9 E	1	181,200 $\pm$ 11,650	4.335 $\pm$ 0.577	0.656
	2	180,500 $\pm$ 11,980	4.315 $\pm$ 0.598	0.661
R - 9 I	1	205,600 $\pm$ 16,040	3.901 $\pm$ 0.776	1.426
	2	204,300 $\pm$ 15,860	3.855 $\pm$ 0.778	1.358
R - 1 0 C	1	799,100 $\pm$ 33,710	3.241 $\pm$ 0.157	0.151
	2	799,900 $\pm$ 33,650	3.248 $\pm$ 0.157	0.153
R - 1 0 H	1	981,700 $\pm$ 101,300	3.728 $\pm$ 0.194	0.989
	2	978,900 $\pm$ 94,730	3.728 $\pm$ 0.183	0.907
R - 1 1 D	1	1,614,000 $\pm$ 377,300	3.523 $\pm$ 0.256	1.978
	2	1,589,000 $\pm$ 343,300	3.515 $\pm$ 0.241	1.925
R - 1 1 G	1	1,431,000 $\pm$ 187,500	3.387 $\pm$ 0.170	0.855
	2	1,430,000 $\pm$ 183,100	3.391 $\pm$ 0.167	0.849

TABLE 5.5

Summary of LALLS Results - Linear and Non-Linear Least Squares

Sample	ITYPE	Parameter Estimates $\pm$ 95% Confidence Intervals	
		$\hat{M}_w$	$\hat{A}_2 (x\ 10^4)$
B 1 0 - 5	3	1, 341, 000 $\pm$ 131, 800	1.680 $\pm$ 0.929
	4	1, 339, 000 $\pm$ 158, 900	1.659 $\pm$ 0.923
B 1 0 - 7	3	2, 058, 000 $\pm$ 353, 700	1.385 $\pm$ 0.494
	4	2, 068, 000 $\pm$ 438, 100	1.391 $\pm$ 0.517
B 1 1 - 8	3	1, 171, 000 $\pm$ 137, 200	3.378 $\pm$ 0.421
	4	1, 174, 000 $\pm$ 170, 500	3.378 $\pm$ 0.494
B 1 1 - 9	3	2, 086, 000 $\pm$ 216, 200	0.929 $\pm$ 0.276
	4	1, 979, 000 $\pm$ 268, 200	0.795 $\pm$ 0.320
A - 9 E	3	177, 900 $\pm$ 12, 650	4.183 $\pm$ 0.609
	4	172, 800 $\pm$ 10, 300	3.971 $\pm$ 0.444
A - 9 I	3	210, 500 $\pm$ 14, 600	4.007 $\pm$ 0.541
	4	206, 100 $\pm$ 12, 900	3.863 $\pm$ 0.423
A - 1 0 C	3	837, 000 $\pm$ 88, 690	3.355 $\pm$ 0.196
	4	833, 300 $\pm$ 83, 960	3.336 $\pm$ 0.200
A - 1 0 H	3	1, 051, 000 $\pm$ 207, 300	3.794 $\pm$ 0.309
	4	1, 036, 000 $\pm$ 202, 400	3.748 $\pm$ 0.356
A - 1 1 D	3	1, 791, 000 $\pm$ 521, 500	3.623 $\pm$ 0.248
	4	1, 686, 000 $\pm$ 477, 100	3.545 $\pm$ 0.333
A - 1 1 G	3	1, 475, 000 $\pm$ 260, 500	3.440 $\pm$ 0.209
	4	1, 459, 000 $\pm$ 224, 000	3.420 $\pm$ 0.214

TABLE 5.6

Summary of LALLS Results - Average Recorded Value of G_θ Used

Sample	ITYPE	Parameter Estimates + 95% Confidence Intervals		Variance of the Residuals
		$\widehat{\overline{M}}_w$	$\hat{A}_2 \, (\times 10^4)$	$\sum\limits_{i=1}^{n} \dfrac{e_i^2}{var(e_i)} \Big/ v_e$
B 10-5	1	1,286,000 ± 164,100	1.232 ± 1.301	1.049
	2	1,275,000 ± 159,600	1.183 ± 1.285	1.041
	3	1,352,000 ± 137,500	1.666 ± 0.953	–
	4	1,352,000 ± 171,000	1.654 ± 0.975	–
B 10-7	1	2,164,000 ± 365,000	1.397 ± 0.455	1.827
	2	2,148,000 ± 360,800	1.389 ± 0:455	1.959
	3	2,065,000 ± 343,500	1.355 ± 0.476	–
	4	2,071,000 ± 420,500	1.356 ± 0.493	–
B 11-8	1	1,175,000 ± 69,750	3.316 ± 0.318	0.221
	2	1,177,000 ± 68,820	3.334 ± 0.313	0.212
	3	1,183,000 ± 146,400	3.345 ± 0.441	–
	4	1,183,000 ± 181,900	3.335 ± 0.520	–
B 11-9	1	2,160,000 ± 356,200	0.981 ± 0.413	2.522
	2	2,134,000 ± 373,300	0.964 ± 0.446	2.400
	3	2,216,000 ± 298,300	0.999 ± 0.337	–
	4	2,056,000 ± 324,700	0.827 ± 0.361	–

lower envelope value in the analysis is preferred.

5.2.2.5 Summary

From the above discussions, it is recommended that non-linear regression of R_θ be used to analyze LALLS data. This is preferred over linear regression of $K^x c/R_\theta$ since the quantity containing the majority of the measurement error, R_θ, does not appear in the denominator. However, if good estimates of the error structure can be obtained, or are available, use the method of error propagation to make effective use of this information. Recall that it was found that measurement error in the polymer concentration had little or no effect on the error structure while those in the measurement of G_0 had the greatest effect.

Finally, it was recommended that the lower envelope value should be used when recording a value for G_θ from a chart recording.

5.3 Dynamic Light Scattering

The objective here was to determine the suitability of an analytical dynamic light scattering instrument (NICOMP Model TC-200 Computing Autocorrelator) in analysing samples of known particle size distributions (PSD's), and to demonstrate some of the difficulties in re-constructing PSD's from raw autocorrelation data. The latter objective was served by the analysis routines discussed previously. This was the sole purpose of these routines and were in no way an

attempt to reproduce the results obtained from the analytical instrument.

Eleven samples were studied, four of which were two sets of replicate pairs. Five of the samples were monodisperse standards of Dow polystyrene latex particles. From these standards, three different types of distributions were made. Finally, there was one unknown polydisperse sample. Table 5.7 lists all of the samples examined.

5.3.1 Results from the NICOMP Model TC-200

The samples listed in table 5.7 were taken to the C-I-L Research Laboratory in Toronto for analysis on their NICOMP instrument. Figure 5.6 is typical of the results obtained from this instrument. Note that a distribution of particle sizes has been fit, thus the "mean diameter" reported by the instrument is actually an estimate of the weighted particle size diameter. This instrument allows the user to choose one of three weightings that may be applied in the estimation of the mean diameter. These were (1) mass weighted, $\overline{D}_m$; (2) area weighted, $\overline{D}_a$; and (3) intensity weighted, $\overline{D}_I$ particle size diameter estimates. A summary of the analysis results using the default fit number of two and the mass weighting option, is given in table 5.8. The standard deviations reported in table 5.8 were calculated based on a normal Gaussian fit of the sample results.

TABLE 5.7

Composition of Sample Studied Using DLS

Sample ID	Particle Composition (nm)	
M34	34	
M98	98	
M175	176	
M220	220	
M275	275	
B98/275	1.000 part 98	
	0.901 part 275	
D176-A	0.496 part 176	
D176-B	1.000 part 220	$\bar{D}_i = 222$
	0.505 part 275	$\bar{D}_m = 226$
B98/D176-A	1.136 part 98	
B98/D176-B	0.496 part 176	
	1.000 part 220	
	0.505 part 275	
R2-20	unknown broad polyvinylacetate distribution	

TABLE 5.8

Summary of Results Obtained from a NICOMP Model TC-200
Computing Autocorrelator *

Sample ID	$(\widehat{\overline{D_m}})_1$ (nm)	Range$_1$(nm)	$(\widehat{\overline{D_m}})_2$ (nm)	Range$_2$(nm)	St. Dev. (nm)
M34	32.5	31.5 - 42.8	-	-	**
M98	93.4	85.7 - 100.0	-	-	3.4
M176	166.6	155.1 - 187.5	-	-	7.1
M220	223.0	205.7 - 240.0	-	-	8.6
M275	299.8	272.7 - 321.4	-	-	12.2
B98/275	99.7	94.7 - 109.0	315.1	257.1 - 400.0	-
D176-A	228.3	187.5 - 272.7	-	-	21.5
D176-B	224.6	204.5 - 264.7	-	-	15.5
B98/D176-A	120.5	107.1 - 130.4	257.4	214.2 - 333.3	-
B98/D176-B	104.6	96.7 - 111.1	240.8	200.0 - 300.0	-
R2-20	1279.6	1071.4 - 1500.0	-	-	178.6

* - With the exception of sample R2-20, all the above results were obtained using fit number 2.
R2-20 results were obtained with fit number 6.
** - Standard deviation was unavailable.

Thus, standard deviations were not reported for the bimodal samples since the Gaussian estimate was only unimodal.

From examining the results in table 5.8, two things became apparent that help explain the observed phenomena in the results from the bimodal samples. First, a distribution of particle sizes is always fit regardless of the nature of the sample. This was demonstrated in figure 5.6, which is the result from the monodisperse sample M98. Second, this distribution broadens as the particle size increases. This is evident from the results of the monodisperse samples M34, M98, M176, M220 and M275. The range of particle sizes over which the weight average particle size has been estimated increases from 11.3 nm, for sample M34, to 48.7 nm, for sample M275. This is caused by a decrease in the resolution of the particle size scale as the particle size increases. Comparing the results from sample M220 in figure 5.7 with figure 5.6 clearly demonstrates this. The stacked bar graph in figure 5.8 visually displays the overall trend of increasing distribution breadths (ranges) as the particle size increases. The residual portion of the graph also shows that good estimates of $\bar{D}_i$ were obtained for the unimodal samples; the residuals being the known $\bar{D}_i$ minus $\hat{\bar{D}}_i$. All of the $\hat{\bar{D}}_i$'s were within 10% of the known $\bar{D}_i$ and most were within 5%.

As mentioned previously, the above two points help explain two problems that prevent an accurate analysis of bimodal samples. The first problem was that the results from the mode containing the larger

NICOMP Distribution Analysis
SIZE nanometers   RELATIVE MASS

```
****************
**************************************
********************************************************** ****
***********************************************
*****************
*
```

980 A CIL   25/2/85

Figure 5.6 – Reconstructed NICOMP PSD for sample M98

NICOMP Distribution Analysis
SIZE nanometers   RELATIVE MASS

Figure 5.7 - Reconstructed NICOMP PSD for sample M220

Figure 5.8 – Residual/Range Bar Graph

NICOMP Model TC–200 Results
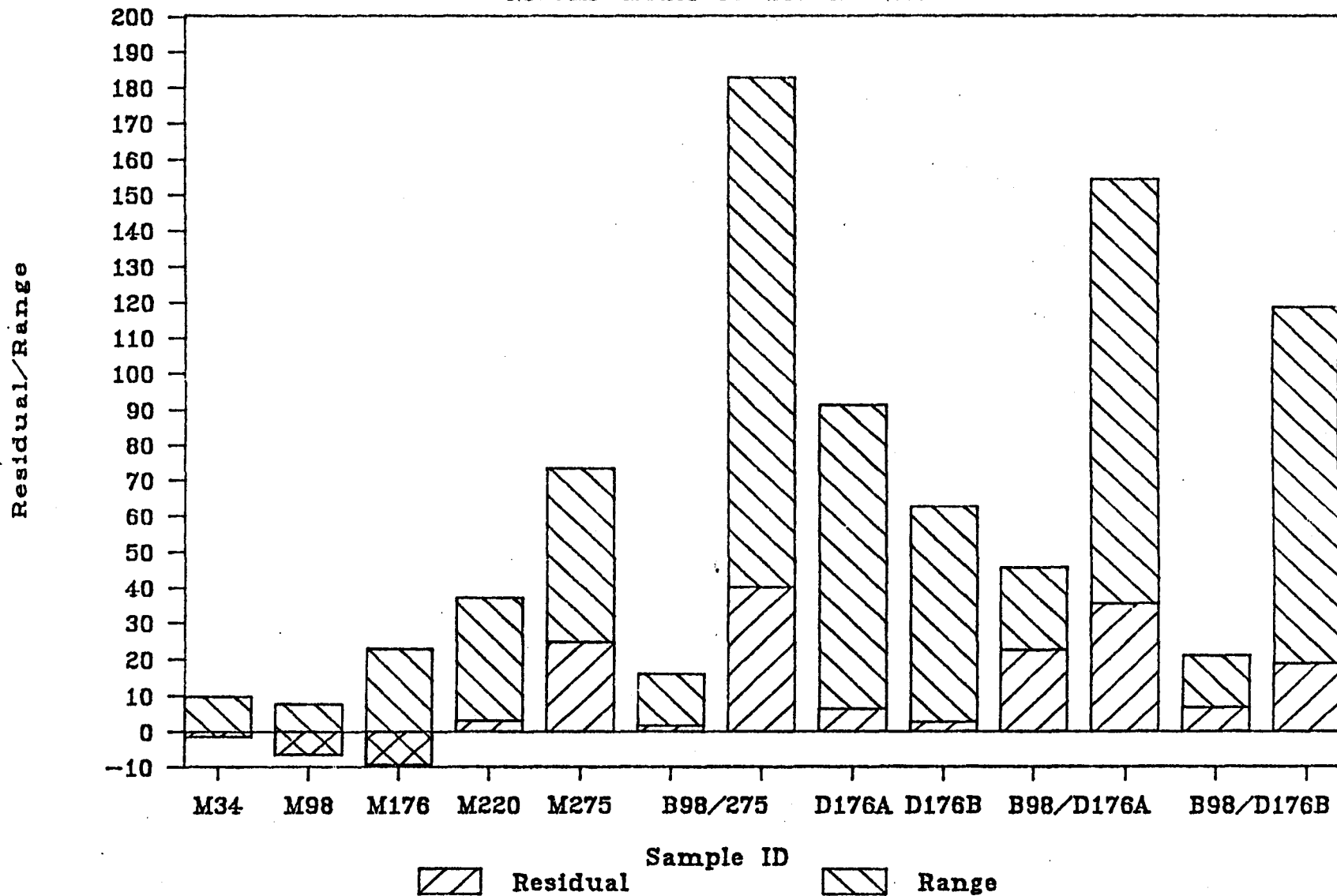
particles were not as reliable as those from the mode containing the smaller particles. This was especially evident in. sample B98/275 where both modes were monodisperse. We would expect the distribution of the second mode to be wider in light of the second point mentioned above, but it was nearly three times as broad as the distribution resulting from sample M275, see figure 5.8. This broadening was caused by the presence of the first mode which requires fitting at lower particle diameters. This then forced the second mode to be fit at a position on the logarithmic diameter scale where the resolution is even poorer than it was in the monodisperse sample M275. As a result, the estimate of the weight average particle size of the second mode was biased towards higher values. This is evident in the residual portion of figure 5.8. However, this problem is reduced if the two modes are closer together, or if they are polydisperse, instead of monodisperse. Such were the observations made in samples B98/176-A and B98/176-B. The presence of the smaller particles that make up the second modes distribution brings the fitted results into an area of increased resolution on the particle size scale. Notice however, that it is impossible to discern the nature of the second mode. No indication of the polydisperse second mode in these samples was given by the width of the distribution fit. It is actually narrower than the width of the fit to the monodisperse second in sample B98/275. Thus, one might erroneously conclude that the second modes in samples B98/275, and B98/176-A or B98/176-B were polydisperse and monodisperse respectively.

The second problem was that good estimates of the mass ratios of the two modes in the bimodal samples were difficult to obtain. For sample B98/275, the estimated mass ratio of 275 nm particles to 98 nm particles was 1.02:1.0. The known mass ratio is 0.90:1.0. It is not surprising that the estimated mass ratio is too high since the $\hat{D}_i$ for the second mode was over-estimated due to the reasons discussed above. For sample B98/D176-A and B98/D176-B, the estimated mass ratios of the polydisperse mode to the monodisperse mode were 1.14:1.0 and 1.46:1.0 respectively. The known ratio here is 1.76:1.0. In these two samples, the mass ratio was under-estimated. Since it is difficult to discern a polydisperse second mode from a monodisperse mode, it must be assumed that, in the polydisperse case, the total mass of particles would be under-estimated, thus yielding a smaller mass ratio.

There is quite likely an ideal bimodal sample that rests at a transition point for which good estimates of the weight average particle sizes and mass ratio may be obtained. There is a transition between over-estimating and under-estimating the $\bar{D}_i$'s and mass ratios as the difference between the $\bar{D}_i$'s of the two modes decreases and the mass ratio increases, see figure 5.9. Any samples deviating from this ideal will be improperly fit. Thus, care must be taken when interpreting results from bimodal samples.

For unimodal polydisperse samples, an indication of their polydispersity may be obtained. The simulated polydisperse samples D176-A and D176-B were fit over a significantly wider range of

decreasing resolution

ideal sample with respect to average particle sizes and polydispersity
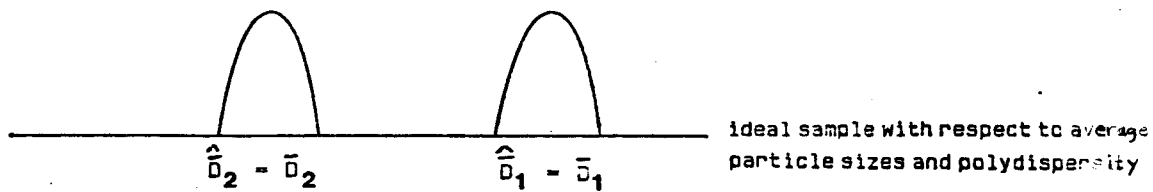
correct mass ratio

same polydispersity
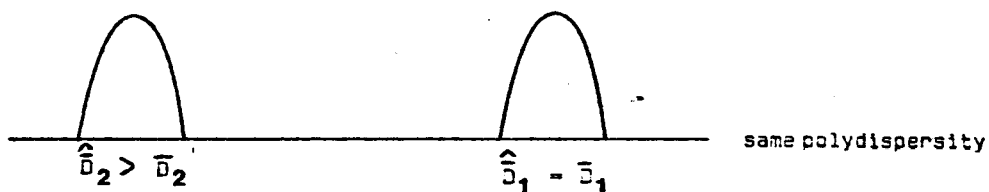
mass ratio over-estimated as difference between particle sizes increase

same average particle sizes
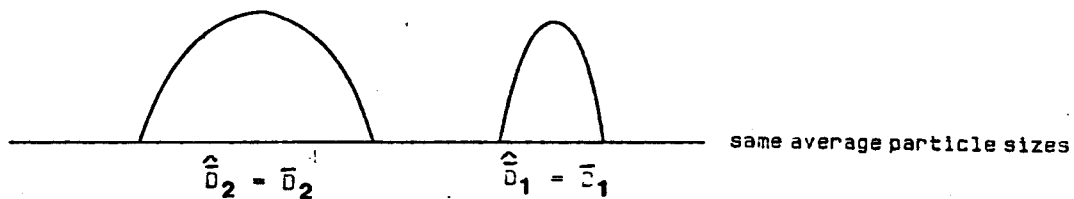
mass ratio under-estimated as polydispersity increases

Figure 5.9 – Transition exists between obtaining good estimates of both D_i 's and the mass ratio for bimodal samples

particle sizes than any of the monodisperse samples from which they were composed. The analysis of the unknown sample, R2-20, also indicates that it is polydisperse. However, this analysis is suspect since results from previous size exclusion chromatography tests yielded a mean particle size of 160 nm. This result is one order of magnitude smaller than the DLS estimate of 1280 nm. It may be that coagulation of the sample occurred between the time of the two analyses.

In conclusion, it can be stated that reliable results may be obtained from this instrument if the sample is unimodal. However, care must be taken when interpreting bimodal results. Any prior knowledge the user has concerning his samples will certainly aid in a correct interpretation of his results.

5.3.2   Reconstruction of Particle Size Distributions By Fitting Sums of Exponentials

The exponential models listed in table 4.15 were used to estimate the particle sizes and distributions from the first-order, normalized autocorrelation fuction $g^{(1)}(\tau)$. This function is easily constructed from the channel contents, which represent the second-order, un-normalized autocorrelation function $G^{(2)}(\tau)$; refer to figure 4.10. The function $g^{(1)}(\tau)$ is computed automatically by the analysis program using equation (2.95) and was used as the objective function in the

exponential models. The results and conclusions from these models are presented in three section, depending upon the fitting technique; (1) non-linear least squares estimation; (2) linear least squares estimation; and (3) exponential sampling.

5.3.2.1 Non-Linear Least Squares Estimation

This section covers the results from model types four and five, a single exponential, and a sum of two exponentials respectively. Here, both the exponential co-efficient and exponent of the models were estimated. The results are presented in table 5.9. It should be noted that the estimates of β_1 for a single exponential were merely the initial value of $g^{(1)}(\tau)$ at zero time lag and have no physical significance. However, when fitting a sum of two exponentials to a bimodal sample, the estimates of β_1 and β_2 represent the relative contribution of each model to the total measured intensity autocorrelation function. Thus, an estimate of the intensity ratio may be obtained. This may be compared with a predicted intensity ratio that can be calculated from the known mass ratio through the Mie theory.

The particle size estimates in table 5.9 exhibit, with the exception of sample M176, a bias towards being over-estimated. Figure 5.10 is a bar graph of the residuals between the known particle size diameter (or intensity average diameter for the polydisperse samples)

and the estimated value. This bias suggests that too much emphasis is put on the data at higher time lags. This would tend to give a higher estimate of the mean decay time. This corresponds to larger particles which diffuse more slowly through the solution. Therefore, the parameters were re-estimated using Morrison's suggested fitting criterion which places more weight on the data at lower time lags (refer to equation 4.17). The resulting estimates were, however, only marginally smaller. For example, 41.5 nm and 238.4 nm for samples M34 and D176-A respectively. The weighting factor NEX was increased from a value of two to five in increments of one in an attempt to realize a significant decrease in the parameter estimates. However, the final estimates for each value of NEX were still only marginally smaller than those from the unweighted case. Thus, it was concluded that Morrison's weighted model as presented in equation (4.17) offered little benefit over the simpler unweighted model.

To effect a real shifting of weight to the data at lower time lags, Morrison's formula was modified to include a second factor, NEX2 as follows. Minimize

$$\sum_{i=1}^{n} [\, g_i^{(1)}(\tau)^{NEX1} - \sum_{j=1}^{m} g_i^{(1)}(\tau)^{NEX1-NEX2} \;\beta_j \exp(-\Gamma_j \, t_i) \,]^2 \qquad (5.12)$$

where 1 < NEX2 < NEX1. Setting NEX1 = NEX2 = 1 is equivalent to Morrison's origonal formula. The introduction of NEX2 compounds the effect of NEX1 in shifting the weight to the data at smaller time lags. After re-estimating the model parameters with several

combinations of NEX1, NEX2 values, it was found that NEX1 = 2 and NEX2 = 1.1 offered the best overall estimates; see table 5.10. The overall effectiveness of using these weights in the model was assessed by comparing figure 5.11 with figure 5.10. Figure 5.11 shows that the residuals were smaller and better behaved than previously. Indeed, the sum of squares of the residuals was reduced to 1,662 nm^2 from 6,677 nm^2.

As mentioned previously, the estimated intensity ratios of the bimodal samples may be compared with the intensity ratios calculated from the known mass ratios. Appendix 5 outlines these calculations for the bimodal samples B98/275 and B98/D176-A and B. The results of these calculations are compared with the experimental results in table 5.11. Comparing the weighted results with the unweighted, one can clearly see the shifting of weight from larger to smaller particle sizes. This is more evident in sample B98/275 where the over-estimation of the intensity ratio has been reduced by 15%. It is less obvious for the other two samples since the intensity ratio already appears to be grossly under-estimated. However, recall that the second mode of these samples was an aggregate of three different particle sizes as shown in figure 5.12. This figure shows the theoretically predicted intensities for each particle size, the sum being the total intensity ratio of 9.17:1. The estimate of the total intensity ratio is more of a point estimate along the distribution, the remaining information being unavailable. This is a serious limitation of this method of estimation. Without prior information on a bimodal sample, the nature of the sample can never be resolved.

TABLE 5.9

Summary of Results Obtained from Non-Linear Least Squares Estimation
ITYPE = 4, 5

Sample ID	ITYPE	Parameter Estimates			
		$\hat{\beta}_1$	$\hat{D}_1$ (nm)	$\hat{\beta}_2$	$\hat{D}_2$ (nm)
M34	4	0.6414	41.9	–	–
M98	4	0.6527	102.1	–	–
M176	4	0.6869	176.0	–	–
M220	4	0.7408	230.0	–	–
M275	4	0.6525	303.8	–	–
B98/275	5	0.0977	102.0	0.5354	312.7
D176-A	4	0.6689	239.2	–	–
D176-B	4	0.6739	236.0	–	–
B98/D176-A	5	0.1331	119.8	0.5464	259.5
B98/D176-B	5	0.1640	125.7	0.5395	265.9
R2-20	4	0.5404	1235.1	–	–

TABLE 5.10

Summary of Results Obtained from Weighted Non-Linear Least Squares Estimation

ITYPE = 4, 5   (NEX1 = 2, NEX2 = 1.1)

Sample ID	ITYPE	Parameter Estimates			
		$\hat{\beta}_1$	$\hat{D}_1$ (nm)	$\hat{\beta}_2$	$\hat{D}_2$ (nm)
M34	4	0.6155	37.7	—	—
M98	4	0.6272	92.0	—	—
M176	4	0.6622	159.5	—	—
M220	4	0.7195	208.4	—	—
M275	4	0.6255	275.8	—	—
B98/275	5	0.1071	100.6	0.4976	286.5
D176-A	4	0.6432	216.7	—	—
D176-B	4	0.6486	213.7	—	—
B98/D176-A	5	0.1353	112.7	0.5184	235.2
B98/D176-B	5	0.1602	116.5	0.5190	239.6
R2-20	4	0.5088	1235.1	—	—

TABLE 5.11

Comparison of Calculated (Mie Theory) and Experimentally Determined (DLS) Bimodal Intensity Ratios. ITYPE = 4, 5

Sample ID	Ratio	Intensity Ratios		
		Calculated	Experimental (unweighted)	Experimental (weighted)
B98/275	$\dfrac{2750}{980}$	$\dfrac{2.45}{1}$	$\dfrac{5.48}{1}$	$\dfrac{4.65}{1}$
B98/D176-A	$\dfrac{D1760}{980}$	$\dfrac{9.17}{1}$	$\dfrac{4.11}{1}$	$\dfrac{3.83}{1}$
B98/D176-B	$\dfrac{D1760}{980}$	$\dfrac{9.17}{1}$	$\dfrac{3.29}{1}$	$\dfrac{3.24}{1}$

Figure 5.10 – Residual Bar Graph

Non-Linear Least Squares
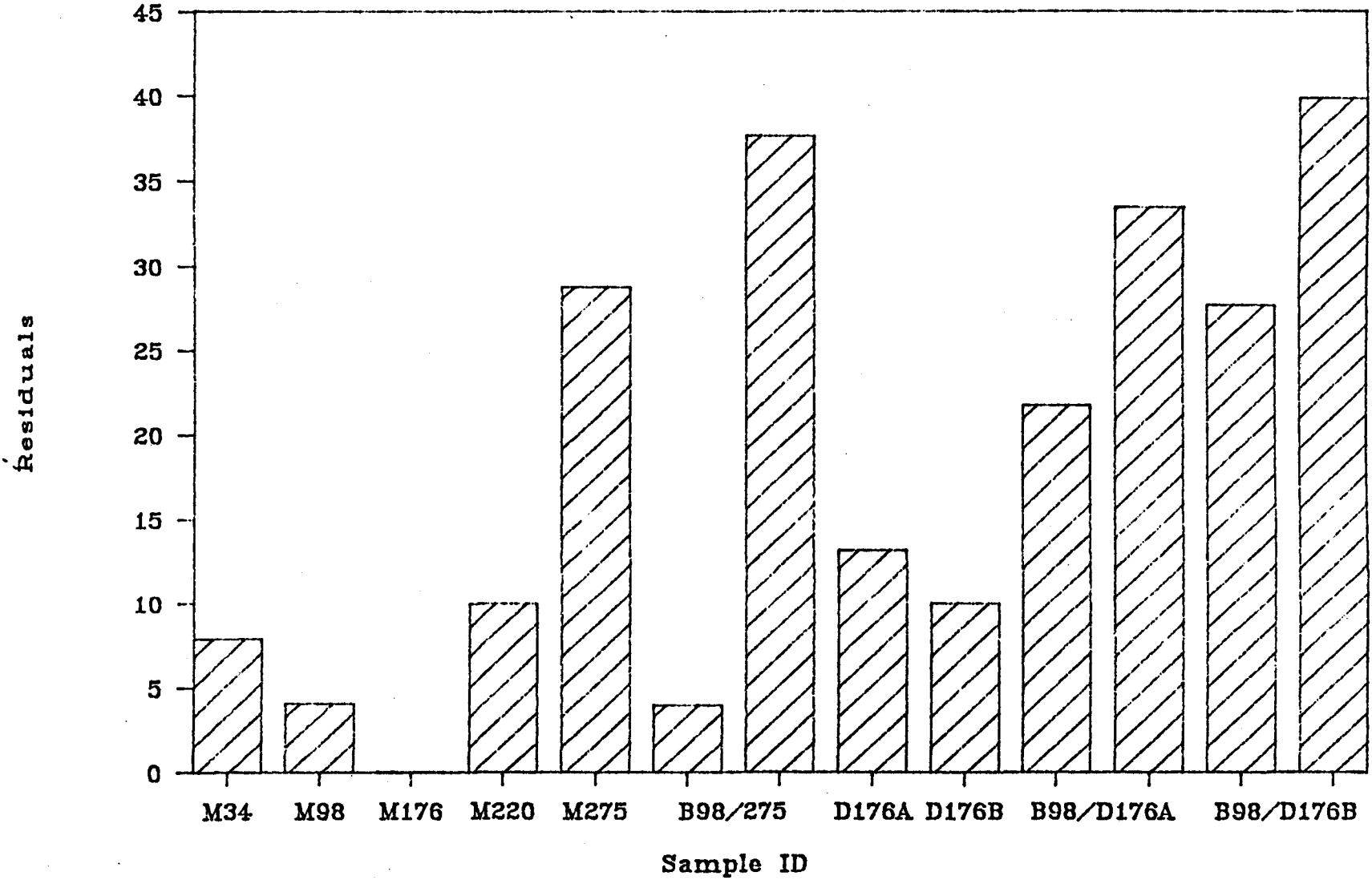
Figure 5.11 – Residual Bar Graph

Weighted Non-Linear Least Squares
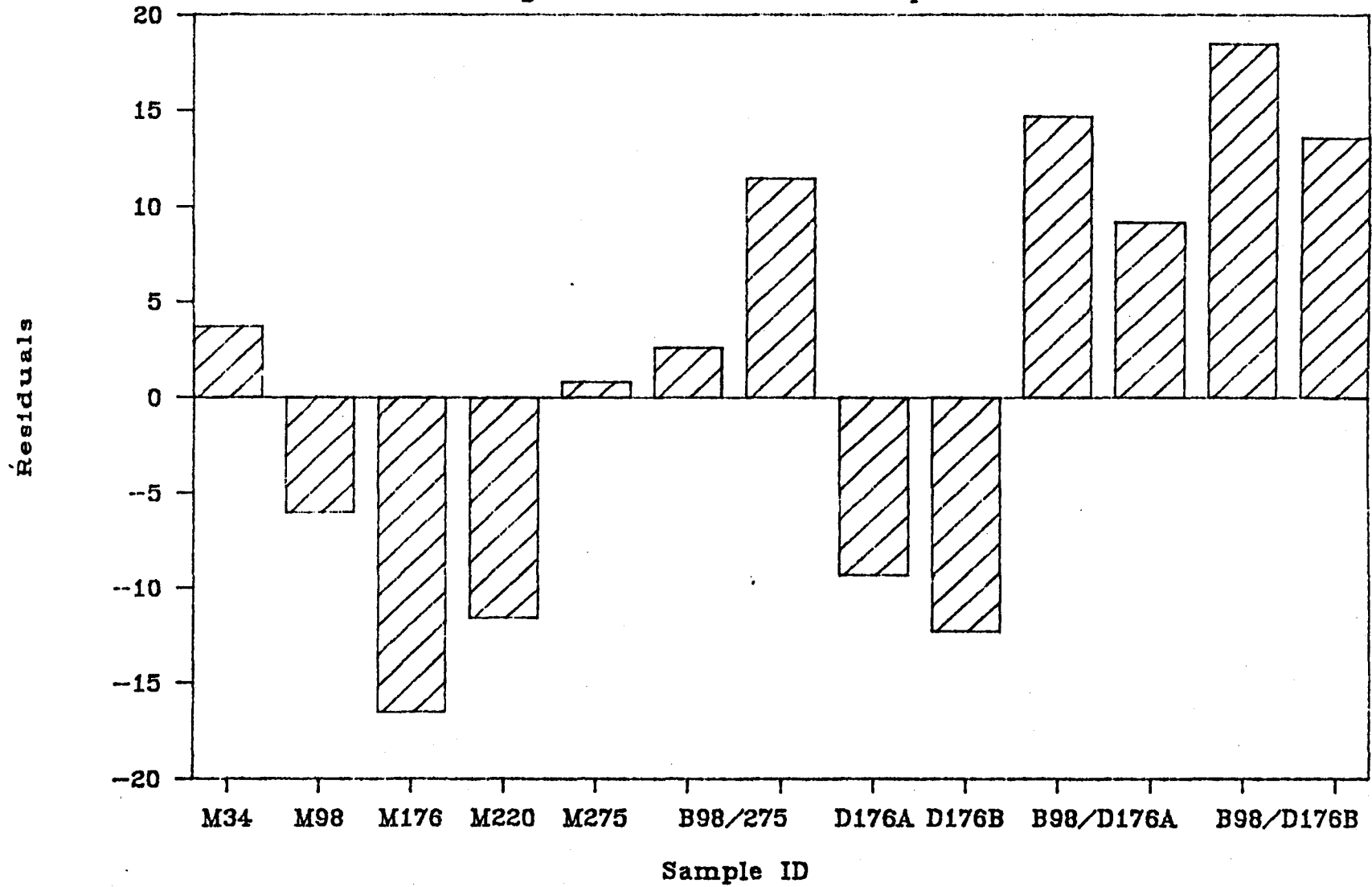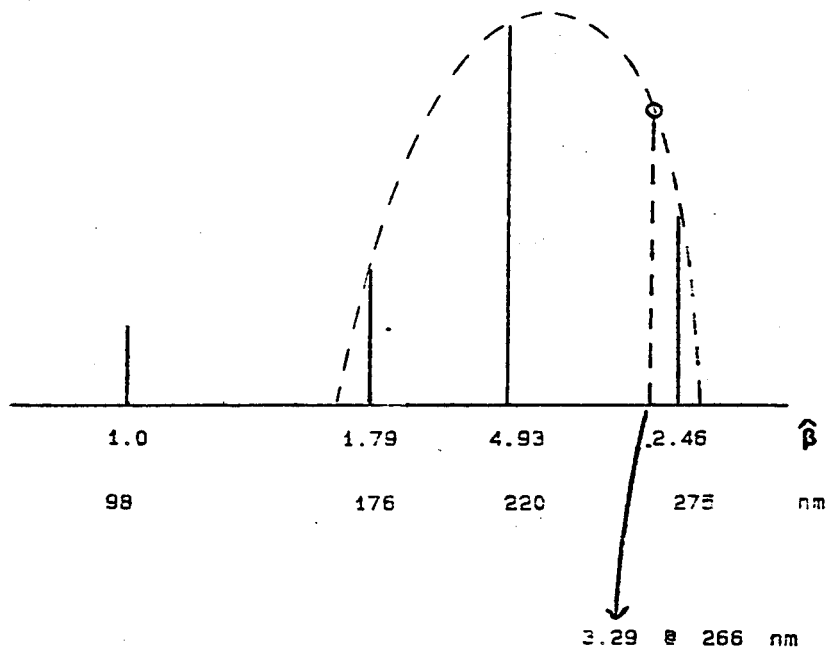
Figure 5.12 – Intensity ratio diagram for sample B98/275

This, of course, also holds for the unimodal polydisperse samples D176-A and D176-B.

A further drawback of these types of models is that they are too simple to adequately fit the data. Figures 5.13 and 5.14 are the residual plots from the analyses of samples M34 (ITYPE=4) and B98/275 (ITYPE=5) respectively. The residuals in these figures are the difference between the first-order, normalized autocorrelation function, $g^{(1)}(\tau)$, and that reconstructed from the model parameters. From the behaviour of the residuals, it is apparent that the model is not sufficiently utilizing all the information available in the data.

5.3.2.2 Linear Least Squares Estimation

Parameter estimation results from model types six, seven and eight are presented in this section; refer to table 4.15. Respectively, these models contain two, three and four parameters. These parameters were all pre-exponential coefficients of a linear model. Thus, a linear least squares approach was used for parameter estimation. Estimates were obtained for given values of Γ corresponding to the known particle sizes; refer to equation (4.14). The focus of these models was on samples B98/275, D176-A, D176-B, B98/D176-A and B98/D176-B. The results are summarized in table 5.12.

Figure 5.13 – DLS Residuals
Sample M34 – Non-Linear Least Squares
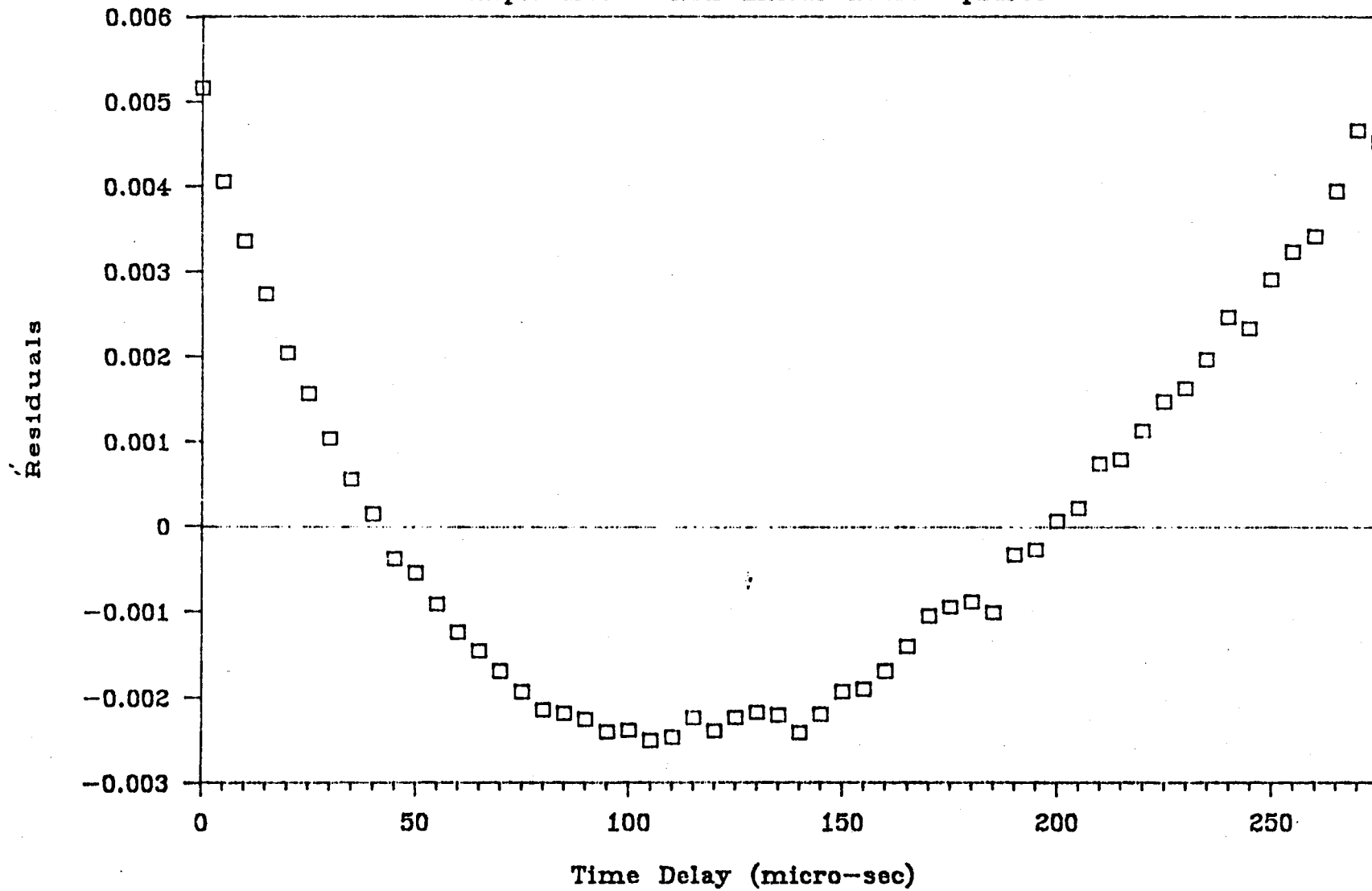
Figure 5.14 – DLS Residuals

Sample B98/275 – Non-Lin. Least Squares
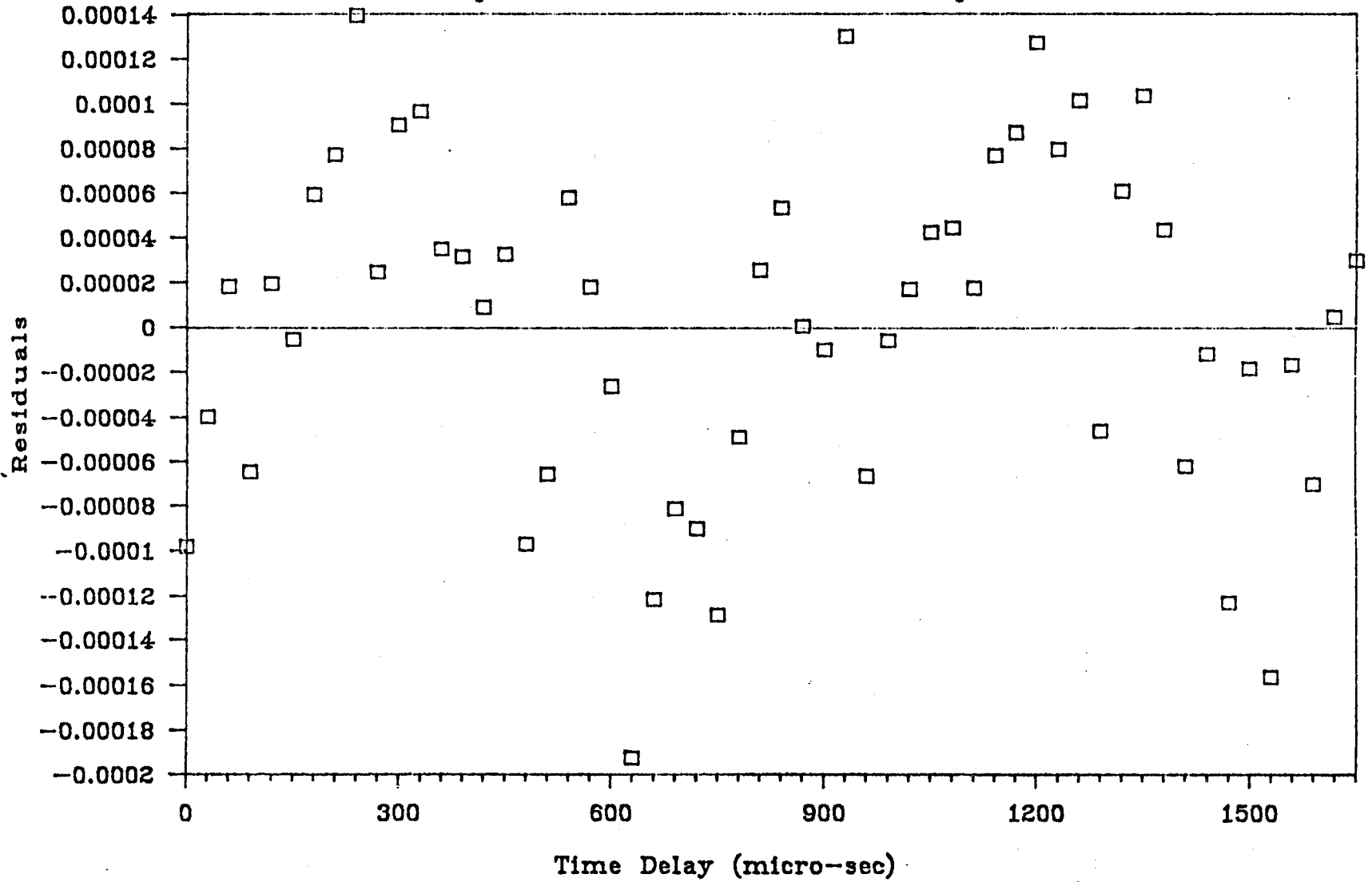
The first thing that is apparent from these results is that, with the exception of sample B98/275, one parameter estimate was negative indicating a negative contribution to the total measured intensity for that given particle size. These negative results are entirely spurious and offer no insight into the nature of the sample.

Once again, the tendency to place more emphasis on the contribution to the total intensity by the larger particles is evident by the greater parameter estimates at the larger given particle sizes. Employing the weighting factors from the previous section did little to improve these results.

Converting the results to intensity ratios relevant to 98 nm particles, and comapring them with those predicted from the Mie theory proved the experimental results to be wildly divergent from what might be expected. Here, we run across a problem inherent in fitting linear sums of exponentials; extremely high correlation between the parameter estimates. In the models with greater than two parameters, the elements of the parameter correlation matrix exceeded 0.99, and were often greater than 0.999. High correlation between parameter estimates was also present in the results from ITYPE=5 discussed previously. However, in the case of applying a linear exponential model to dynamic light scattering data, the physical relationship between the model and the light scattering process has been removed by eliminating the degree of freedom offered in fitting the exponent in

TABLE 5.12

Summary of Results Obtained from Linear Least Squares Estimation
ITYPE = 6, 7, 8

| Sample ID | ITYPE | Parameter Estimates | | | |
		$\hat{\beta}_1$	$\hat{\beta}_2$	$\hat{\beta}_3$	$\hat{\beta}_4$
B98/275	6	0.0266	0.6017	—	—
D176-A	7	0.2205	-0.0252	0.4754	—
D176-B	7	0.2464	-0.0334	0.4628	—
B98/D176-A	6	-0.0145	0.6889	—	—
	8	0.0478	0.2529	-0.0928	0.4716
B98/D176-B	6	-0.0063	0.7048	—	—
	8	0.0427	0.3615	-0.2669	0.5662

the model. The linear exponential model is entirely empirical in nature.

A further serious drawback to this method is that prior knowledge regarding the particle sizes is required.

5.3.2.3 Exponential Sampling

The discussion of the results from the exponential sampling technique is presented in two parts corresponding to Ostrowsky's method using linear least squares, and Morrison's method using non-negatively constrained linear least squares.

Ostrowsky's Method

In all of the results presented below, Ostrowsky's method was applied to fit five pre-exponential coefficients (m=5) over six shifts (n=6). Thus, thirty parameter estimates were used to re-construct the particle size distributions.

Figure 5.15 is a re-constructed particle size distribution (PSD) from 30 parameter estimates for the monodisperse sample M98. This figure is typical of the results obtained using Ostrowsky's method. While the intensity average particle size diameter of the re-constructed distribution is 112.4 nm, the range of particle sizes for which positive estimates were is obtained was quite broad; 34 – 280 nm. As with the linear models, ITYPE = 6, 7, 8, several small negative parameter estimates were obtained. A summary of results from

the remaining samples is given in table 5.13.

The results in table 5.13 represent the smoothest re-constructed PSD's obtained over a variety of trials with different values of ω_{max} and the initial starting diameter D_0. It was found that the quality of the fit was greatly dependent upon the choices of ω_{max} and D_0. Generally, as the starting diameter value increased, nonsensical estimates were obtained. This is a result of forcing the model to estimate parameters at higher and higher particle sizes far beyond the actual value. Recall that the scale is logarithmic with respect to the particle sizes. Also, as the value of ω_{max} decreased, the re-constructed PSD deteriorated into an oscillatory function with large negative parameter estimates. This is a result of restricting the parameter estimates to a narrower range of particle sizes. The results presented in table 5.13 strike a balance between these two extremes. Ostrowsky's recommendation of a minimum ω_{max} value of 3.0 provided consistent results for the unimodal samples. Note that the initial starting diameter increased as the size of the particles in the sample increased. For the bimodal samples, the chosen value of ω_{max} is consistent with Ostrowsky's recommendation that adjacent maxima positions be approximately in the ratio $\exp(2\eta/\omega_{max})$ in order for resolution of the peaks to occur. While the peaks of the bimodal samples were resolved, the re-constructed distribution itself was poorly behaved as figure 5.16 demonstrates.

As in section 5.3.2.1 , the $\hat{D}_i$'s in table 5.13 were biased towards over estimation. Therefore, the parameters were re-estimated and the $\hat{D}_i$'s re-calculated with the data weighted according to equation (5.12) with NEX1 = 2 and NEX2 = 1.1 as before. These results are summarized in table 5.14. Figures 5.17 and 5.18 are stacked bar graphs of the $\hat{D}_i$ residuals and the estimated distribution width for the unweighted and weighted cases respectively. The residuals are the estimated $\hat{D}_i$'s minus the known value. Looking at the residuals portion of the graph, it is apparent that weighing the data has yielded better overall results. The sum of squares of the residuals was reduced to 8,930 from 36,500, and the residuals themselves were not all positive. However, weighing the data had little effect on the width of the estimated distribution.

With respect to the estimated intensity ratios, the weighted data shifted the emphasis far too greatly on the data at low time lags. This is shown in table 5.15 where the unweighted estimates of the intensity ratios for samples B98/D176-A and B98/D176-B are much closer to the expected ratio of 9.17:1 than are the weighted estimates. This was not entirely unexpected since, in the weighted case, we are now placing more emphasis on an entire distribution of parameter estimates as opposed to just one, as was the case in section 5.3.2.1.

Thus, as was the case with the NICOMP Model TC-200, there are some trade-offs between obtaining good estimates of the particle sizes and the modal ratio for bimodal samples.

Figure 5.15 – Reconstructed PSD

Sample M98 – Ostrowsky's Method
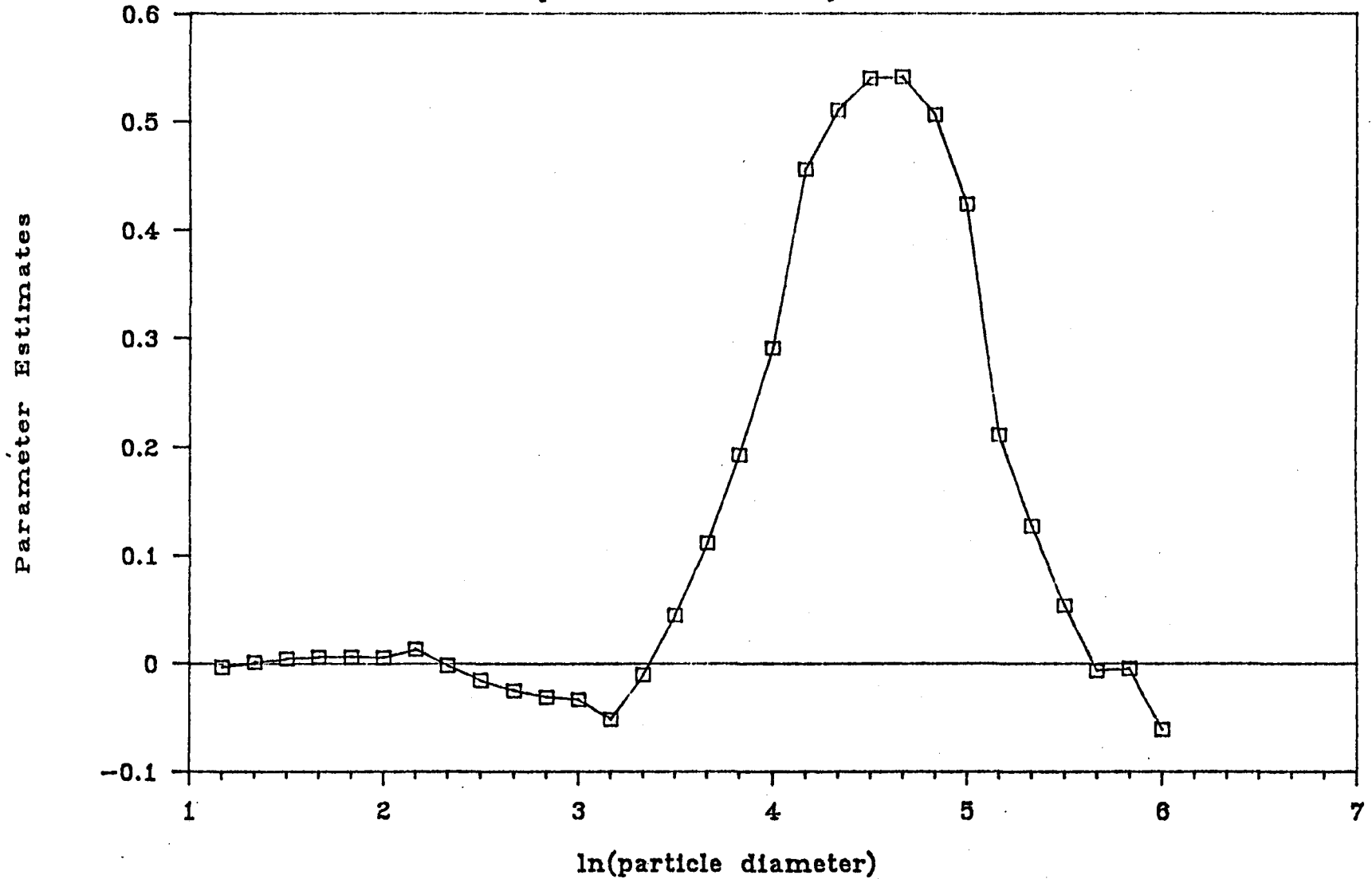
Figure 5.16 – Reconstructed PSD

Sample B98/275 – Ostrowsky's Method
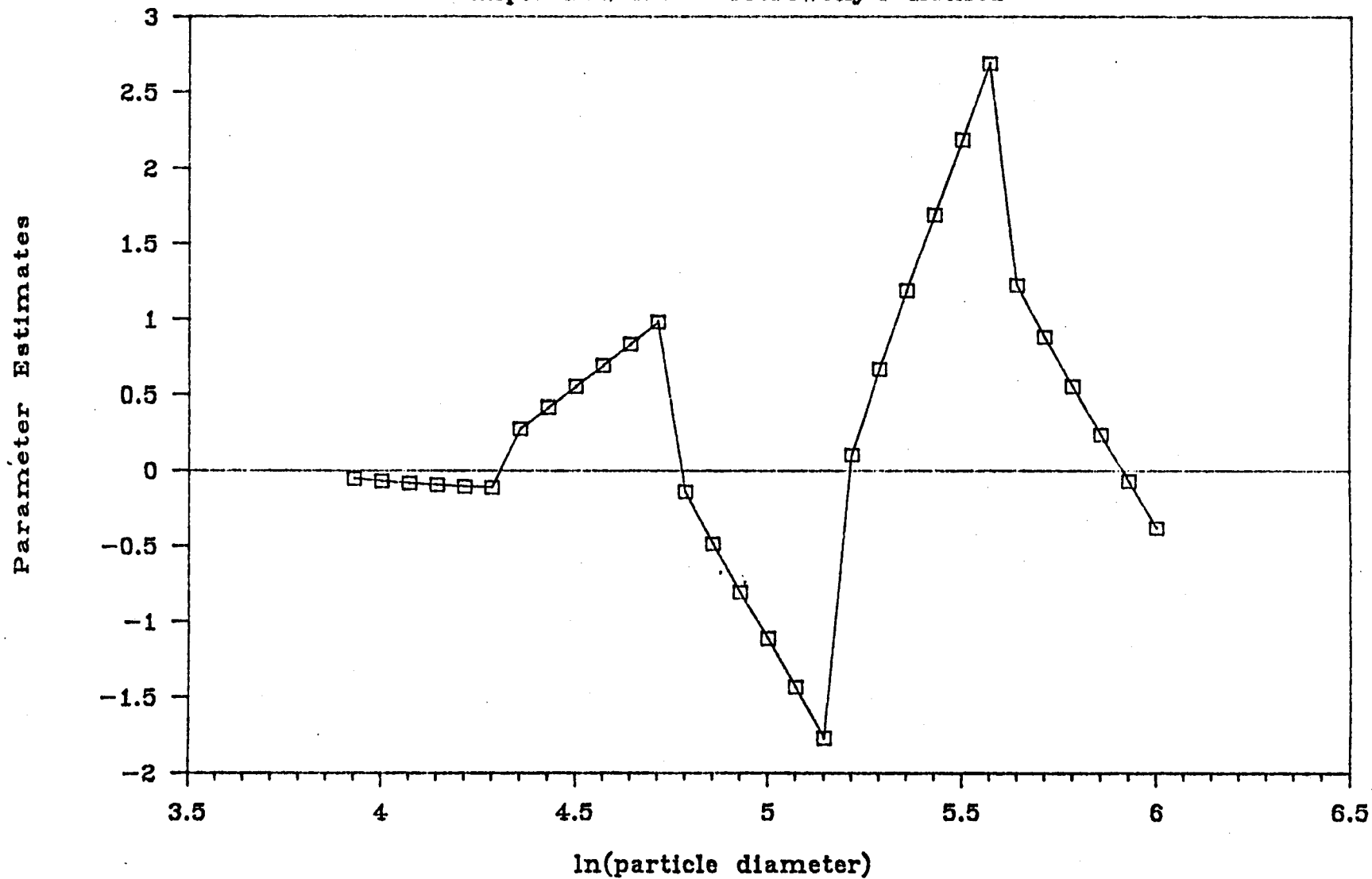
TABLE 5.13

Summary of Results Obtained from Ostrowsky's Method of Exponential Sampling
ITYPE - 3

| Sample ID | ω_{max} | D_o | Estimated Weight Average Particle Size and Range (nm) | | | |
			$(\widehat{D_i})_1$	$Range_1$	$(\widehat{D_i})_2$	$Range_2$
M34	3.5	2.0	46.3	14 - 153	-	-
M98	3.0	3.0	112.4	34 - 280	-	-
M176	3.0	5.0	196.2	57 - 467	-	-
M220	3.0	10.0	287.8	81 - 600	-	-
M275	3.0	10.0	355.3	115 - 785	-	-
B98/275	7.0	50.0	99.8	78 - 114	270.1	192 - 377
D176-A	3.0	10.0	294.1	81 - 600	-	-
D176-B	3.0	10.0	283.3	81 - 600	-	-
B98/D176-A	7.0	50.0	101.5	78 - 122	251.9	132 - 377
B98/D176-B	6.0	30.0	104.7	65 - 132	248.9	157 - 377
R2-20	3.0	40.0	1454.0	460 - 3140	-	-

TABLE 5.14

Summary of Results Obtained from Ostrowsky's Method of Exponential Sampling
with Weighting Applied, ITYPE = 3 (NEX1 = 2, NEX2 = 1.1)

Sample ID	ω_{max}	D_o	Estimated Weight Average Particle Size and Range (nm)			
			$(\widehat{D_i})_1$	Range$_1$	$(\widehat{D_i})_2$	Range$_2$
M34	3.5	2.0	41.2	10 - 114	-	-
M98	3.0	3.0	104.0	29 - 280	-	-
M176	3.0	5.0	182.1	57 - 467	-	-
M220	3.0	10.0	262.2	81 - 554	-	-
M275	3.0	10.0	331.8	97 - 785	-	-
B98/275	7.0	50.0	99.4	78 - 114	256.3	192 - 350
D176-A	3.0	10.0	264.3	81 - 554	-	-
D176-B	3.0	10.0	260.4	81 - 554	-	-
B98/D176-A	7.0	50.0	84.7	60 - 105	211.0	110 - 352
B98/D176-B	6.0	30.0	80.0	55 - 102	217.8	111 - 377
R2-20	3.0	40.0	1348.3	387 - 3140	-	-

Figure 5.17 − Residual/Range Bar Graph

Ostrowsky's Unweighted Results
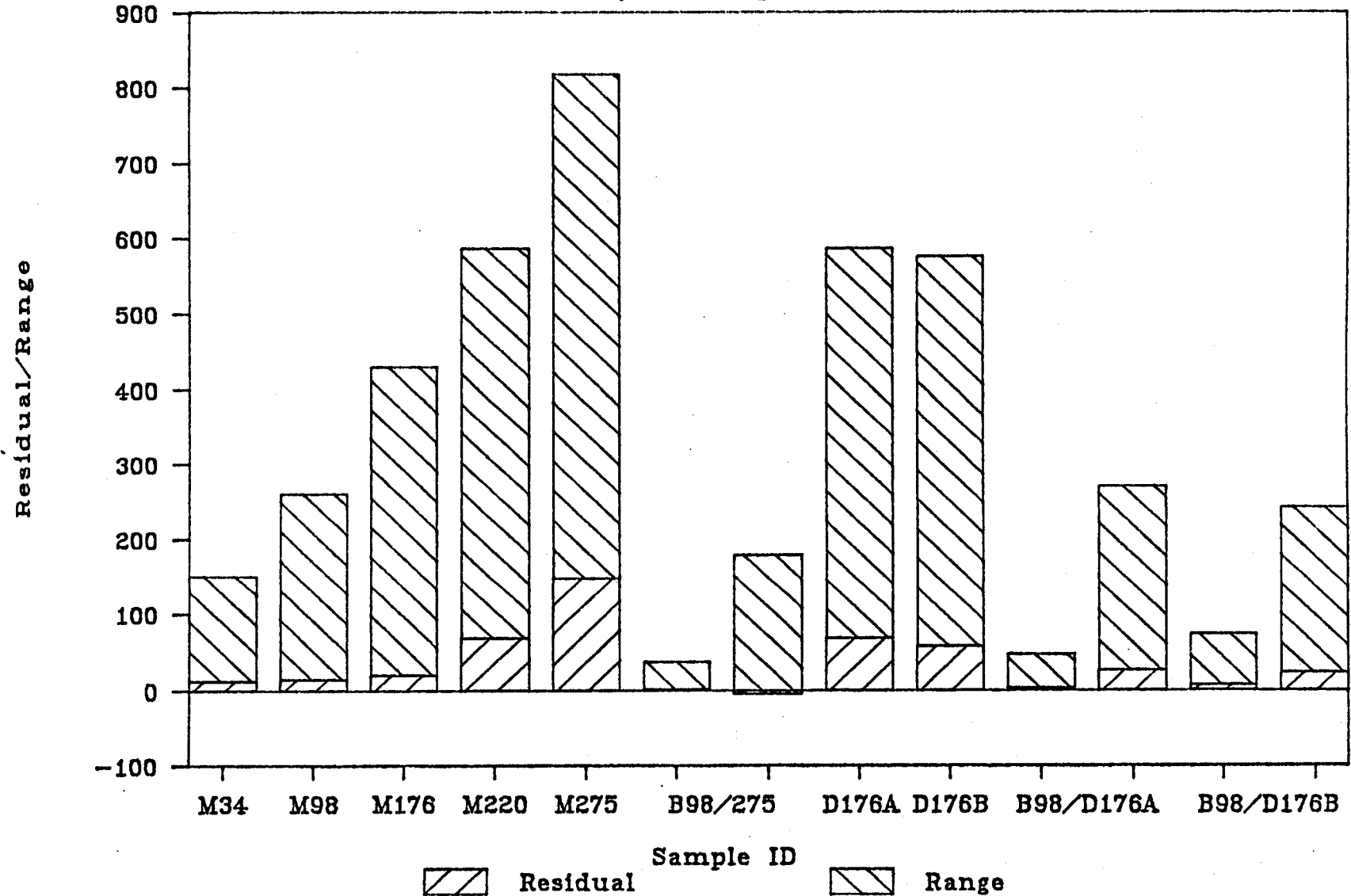
Figure 5.18 – Residual/Range Bar Graph

Ostrowsky's Weighted Results
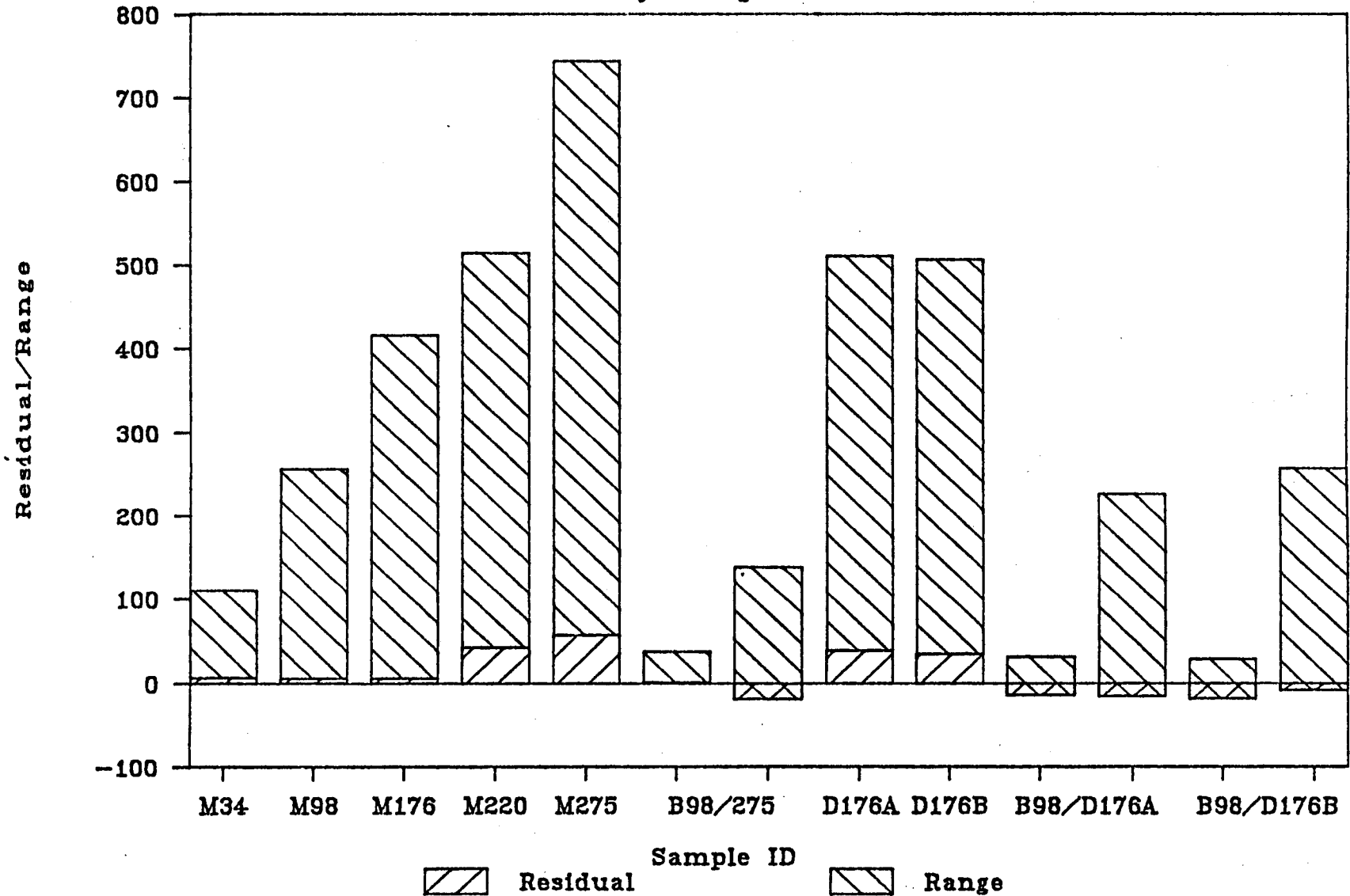
TABLE 5.15

Comparison of Calculated (Mie Theory) and Experimentally Determined (DLS)
Bimodal Intensity Ratios, ITYPE = 3

| Sample ID | Ratio | Intensity Ratios | | |
		Calculated	Experimental (unweighted)	Experimental (weighted)
B99/275	$\dfrac{2750}{980}$	$\dfrac{2.45}{1}$	$\dfrac{3.04}{1}$	$\dfrac{2.92}{1}$
B99/D176-A	$\dfrac{D1760}{980}$	$\dfrac{9.17}{1}$	$\dfrac{7.46}{1}$	$\dfrac{2.56}{1}$
B98/D176-B	$\dfrac{D1760}{980}$	$\dfrac{9.17}{1}$	$\dfrac{6.97}{1}$	$\dfrac{2.12}{1}$

Morrison's Method

In this section, results from Morrison's method of exponential sampling using non-negative linear least squares (NNLLS) will be presented. For comparison purposes, 30 parameter estimates for all the samples were obtained using the exact same ω_{max} and D_0 values given in table 5.13 (unweighted case). The results from these runs were virtually identical to those given in table 5.13. Figure 5.19 demonstrates how closely the re-constructed PSD's matched for sample M98. The major difference was that there were no negative estimates obtained with the NNLLS. This comparison establishes the near equivalency of the two methods for given values of ω_{max} and D_0.

As Morrison suggested, a sum of 20 exponentials per shift was then fit to the data. Again, six shifts were used, thus a total of 120 estimates were obtained for distribution re-construction. Table 5.16 summarizes the results obtained. The value of ω_{max} was no longer constrained to being less than ten as it was in Ostrowsky's method as none of the problems with large negative parameter estimates and oscillatory behaviour were encountered. Thus, the resolution on the logarithmic scale was greatly increased and superior PSD's were estimated as figure 5.20 and 5.21 demonstrate. The stacked bar graph in figure 5.22 is clearly an improvement from that in figure 5.18. The width of the fitted distributions are much narrower than previously giving a more accurate picture of the nature of the sample, and overall, the residuals were smaller. The sum of squares of the

TABLE 5.16

Summary of Results Obtained from Morrison's Method of Exponential Sampling
ITYPE = 1

Sample ID	ω_{max}	D_o	Estimated Weight Average Particle Size and Range (nm)			
			$(\widehat{\overline{D_i}})_1$	$Range_1$	$(\widehat{\overline{D_i}})_2$	$Range_2$
M 3 4	10.0	2.0	37.2	27 - 49	-	-
M 9 8	10.0	4.0	95.4	71 - 127	-	-
M 1 7 6	10.0	20.0	171.2	125 - 222	-	-
M 2 2 0	30.0	120.0	219.9	198 - 240	-	-
M 2 7 5	50.0	150.0	291.0	275 - 309	-	-
B98/275	30.0	50.0	105.5	95 - 115	315.7	286 - 347
D 1 7 6 - A	15.0	50.0	230.0	188 - 277	-	-
D 1 7 6 - B	15.0	50.0	226.3	182 - 267	-	-
B99/D176-A	25.0	50.0	120.0	106 - 134	259.1	231 - 290
B98/D176-B	20.0	50.0	88.8	76 - 101	223.2	195 - 260
R 2 - 2 0	20.0	200.0	1188.0	1014 - 1352	-	-

Figure 5.19 — Reconstructed PSD's

Sample M98 — Ost. and Morr. Methods
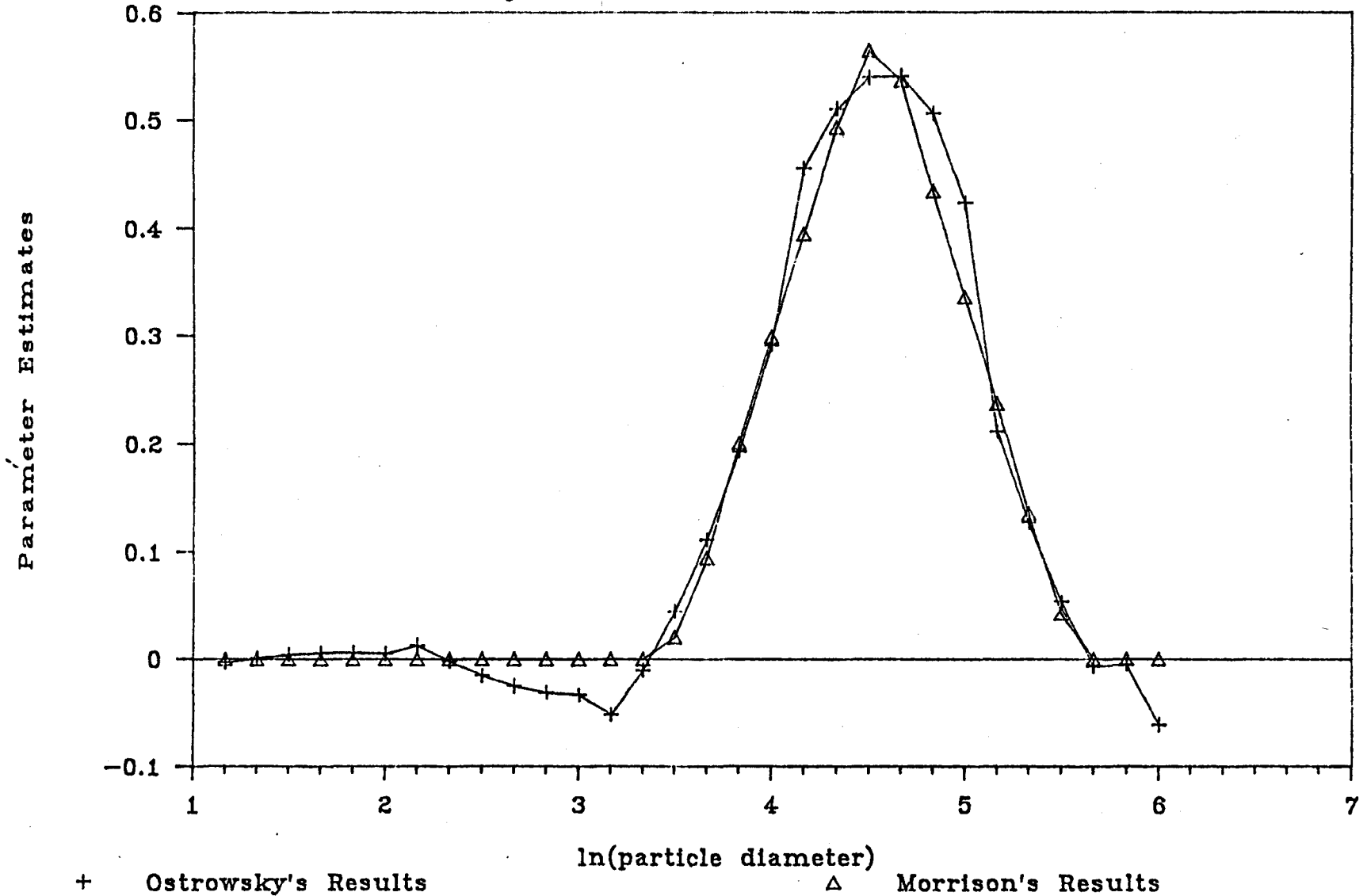
Figure 5.20 – Reconstructed PSD

Sample M220 – Morrison's Method

Parameter Estimates

ln(particle diameter)
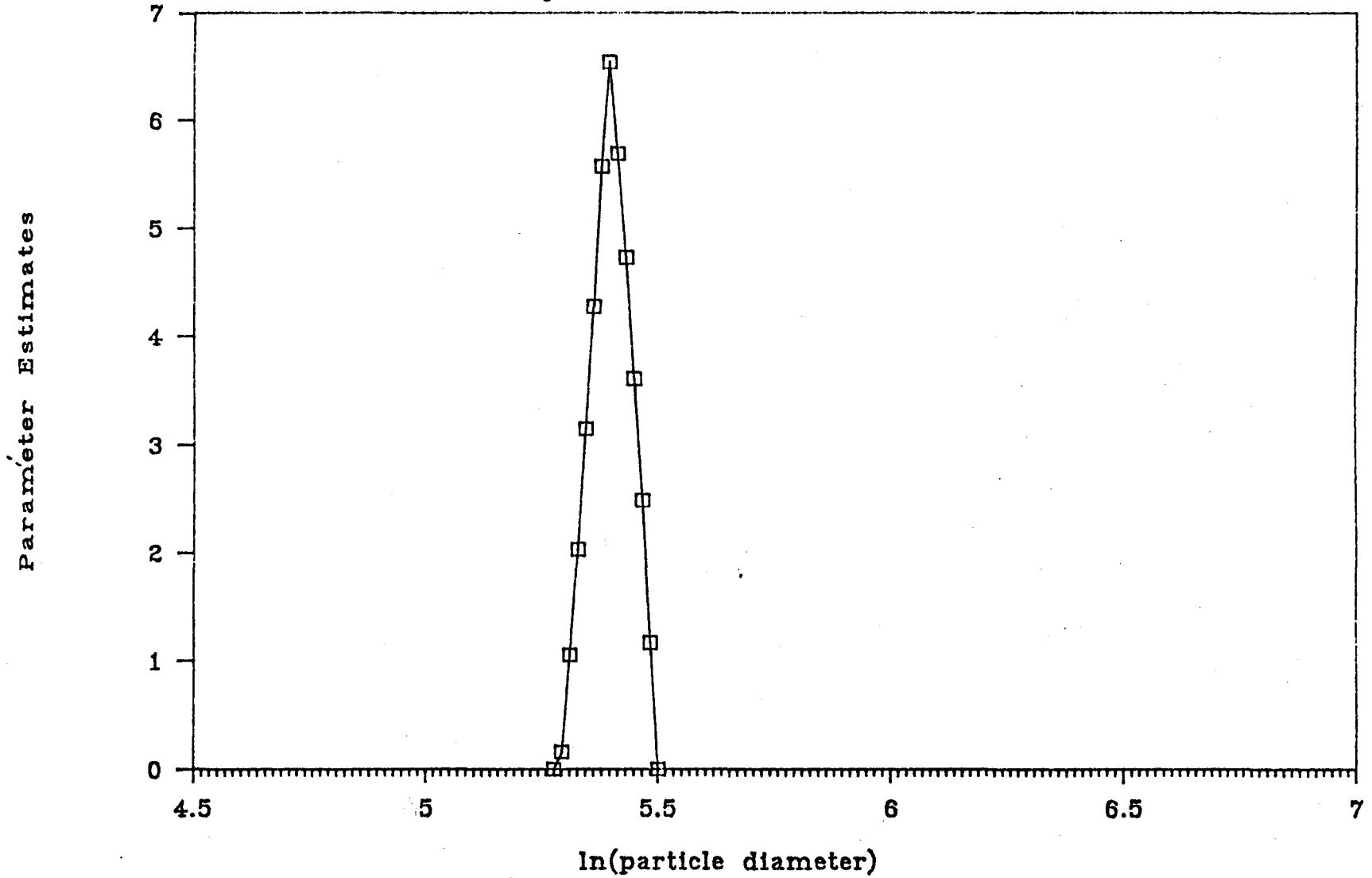
Figure 5.21 – Reconstructed PSD

Sample B98/D176-A – Morrison's Method
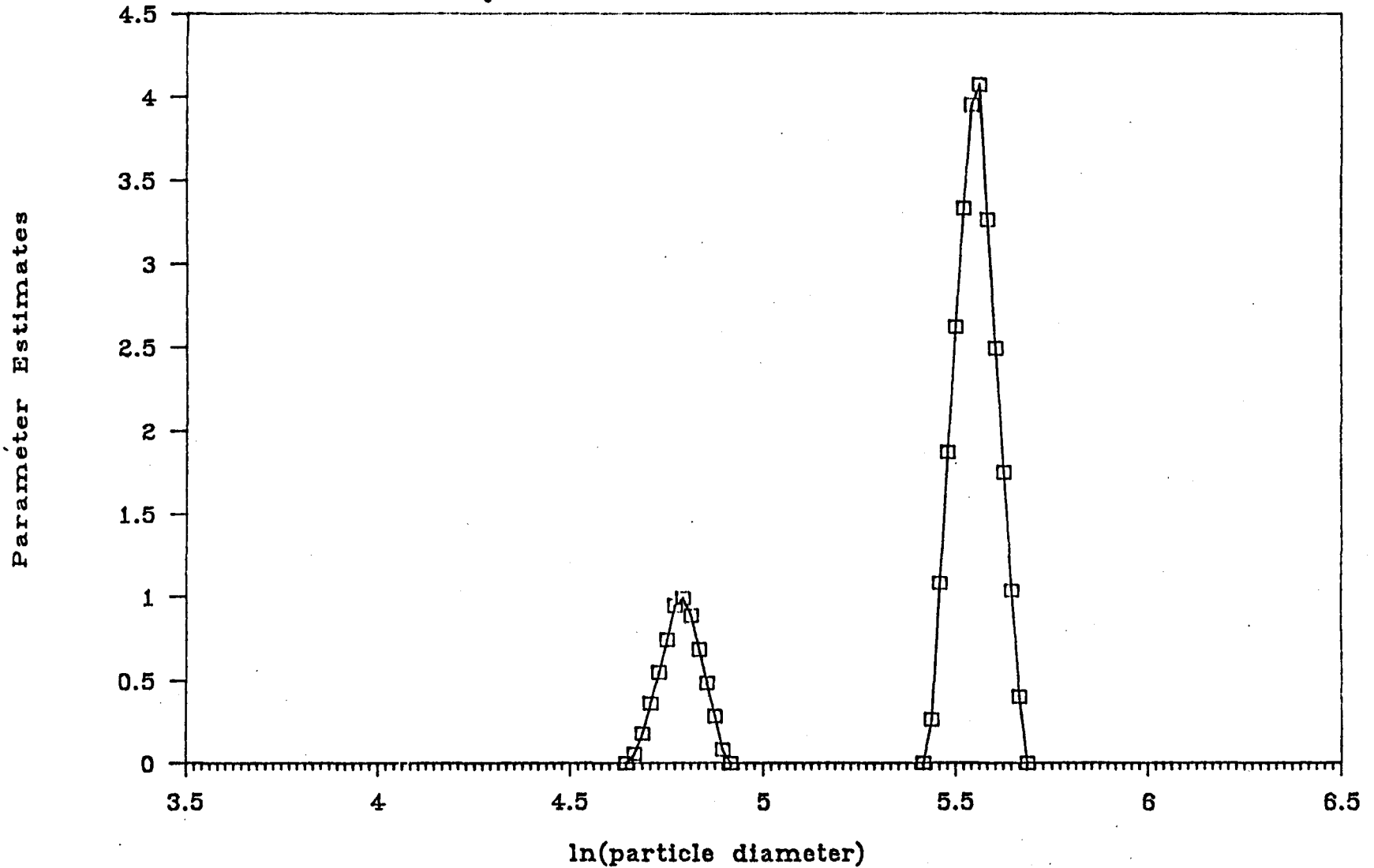
Figure 5.22 – Residual/Range Bar Graph

Morrison's Unweighted Results

163
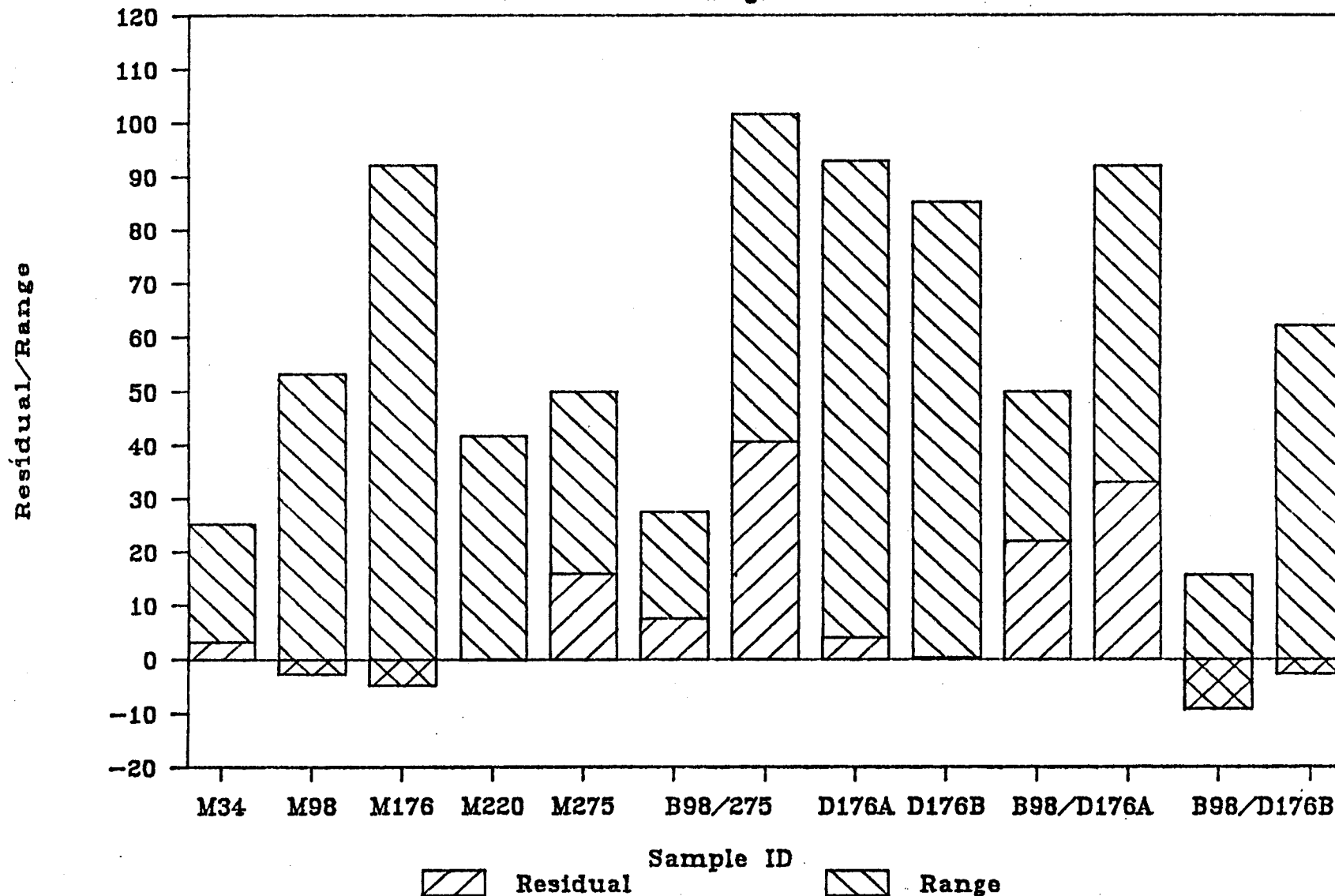
residuals was 3,700; an improvement from 8,930 for the weighted Ostrowsky results.

Morrison's method was also used to fit distributions to weighted data (NEX1 = 2 and NEX2 = 1.1). Since the results from the raw, unweighted data were already quite good, a similar improvement in the results that was obtained with Ostrowsky's method was not expected here. Indeed, the results were very similar, the sum of squares of the residuals being 3,310, compared with 3,670. It may be argued that with the increased resolution available through Morrison's method, weighing the data should be unneccesary. The re-constructed distribution are almost symmetrical about the peak with respect to the absolute diameter (not the logarithmic diameter), and non-zero estimates are not obtained at the higher values on the logarithmic scale. When the resolution is poor, it is these estimates far from the peak on the logarithmic scale that lead to the over-estimation of the average particle sizes observed in Ostrowsky's method. Thus, weighing the data to counteract the emphasis of higher particle sizes was not required.

The estimated intensity ratios for the bimodal sample B98/275, B98/D176-A and B98/D176-B were 5.08:1, 4.18:1 and 14.51:1 respectively. These do not compare very well with 2.45:1 (B98/275) and 9.17:1 (B98/D176-A and B), nor are they as good as the estimates obtained with Ostrowsky's method; refer to table 5.15, unweighted case. Thus, although bimodal peak resolution and position had

improved over Ostrowsky's method, this method does not appear to be as sensitive to relative proportions. Constraining the estimates to be non-zero may also be forcing a mal-distribution of the relative parameter magnitudes in each mode, thus yielding an erroneous intensity ratio estimate.

5.3.2.4 Residuals

The residuals from fitting the autocorrelation function to the sums of exponentials were calculated for each shift. Thus, six sets of residuals were obtained for a total of either 30 or 120 residuals for Ostrowsky's and Morrison's methods respectively. Residual plots for each set of estimated parameters proved to be nearly identical, thus an average of the six residuals was taken as representative. Figures 5.23 and 5.24 are the residual plots from Ostorwsky's and Morrison's methods for sample M98. It is apparent from these figures that the residuals are correlated. This is not too surprising given the nature of the models used to fit the raw data. In the simpler cases of fitting one or two exponential functions to data of exponential form, the residuals from the fit will certainly be correlated as figures 5.13 and 5.14 showed.

For residuals whose behaviour is that of a first-order autocorrelation function, AR(1), a transformation of the data may be applied that will remove this correlation, refer to Kadiyala (1968) and Riddell (1977). Instead of estimating the parameters β in the model

Figure 5.23 — DLS Residuals

Sample M98 — Ostrowsky's Method
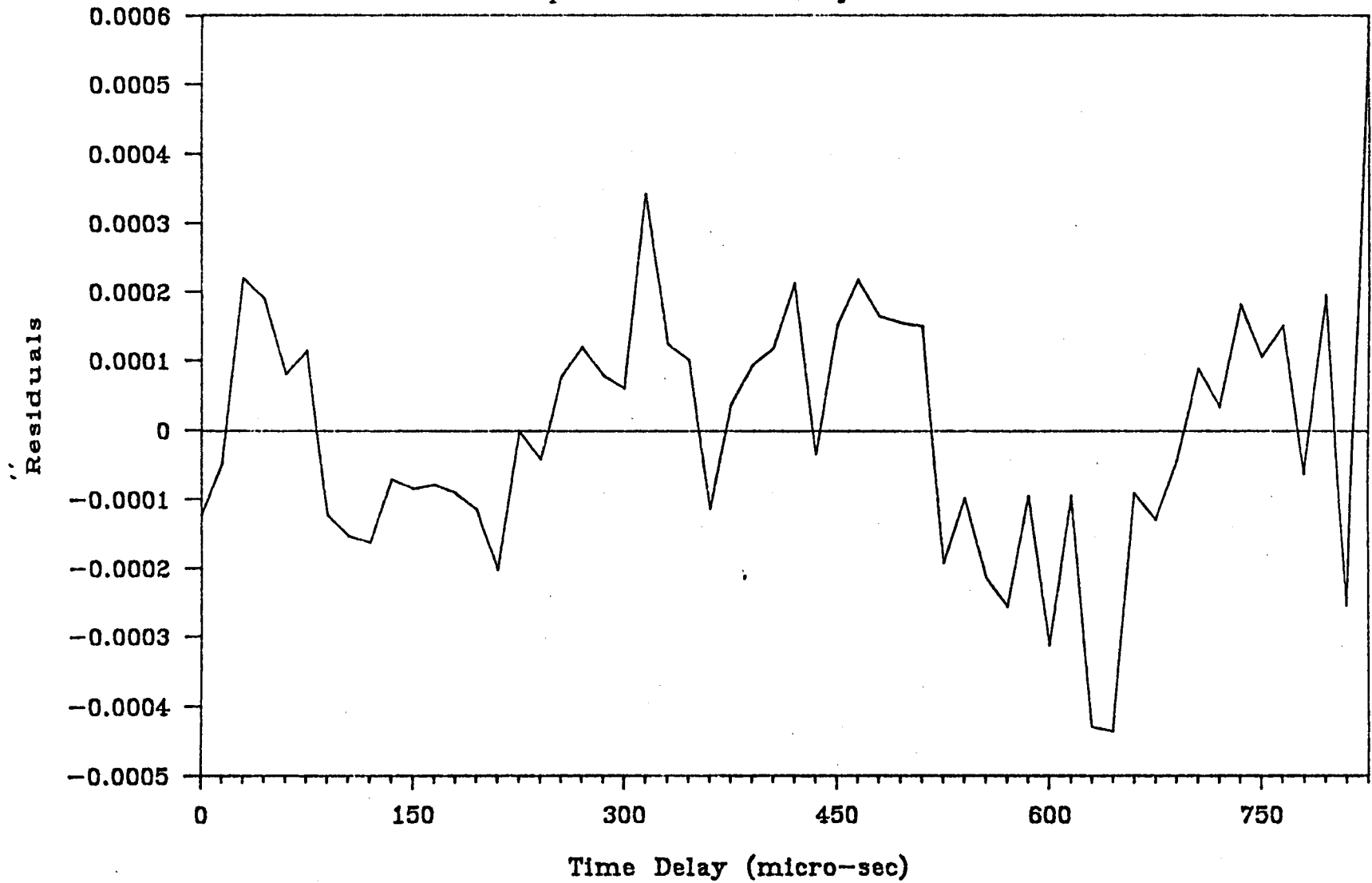
Figure 5.24 – DLS Residuals

Sample M98 – Morrison's Method
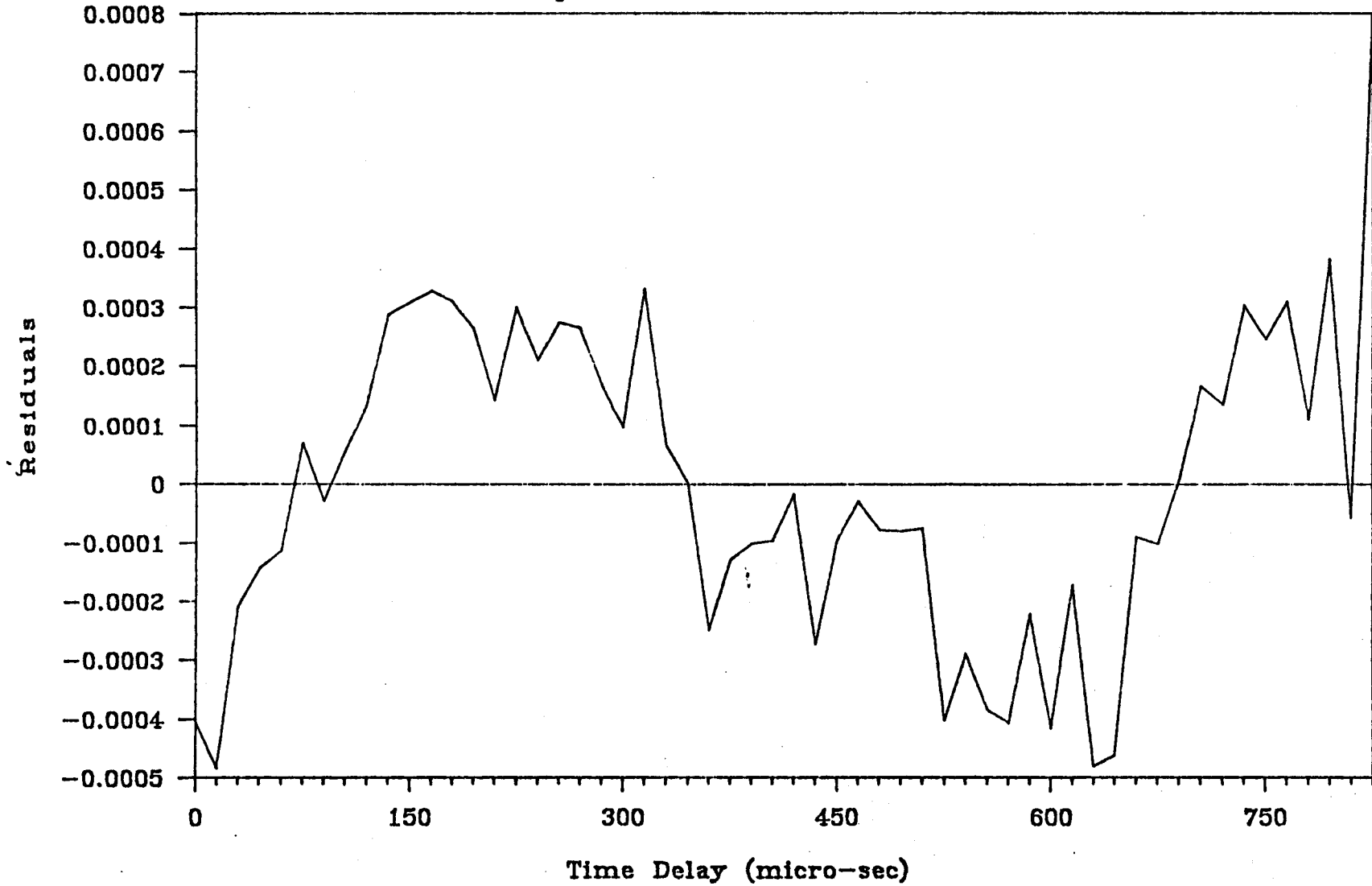
$$\underline{Y} = \underline{X}\beta + \underline{e} \qquad\qquad (5.13)$$

where the residuals, $\underline{e}$, follow an AR(1) behaviour, estimate the parameters β^* in the transformed model

$$\underline{W} = \underline{Z}\beta^* + \underline{u} \qquad\qquad (5.14)$$

where

$$\underline{W} = \underline{C}\underline{Y} \qquad\qquad (5.15)$$
$$\underline{Z} = \underline{C}\underline{X} \qquad\qquad (5.16)$$
$$\underline{u} = \underline{C}\underline{e} \qquad\qquad (5.17)$$

The transformation matrix $\underline{C}$ is

$$\underline{C} = \begin{bmatrix} (1-\phi^2)^{1/2} & 0 & 0 & \dots & 0 & 0 & 0 \\ -\phi & 1 & 0 & \dots & 0 & 0 & 0 \\ \cdot & \cdot & \cdot & & \cdot & \cdot & \cdot \\ \cdot & \cdot & \cdot & & \cdot & \cdot & \cdot \\ 0 & 0 & 0 & \dots & -\phi & 1 & 0 \\ 0 & 0 & 0 & \dots & 0 & -\phi & 1 \end{bmatrix} \qquad (5.18)$$

where ϕ is the autocorrelation coefficient in the first-order autocorrelation function

$$e_t = \phi\, e_{t-1} + a_t \qquad\qquad (5.19)$$

and a_t is random noise.

This type of transformation lends itself very well to the non-negative linear least squares algorithm. Applying the transformation to equation (4.15), we now solve the transformed set of linear equations for $\underline{X}^*$,

$$(\underline{C}\underline{A})_{nxp}\underline{X}^*_{px1} = (\underline{C}\underline{B})_{nx1} \qquad \text{subject to } \underline{X}^* \geqslant 0 \qquad (5.20)$$

This type of analysis was built into the estimation routine DLSPLOT and was chosen by selecting ITYPE = 2. However, an estimate of ϕ must be provided to the routine. This may be obtained from a time series analysis of the residuals by fitting them to an AR(1) model.

Using the time series package INTER84 available on the Chemical Engineering Department's VAX mini-computer at McMaster University, ϕ was estimated to be 0.844 for the data given in figure 5.24. It should be stated that an AR(1) model was found to be adequate for this data and no higher order terms were significant. The parameters in the transformed model were then re-estimated choosing ITYPE = 2. Figure 5.25 was the resulting reconstructed PSD for sample M98. While the shape of the distribution and the estimated intensity weighted particle size diameter did not change greatly ($\hat{D}_I$ = 95.3 as opposed to 95.4 from table 5.16), the residuals were much better behaved, see figure 5.26. This procedure was repeated for the other samples studied with similar results.

5.3.2.5 Summary

In the general case where no prior information regarding the sample is available, exponential sampling using non-negative linear least squares (Morrison's method) is recommended. Good estimates of the intensity weighted particle size diameters were obtained. The distribution of particles sizes fit were narrow for the monodisperse samples and close to the expected distribution for the polydisperse samples. The peaks of the bimodal were samples were also clearly resolved. Finally, the data need not be weighted for this method of analysis.

Figure 5.25 – Reconstructed PSD

Sample M98 – Transformed Morr. Method

Parameter Estimates

ln(particle diameter)
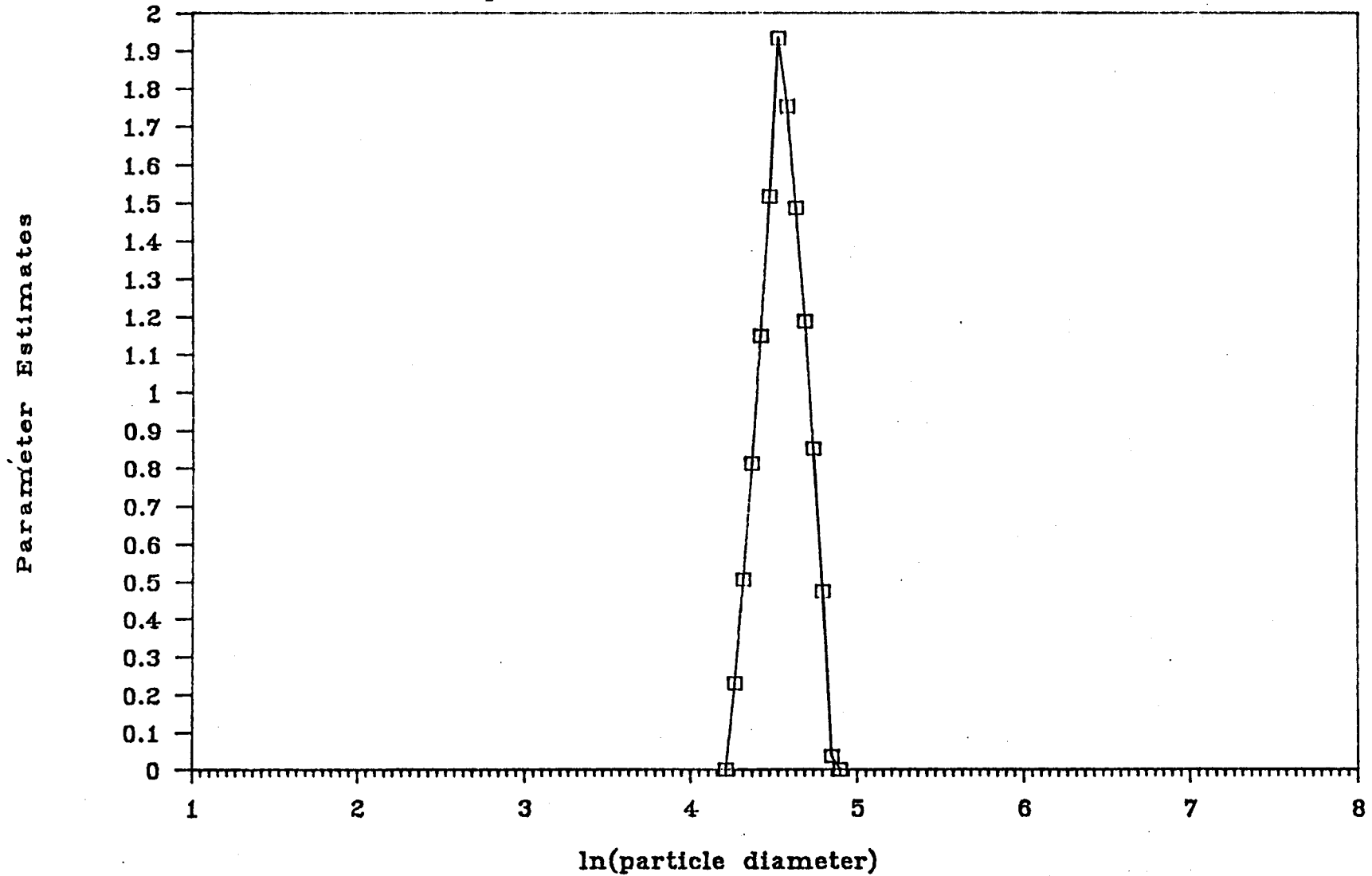
Figure 5.26 — Transformed DLS Residuals

Sample M98 — Morrison's Method

Time Delay (micro-sec)
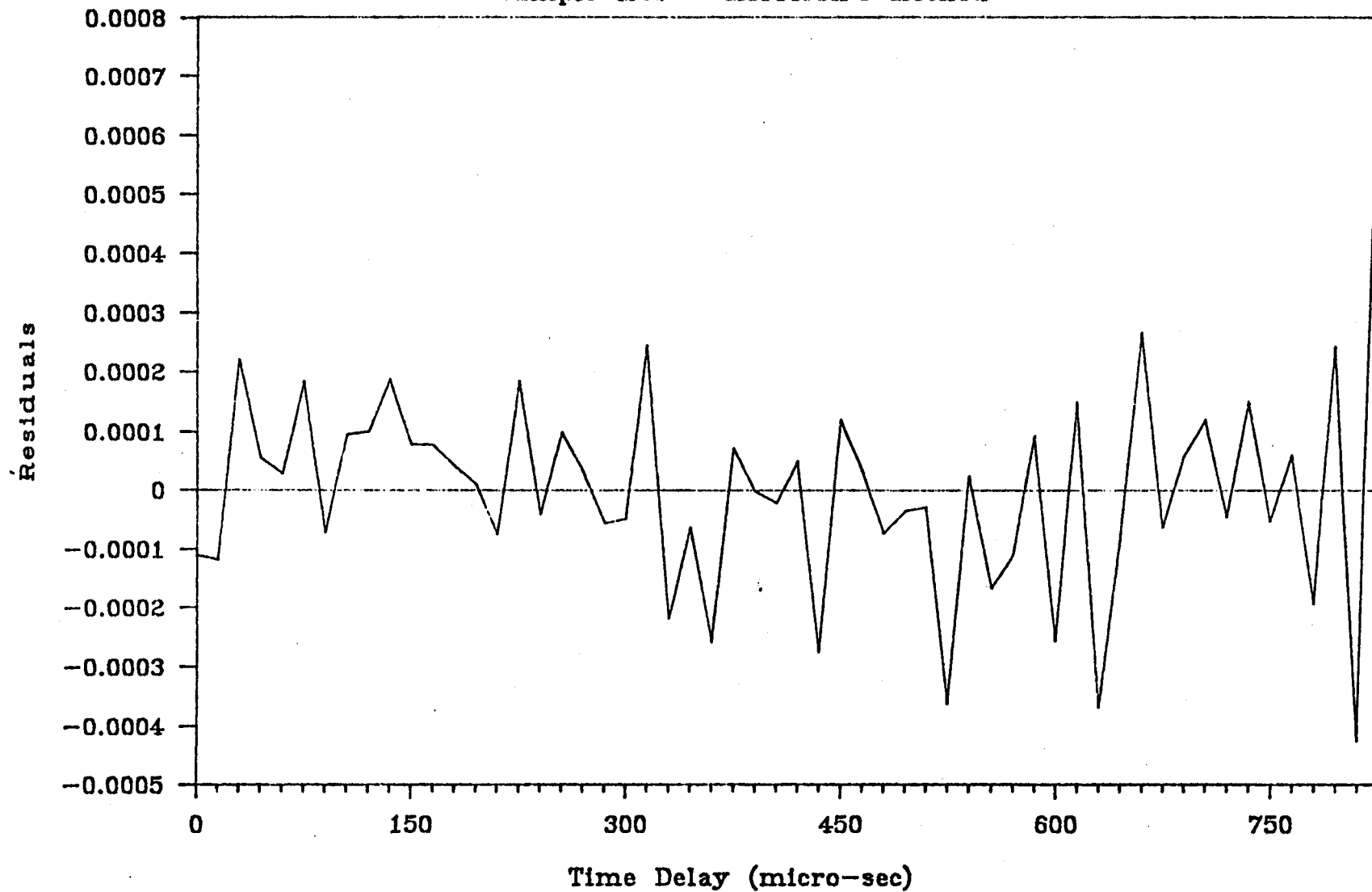
In addition, the transformation matrix in equation (5.18) was easily applied to this method. Although no significant change in the final results was observed, it it still desireable to uncorrelate the residuals to ensure they are not adversely affecting the results. This method does not however, appear to have the freedom that Ostrowsky's method does in providing good intensity ratio estimates for bimodal samples. If this information is important, the user may want to run both methods of analysis and cross-check the intensity ratio results and use those that are deemed the most appropriate, should they differ significantly.

If the experimenter knows his sample to be monodisperse (in one or more modes), or if just an estimate of the average particle size is required, he may use the simpler weighted non-linear least squares approach. However, the user must be wary that the weights used were empirical in nature. Non-negative least squares would still be preferred.

REFERENCES

BILLINGHAM, N.C. (1977), Molar Mass Measurements in Polymer Science, Kogan Page, London.

DEBYE, P. (1915), Ann. Physik, [4], 46, 809.

EINSTEIN, A. (1910), Ann. Physik, [4], 33, 1275.

FLORY, P.J. (1953), Principles of Polymer Chemistry, Cornell University Press, Ithaca, N.Y.

HOWLEY, P. (1981), "Stastical Analysis of Polymer Light Scattering Data", Unpublished, McMaster University, Hamilton.

HUGLIN, M.B., Ed. (1972), Light Scattering from Polymer Solutions, Academic Press, N.Y.

KADIYALA, K.R. (1968), "A Transformation Used to Circumvent the Problem of Autocorrelation", Econometrica, 36, 1, 93.

LAWSON, C.L. and HANSON, R.J. (1974), Solving Least Squares Problems, Prentice-Hall, N.J.

MORRISON, I.D., GRABOWSKI, E.F. and HERB, C.A. (1985), "Improved Techniques for Particle Size Determination", to be published.

OSTER, N. (1948), "The Scattering of Light and its Applications to Chemistry", Chem. Rev., 43, 319.

OSTROWSKY, N., SORNETTE, D., PARKER, P. and PIKE, E.R. (1981), "Exponential Sampling Method for Light Scattering Polydispersity Analsyis", Optical Acta, 28, 8, 1059.

PANGONIS, W.J., and HELLER, H. (1960), Angular Scattering Functions for Spherical Particles, Wayne State University Press, Detroit.

PATINO-LEAL, H., REILLY, P.M. and O'DRISCOLL, K.F. (1980), "On the Estimation of Reactivity Ratios", J. Poly. Sci., Poly. Lett., 18, 219.

PUSEY, P.N., KOPPEL, D.E., SCHAEFER, D.W., CAMERINI-OTERO, R.D. and KOENIG, S.H. (1974), "Intensity Fluctuation Spectroscopy of Laser Light Scattered by Solutions of Spherical Viruses", Biochemistry, 13, 5, 952.

REILLY, P.M. and PATINO-LEAL, H. (1981), "A Bayesian Study of the Error-in-Variables Model", Technometrics, 23, 3, 221.

RIDDEL, W.C. (1977), "Prediction in Generalized Least Squares", The American Statistician, 31, 2, 88.

ROBERTS, K.R., TORKINGTON, J.A., GORDON, M. and ROSS-MURPHY, S.B. (1977), "Computer Analysis of Light Scattering Data", J. Poly. Sci.: Poly. Symp., 61, 45.

RUBIO, L.G., TALATINIAN, A.V. and MacGREGOR, J.F. (1984), "Symposium on Quantitative Characterization of Plastics and Rubber", Proceedings McMaster University, Hamilton, June 1984, 5, 37.

STACEY, K.A. (1956), Light Scattering in Physical Chemistry, Butterworths Scientific Publications, London.

STOCK, R.S. and RAY, W.H. (1985), "Interpretation of Photon Correlation Spectroscopy Data: A Comparison of Analysis Methods", J. Poly. Sci., Poly. Phys. Ed., 23, 7, 1393.

SUTTON, T.L. and MacGREGOR, J.F. (1977), "The Analysis and Design of Binary Vapour-Liquid Equilibrium Experiments", Can. J. Chem. Eng., 55, 602.

TANFORD, C. (1961), Physical Chemistry of Macromolecules, Wiley and Sons, N.Y.

ZIMM, B.H. (1948), "The Scattering of Light and the Radial Distribution Function of High Polymer Solution", J. Chem. Phys., 16, 1093.

APPENDICES

APPENDIX 1

Proof of Equivalent Scattering Geometries

Prove that $\sin^2\theta_1 + \sin^2\theta_2 = 1 + \cos^2\theta$; refer to figure 2.2.

Let:
$$X = r\cos\theta$$
$$Y = r\cos\theta_1$$
$$Z = r\cos\theta_2$$

Then $\quad \sin\theta_1 = \dfrac{A}{r} \qquad \therefore \quad \sin_1^2\theta = \dfrac{A^2}{r^2}$

By the Pythagorean Theorem,

$$A^2 = r^2 - Y^2$$
$$= r^2 - r^2\cos^2\theta_1$$
$$= r^2(1 - \cos^2\theta_1)$$

$\therefore \sin^2\theta_1 = 1 - \cos^2\theta_1$

Now, $\quad \sin\theta_2 = \dfrac{B}{r} \qquad \therefore \quad \sin^2\theta_2 = \dfrac{B^2}{r^2}$

Similarly,

$$B^2 = r^2 - Z^2$$
$$= r^2 - r^2\cos^2\theta_2$$
$$= r^2(1 - \cos^2\theta_2)$$

$\therefore \sin\theta_2 = 1 - \cos^2\theta_2$

Then,
$$\sin^2\theta + \sin^2\theta_2 = 2 - \cos^2\theta_1 - \cos^2\theta_2$$
$$= 2 + \cos^2\theta - \cos^2\theta - \cos^2\theta_1 - \cos^2\theta_2$$
$$= 2 + \cos^2\theta - \frac{X^2}{r^2} - \frac{Y^2}{r^2} - \frac{Z^2}{r^2}$$
$$= 2 + \cos^2\theta - \frac{(X^2 + Y^2 + Z^2)}{r^2}$$

But,
$$X^2 + Y^2 + Z^2 = r^2$$

$\therefore \quad \sin^2\theta_1 + \sin^2\theta_2 = 2 + \cos^2\theta - \dfrac{r^2}{r^2}$
$$= 2 + \cos^2\theta - 1$$
$$= 1 + \cos^2\theta$$

Q.E.D

```
      SUBROUTINE UWHAUS(NPROB,MODEL,NOB,Y,NP,TH,DIFF,SIGNS,
     1   EPS1,EPS2,MIT,FLAM,FNU,SCRAT)
      IMPLICIT REAL*8(A-H,O-Z)
      DIMENSION SCRAT(1)
      OPEN (UNIT=30,FILE='SUMPROP.DAT',STATUS='UNKNOWN')


C     this program is compatible with double precision programs
c     and not with single precision programs
c

      IA=1
      IB=IA+NP
      IC=IB+NP
      ID=IC+NP
      IE=ID+NP
      IF=IE+NP
      IG=IF+NOB
      IH=IG+NOB
      II=IH+NP*NOB
      IJ=IH
      CALL HAUS59(NPROB,MODEL,NOB,Y,NP,TH,DIFF,SIGNS,EPS1,
     1   EPS2,MIT,FLAM,FNU,SCRAT(IA),SCRAT(IB),SCRAT(IC),
     2   SCRAT(ID),SCRAT(IE),SCRAT(IF),SCRAT(IG),SCRAT(IH),
     3   SCRAT(II),SCRAT(IJ) )
      RETURN
      END
      SUBROUTINE HAUS59(NPRBO,MODEL,NBO,Y,NQ,TH,DIFZ,SIGNS,
     1   EP1S,EP2S,MIT,FLAM,FNU,    Q,P,E,PHI,TB,F,R,A,D,DELZ)
      IMPLICIT REAL*8(A-H,O-Z)
      DIMENSION TH(1),DIFZ(1),SIGNS(1),Y(1),Q(1),P(1),E(1),
     1   PHI(1),TB(1),F(1),R(1),A(1),D(1),DELZ(1)
      DACOS(X)=DATAN(DSQRT(1.0D0/X**2-1.0D0))
      NP=NQ
      NPROB=NPRBO
      NOB=NBO
      EPS1=EP1S
      EPS2=EP2S
      NPSQ=NP*NP
       NSCRAC=5*NP+NPSQ+2*NOB+NP*NOB
      WRITE(06,1000) NPROB,NOB,NP,NSCRAC
      WRITE(06,1001)
      WRITE (30,1001)
      CALL GASS60(1,NP,TH,TEMP,TMEP)
      WRITE(06,1002)
      WRITE (30,1002)
      CALL GASS60(1,NP,DIFZ,TEMP,TEMP)
      IF(MIN0(NP-1,50-NP,NOB-NP,MIT-1,999-MIT))99,15,15
15    IF(FNU-1.0)99,99,16
16    CONTINUE
      DO 19 I=1,NP
      TEMP=DABS(DIFZ(I))
      IF(DMIN1(1.0D0-TEMP,DABS(TH(I))))99,99,19
19    CONTINUE
      GA=FLAM
      NIT=1
      LAOS=0
      IF(EPS1)  5,70,70
5     EPS1=0
   70 SSQ=0
      CALL MODEL(NPROB,TH,F,NOB,NP)
      DO 90 I=1,NOB
      R(I)=Y(I)-F(I)
90    SSQ=SSQ+R(I)*R(I)
*
```

```
       WRITE(06,9011)
 9011 FORMAT(' INITIAL FUNCTION VALUES')
       WRITE(06,2001) (F(I),I=1,NOB)
       WRITE(06,9012)
 9012 FORMAT(////' INITIAL RESIDUALS')
       WRITE(06,2001) (R(I),I=1,NOB)
*
       WRITE(06,1003) SSQ
100    GA=GA/FNU
       INTCNT=0
       WRITE(06,1004) NIT
101    JS=1-NOB
       DO 130 J=1,NP
       TEMP=TH(J)
       P(J)=DIFZ(J)*TH(J)
       TH(J)=TH(J)+P(J)
       Q(J)=O
       JS=JS+NOB
       CALL MODEL(NPROB,TH,DELZ(JS),NOB,NP)
       IJ=JS-1
       DO 120 I=1,NOB
       IJ=IJ+1
       DELZ(IJ)=DELZ(IJ)-F(I)
120    Q(J)=Q(J)+DELZ(IJ)*R(I)
       Q(J)=Q(J)/P(J)
130    TH(J)=TEMP
       IF(LAOS) 131,131,414
131    DO 150 I=1,NP
       DO 151 J=1,I
       SUM=O
       KJ=NOB*(J-1)
       KI=NOB*(I-1)
       DO 160 K = 1, NOB
       KI = KI + 1
       KJ = KJ + 1
160    SUM = SUM + DELZ(KI) * DELZ(KJ)
       TEMP= SUM/(P(I)*P(J))
       JI = J + NP*(I-1)
       D(JI) = TEMP
       IJ = I + NP*(J-1)
151        D(IJ) = TEMP
150   E(I) = DSQRT(D(JI))
666   CONTINUE
       DO 153  I = 1, NP
       IJ = I-NP
       DO 153 J=1,I
       IJ = IJ + NP
       A(IJ) = D(IJ) / (E(I)*E(J))
       JI = J + NP*(I-1)
153   A(JI) = A(IJ)
C                                        A= SCALED MOMENT MATRIX
       II = - NP
       DO 155 I=1,NP
       P(I)=Q(I)/E(I)
       PHI(I)=P(I)
       II = NP + 1 + II
155   A(II) = A(II) + GA
C
       I=1
       CALL MATIN(A, NP, P, I, DET)
C                                        P/E = CORRECTION VECTOR
       STEP=1.0
       SUM1=0.
       SUM2=0.
       SUM3=0.
```

```
      DO 231 I=1,NP
      SUM1=P(I)*PHI(I)+SUM1
      SUM2=P(I)*P(I)+SUM2
      SUM3= PHI(I) * PHI(I) + SUM3
231   PHI(I) = P(I)
      TEMP = SUM1/(DSQRT(SUM2)*DSQRT(SUM3))
      TEMP = DMIN1(TEMP, 1.0D0)
      TEMP = 57.295*DACOS(TEMP)
      WRITE(06,1041)  DET,TEMP
170   DO 220 I = 1, NP
      P(I) = PHI(I) *STEP / E(I)
      TB(I) = TH(I) + P(I)
220   CONTINUE
      WRITE(06,7000)
7000  FORMAT(30H0TEST POINT PARAMETER VALUES      )
      WRITE(06,2006)  (TB(I),I=1,NP)
      DO 221 I = 1, NP
      IF(SIGNS(I)) 221, 221, 222
222   IF(DSIGN(1.0D0,TH(I))*DSIGN(1.0D0,TB(I))) 663, 221, 221
221   CONTINUE
      SUMB=0
      CALL MODEL(NPROB, TB, F, NOB, NP)
      DO 230 I=1,NOB
      R(I)=Y(I)-F(I)
230   SUMB=SUMB+R(I)*R(I)
      WRITE(06,1043)  SUMB
      IF(SUMB - (1.0+EPS1)*SSQ) 662, 662, 663
663   IF( DMIN1(TEMP-30.0D0, GA)) 665, 665, 664
665   STEP=STEP/2.0
      INTCNT = INTCNT + 1
      IF(INTCNT - 36) 170, 2700, 2700
664   GA=GA*FNU
      INTCNT = INTCNT + 1
      IF(INTCNT - 36) 666, 2700, 2700
662   WRITE(06,1007)
      DO 669 I=1,NP
669   TH(I)=TB(I)
      CALL GASS60(1, NP, TH, TEMP, TEMP)
      WRITE(06,1040)  GA,SUMB
      IF(EPS2) 229,229,225
229   IF(EPS1) 270,270,265
225   DO 240 I = 1, NP
      IF(DABS(P(I))/(1.E-20+DABS(TH(I)))-EPS2) 240, 240, 241
241   IF(EPS1) 270,270,265
240   CONTINUE
      WRITE(06,1009)  EPS2
      GO TO 280
265   IF(DABS(SUMB - SSQ) - EPS1*SSQ) 266, 266, 270
266   WRITE(06,1010)  EPS1
      GO TO 280
270   SSQ=SUMB
      NIT=NIT+1
      IF(NIT - MIT) 100, 100, 280
2700  WRITE(06,2710)
2710  FORMAT(//115H0**** THE SUM OF SQUARES CANNOT BE REDUCED TO THE SUM
     1OF SQUARES AT THE END OF THE LAST ITERATION - ITERATING STOPS    /)
C
C                                              END ITERATION
C
280   WRITE (30,1007)
      CALL GASS60(1,NP,TH,TEMP,TEMP)
      WRITE (30,1040) GA,SUMB
      WRITE (30,1045) NIT
1045  FORMAT(//1X,' NUMBER OF ITERATIONS = ',I3,//)
      WRITE(06,1011)
```

```
      WRITE(06,2001) (F(I),I=1,NOB)
      WRITE(06,1012)
      WRITE(06,2001) (R(I),I=1,NOB)
      WRITE(06,1017)
      WRITE (30,1017)
 1017 FORMAT(////16H XPRIME-X MATRIX)
      CALL GASS60(4,NP,TEMP,TEMP,D)
      SSQ=SUMB
      IDF=NOB-NP
      WRITE(06,1016)
      WRITE (30,1016)
      I=0
       CALL MATIN(D, NP, P, I, DET)
        CALL GASS60(4,NP,TEMP,TEMP,D)
      DO 7692 I=1,NP
      II = I + NP*(I-1)
 7692 E(I) = DSQRT(D(II))
      DO 340 I=1,NP
      JI = I + NP*(I-1) - 1
      IJ = I + NP*(I-2)
      DO 340 J = I, NP
      JI = JI + 1
      A(JI) = D(JI) / (E(I)*E(J))
      IJ = IJ + NP
  340    A(IJ) = A(JI)
         WRITE (06,1015)
         WRITE (30,1015)
         CALL GASS60(3, NP, TEMP, TEMP, A)
      IF(IDF) 341, 410, 341
  341 SDEV = SSQ/FLOAT(IDF)
      WRITE(06,1014) SDEV,IDF
      WRITE (30,1014) SDEV,IDF
       SDEV = DSQRT(SDEV)
      DO 391 I=1,NP
      P(I)=TH(I)+2.0*E(I)*SDEV
  391 TB(I)=TH(I)-2.0*E(I)*SDEV
      WRITE(06,1039)
      WRITE (30,1039)
       CALL GASS60(2, NP, TB, P, TEMP)
        WRITE (06,1050)
 1050   FORMAT(/19H0CONFIDENCE FIGURES )
        DO 392 I=1,NP
  392       TB(I)=2*E(I)*SDEV
        CALL GASS60(1, NP, TB, TEMP, TEMP)
      LAOS = 1
      GO TO 101
  414 DO 415 K = 1, NOB
      TEMP = 0
      DO 420 I=1,NP
      DO 420 J=1,NP
      ISUB = K+NOB*(I-1)
      DEBUG1 = DELZ(ISUB)
C     DEBUG1 = DELZ(K + NOB*(I-1))
      ISUB = K+NOB*(J-1)
      DEBUG2 = DELZ(ISUB)
C     DEBUG2 = DELZ(K + NOB*(J-1))
      IJ = I + NP*(J-1)
      DEBUG3 = D(IJ)/(DIFZ(I)*TH(I)*DIFZ(J)*TH(J))
  420 TEMP = TEMP + DEBUG1 * DEBUG2 * DEBUG3
       TEMP = 2.0*DSQRT(DABS(TEMP))*SDEV
      R(K)=F(K)+TEMP
  415 F(K)=F(K)-TEMP
      WRITE(06,1008)
       IE=0
      DO 425 I=1,NOB,10
```

```
         IE=IE+10
         IF(NOB-IE) 430,435,435
  430 IE=NOB
  435 WRITE(06,2001) (R(J),J=I,IE)
  425 WRITE(06,2006) (F(J),J=I,IE)
  410 WRITE(06,1033) NPROB
         RETURN
   99 WRITE(06,1034)
         GO TO 410
 1000 FORMAT(38H1NON-LINEAR ESTIMATION, PROBLEM NUMBER   I3,// I5,
    1  14H OBSERVATIONS, I5, 11H PARAMETERS  I14, 17H SCRATCH REQUIRED)
 1001 FORMAT(/25H0INITIAL PARAMETER VALUES  )
 1002 FORMAT(/54H0PROPORTIONS USED IN CALCULATING DIFFERENCE QUOTIENTS )
 1003 FORMAT(/25H0INITIAL SUM OF SQUARES =   E12.4)
 1004 FORMAT(/////45X,13HITERATION NO.  I4)
 1007 FORMAT(/32H0PARAMETER VALUES VIA REGRESSION  )
 1008 FORMAT(////54H0APPROXIMATE CONFIDENCE LIMITS FOR EACH FUNCTION VAL
    1UE     )
 1009 FORMAT(/62H0ITERATION STOPS - RELATIVE CHANGE IN EACH PARAMETER LE
    1SS THAN   E12.4)
 1010 FORMAT(/62H0ITERATION STOPS - RELATIVE CHANGE IN SUM OF SQUARES LE
    1SS THAN   E12.4)
 1011 FORMAT(22H1FINAL FUNCTION VALUES  )
 1012 FORMAT(////10H0RESIDUALS  )
 1014 FORMAT(//24H0VARIANCE OF RESIDUALS =    ,E12.4,1H,I4,
    120H DEGREES OF FREEDOM    )
 1015 FORMAT(////19H0CORRELATION MATRIX  )
 1016 FORMAT(////17H0XPRIME-X INVERSE)
 1033 FORMAT(//19H0END OF PROBLEM NO.  I3)
 1034 FORMAT(/16H0PARAMETER ERROR  )
 1039 FORMAT(/71H0INDIVIDUAL CONFIDENCE LIMITS FOR EACH PARAMETER (ON LI
    1NEAR HYPOTHESIS)   )
 1040 FORMAT(/9H0LAMBDA =E10.3,40X,33HSUM OF SQUARES AFTER REGRESSION =
    1E15.7)
 1041 FORMAT(14H DETERMINANT =  E12.4, 6X, 25H ANGLE IN SCALED COORD. =
    1  F5.2, 8HDEGREES   )
 1043 FORMAT(28H0TEST POINT SUM OF SQUARES =   E12.4)
 2001 FORMAT(/10E12.4)
 2006 FORMAT(10E12.4)
         END
         SUBROUTINE MATIN(A, NVAR, B, NB, DET)
           IMPLICIT REAL*8(A-H,O-Z)
         DIMENSION A(NVAR, 1), B(NVAR, 1)
          PIVOTM = A(1,1)
          DET = 1.0
         DO 550 ICOL = 1, NVAR
          PIVOT = A(ICOL, ICOL)
         PIVOTM = DMIN1(PIVOT, PIVOTM)
          DET = PIVOT * DET
C
C       DIVIDE PIVOT ROW BY PIVOT ELEMENT
C
         A(ICOL, ICOL) = 1.0
         PIVOT = DMAX1(PIVOT, 1.0D-30)
          PIVOT = A(ICOL, ICOL)/PIVOT
         DO 350 L=1,NVAR
  350    A(ICOL, L) = A(ICOL, L)*PIVOT
         IF (NB) 371,371,372
  372 DO 370 L=1,NB
  370    B(ICOL, L) = B(ICOL, L)*PIVOT
C
C       REDUCE NON-PIVOT ROWS
C
  371 DO 550 L1=1,NVAR
         IF (L1-ICOL) 551,550,551
```

```
551   T = A(L1, ICOL)
      A(L1, ICOL) = 0.
      DO 450 L=1,NVAR
450   A(L1, L) = A(L1, L) - A(ICOL, L)*T
      IF (NB) 552,550,552
552 DO 500 L=1,NB
500   B(L1, L) = B(L1, L)-B(ICOL,L)*T
550 CONTINUE
      RETURN
      END
      SUBROUTINE GASS60(ITYPE, NQ, A, B, C)
       IMPLICIT REAL*8(A-H,O-Z)
      DIMENSION A(NQ),B(NQ),C(NQ,NQ)
      NP = NQ
      NR = NP/10
      LOW = 1
      LUP = 10
10    IF( NR )15,20,30
15    RETURN
20    LUP=NP
      IF (LOW-LUP) 30,30,15
30 WRITE(06,500) (J,J=LOW,LUP)
      WRITE (30,500) (J,J=LOW,LUP)
      GO TO (40,60,80,80), ITYPE
40 WRITE(06,600) (A(J),J=LOW,LUP)
      WRITE (30,600) (A(J),J=LOW,LUP)
      GO TO 100
60 WRITE(06,600) (B(J),J=LOW,LUP)
      WRITE (30,600) (B(J),J=LOW,LUP)
      GO TO 40
80 IF(ITYPE.EQ.4) GO TO 70
      DO 90 I=LOW,LUP
      WRITE(06,720) I,(C(J,I),J=LOW,I)
90 WRITE (30,720) I,(C(J,I),J=LOW,I)
      GO TO 71
70 DO 72 I=LOW,LUP
      WRITE(06,721) I,(C(I,J),J=LOW,I)
72 WRITE (30,721) I,(C(I,J),J=LOW,I)
71 CONTINUE
      LOW2=LUP+1
      IF (LOW2-NP) 96,96,100
96 IF (ITYPE.EQ.4) GO TO 97
      DO 95 I=LOW2,NP
      WRITE(06,720) I,(C(J,I),J=LOW,LUP)
95 WRITE (30,720) I,(C(J,I),J=LOW,LUP)
      GO TO 100
97 DO 98 I=LOW2,NP
      WRITE(06,721) I,(C(I,J),J=LOW,LUP)
98 WRITE (30,721) I,(C(I,J),J=LOW,LUP)
100    LOW = LOW + 10
       LUP = LUP + 10
       NR = NR - 1
       GO TO 10
500   FORMAT(/I8,9I12)
600   FORMAT(10E12.4)
720   FORMAT(1H0,I3,1X,F7.4,9F12.4)
721   FORMAT(1H0,I3,1X,E10.4,9E12.4)
1     CONTINUE
      RETURN
      END
```

```
C
C     This program performs a data analysis on user supplied Wide Angle
C     Light Scattering data.  It is currently dimensioned to handle a
C     problem where galvanometer measurements have been taken over a grid
C     of five polymer concentrations and 12 scattering angles.
C
C     All variables are double precision
C
      IMPLICIT REAL*8(A-H,O-Z)
      DIMENSION BETA(4),DIFF(4),SIGNS(4),SCRAT(500),X(60),Z(60),OBJEC(60),
     #          DTHETA(60),GSOLN(60),GSOLV(60)
      COMMON/PH/C(60),THETA(60),KCROBS(60),W(60),HTHETA(60),RTHETA(60),
     #          VARH(60),VARC(60),VART(60),VARE(60),GBAR(60),
     #          KSTAR,RB,GB,CVAR,TVAR,ITYPE
C
C     The user must define an external MODEL subroutine for the estimation
C     program UWHAUSDD.
C
      EXTERNAL MODEL
      REAL*8 KCROBS,KCRCAL,KSTAR
C
C     Only one input data file, WALSPROP.DAT is required by the program.  Inputs
C     are described below.
C
      OPEN(UNIT=1,FILE='WALSPROP.DAT',STATUS='OLD')
C
C     The following output data files are created by the program:
C
C     ZIMMPROP.DAT        - stores the absissa and ordinate data required to
C                           construct a Zimm plot
C     VARPROP.DAT         - contains the relative contributions of each error
C                           variance term accounted for in the error
C                           propogation model to the total error variance
C     STATPROP.DAT        - store the complete UWHAUSDD results for later
C                           viewing if desired
C     SUMPROP.DAT         - contains a summary of UWHAUSDD results such as
C                           parameter estimates, confidence intervals and
C                           correlation matrix
C     RESIDS.DAT          - contains the residuals from the fit
C
      OPEN(UNIT=10,FILE='ZIMMPROP.DAT',STATUS='UNKNOWN')
      OPEN(UNIT=11,FILE='VARPROP.DAT',STATUS='UNKNOWN')
      OPEN(UNIT=20,FILE='STATPROP.DAT',STATUS='UNKNOWN')
      OPEN(UNIT=40,FILE='RESIDS.DAT',STATUS='UNKNOWN')
      IZERO=0
C
C     Choose a parameter estimation routine
C
      PRINT *, 'ENTER ITYPE - 1,2,3,4:'
      PRINT *, '    1.  Error propogation on Kc/R'
      PRINT *, '    2.  Error propogation on R'
      PRINT *, '    3.  Non-linear least squares on Kc/R'
      PRINT *, '    4.  Non-linear least squares on R'
      READ *, ITYPE
C
C     Input data file WALSPROP.DAT, must contain:
C
C     KPRIME              - an arbitrary constant used in the absissa to
C                           construct a Zimm plot
C     CVAR, DTVAR         - estimates of the standard deviations in measuring
C                           the polymer concentration (in percent of the
C                           concentration) and scattering angle (in degrees)
C     UWHAUSDD parameters NOB, NP, ESP1, EPS2, MIT, FLAM, FNU
C     BETA                - Initial guesses of model parameters
C     C, DTHETA           - polymer concetrations and scattering angles at
```

```
C                        which measurements were recorded
C     GSOLV              - measured galvanometer readings for the solvent at
C                        angle of measurement
C     GSOLN              - measured galvanometer readings for the polymer
C                        solutions
C
      READ (1,*) KPRIME
      READ (1,*) CVAR,DTVAR
      READ (1,*) NPROB,NOB,NP,EPS1,EPS2,MIT,FLAM,FNU
      WRITE (6,*) NPROB,NOB,NP,EPS1,EPS2,MIT,FLAM,FNU
      WRITE (6,*) CVAR,DTVAR
      WRITE (20,*) KPRIME,CVAR,DTVAR
      WRITE (20,*) NPROB,NOB,NP,EPS1,EPS2,MIT,FLAM,FNU
      READ (1,*) (BETA(I),I=1,NP)
      WRITE (6,*) (BETA(I),I=1,NP)
      READ (1,*) (C(I),I=1,5)
      READ (1,*) (DTHETA(I),I=1,56,5)
      READ (1,*) (GSOLV(I),I=1,56,5)
      READ (1,*) (GSOLN(I),I=1,NOB)
      READ (1,*) KSTAR,RB,GB
C
C     Fill the concentration vector (C) with the appropriate values
C
      DO J=1,5
         DO K=1,11
            C(J+5*K)=C(J)
         END DO
      END DO
C
C     Convert DTVAR from degrees to radians and CVAR from a percentage
C
      PI=4.0*DATAN(1.D0)
      TVAR=DTVAR*PI/180.0
      CVAR=CVAR/100
C
C     Calculate GBAR, the average galvanometer reading at each angle, and fill
C     GBAR, GSOLV, DTHETA, THETA vectors with the appropriate values
C
      DO J=1,56,5
         GBAR(J)=GSOLN(J)
         THETA(J)=DTHETA(J)*PI/180.0
         DO K=1,4
            GBAR(J)=GBAR(J)+GSOLN(J+K)
            GSOLV(J+K)=GSOLV(J)
            DTHETA(J+K)=DTHETA(J)
            THETA(J+K)=THETA(J)
         END DO
         GBAR(J)=GBAR(J)/5
         DO K=1,4
            GBAR(J+K)=GBAR(J)
         END DO
      END DO
      WRITE (6,*) GBAR
C
C     Calculate HTHETA, the difference between the galvanometer readings of
C     the solution and the solvent; RTHETA, the polymer Rayleigh ratio;
C     KCROBS, the observed value of Kc/R; and X, the values of the absissa
C     for the Zimm plot
C
      DO J=1,60
         HTHETA(J)=GSOLN(J)-GSOLV(J)
         RTHETA(J)=RB/GB*DSIN(THETA(J))*HTHETA(J)
         KCROBS(J)=KSTAR*C(J)/RTHETA(J)
         X(J)=DSIN(THETA(J)/2.0)**2+KPRIME*C(J)
      END DO
```

```
          PRINT 49
          PRINT 50,(C(I),KCROBS(I),DTHETA(I),I=1,NOB)
C
C   Arbitrarily set the objective vector (used by UWHAUSDD) to zero, which
C   is appropriate for the error propogation applications
C
          DO I=1,NOB
             OBJEC(I)=0.0
          END DO
C
C   Set the step differential used by UWHAUSDD to evaluate the objective
C   function and set SIGNS equal to 1, thus not allowing negative parameter
C   estimates
C
          DO I=1,NP
             DIFF(I)=0.0001
             SIGNS(I)=1
          END DO
C
C   If either of the non-linear least squares applications has been chosen,
C   set the objective vector to the appropriate function values
C
          IF (ITYPE.EQ.3) THEN
             DO I=1,NOB
                OBJEC(I)=KCROBS(I)
             END DO
          ELSE IF (ITYPE.EQ.4) THEN
             DO I=1,NOB
                OBJEC(I)=RTHETA(I)
             END DO
          END IF
C·
C   Call the estimation subroutine UWHAUS
C
          CALL UWHAUS(NPROB,MODEL,NOB,OBJEC,NP,BETA,DIFF,SIGNS,EPS1,EPS2,MIT,
     #              FLAM,FNU,SCRAT)
C
C   Calculate the predicted values of Kc/R using the final parameter estiamtes
C   and the residuals
C
          DO I=1,NOB
             KCRCAL=1.0/BETA(1)*(1.0+BETA(2)*DSIN(THETA(I)/2.0)**2)
     #             +2.0*BETA(3)*C(I)+3.0*BETA(4)*C(I)**2
             RES=KCROBS(I)-KCRCAL
             WRITE (10,300) X(I),IZERO,KCROBS(I),KCRCAL
300          FORMAT(' ',F9.7,5X,I2,5X,E11.5,5X,E11.5)
             WRITE (40,310) I,RES
310          FORMAT(' ',I3,5X,E11.5)
          END DO
          CVAR=CVAR*100
          WRITE (30,120) ITYPE
          WRITE (30,500) CVAR
          WRITE (30,505) DTVAR
500       FORMAT(///,' ','CONC ST. DEV.= ',F6.4,' % OF CONC')
505       FORMAT(' ','ANGLE ST. DEV.= ',F6.4,' DEGREES')
C
C   If the method of error propgation was employed, calculate the relative
C   contribution made by each term in the error propogation formula to the
C   total error variance
C
          IF (ITYPE.LE.2) THEN
             DO I=1,NOB
                VARH(I)=VARH(I)/VARE(I)
                VARC(I)=VARC(I)/VARE(I)
                VART(I)=VART(I)/VARE(I)
```

```
              VARE(I)=VARE(I)/VARE(I)
              WRITE (11,400) VARH(I),VARC(I),VART(I),VARE(I)
          END DO
        END IF
400     FORMAT(' ',4(E11.5,3X))
        PRINT 100
        PRINT 110,(C(I),DTHETA(I),W(I),I=1,NOB)
        WRITE (20,999) (W(I),I=1,NOB)
        WRITE (30,999) (W(I),I=1,NOB)
999     FORMAT (' ',5X,D24.16)
49      FORMAT ('1',8X,'C',11X,'KCROBS',11X,'THETA'//)
50      FORMAT (5X,F7.5,5X,E11.5,5X,F6.2)
100     FORMAT ('1',5X,'C',7X,'THETA',5X,'W'//)
110     FORMAT (3X,F7.5,3X,F6.2,3X,E11.5)
120     FORMAT (///,' ','ITYPE = ',I2//)
        STOP
        END
C
C
C
        SUBROUTINE MODEL(NPROB,BETA,F,NOB,NP)
        IMPLICIT REAL*8(A-H,O-Z)
        DIMENSION BETA(NP),F(NOB)
        COMMON/PH/C(60),THETA(60),KCROBS(60),W(60),HTHETA(60),RTHETA(60),
     #          VARH(60),VARC(60),VART(60),VARE(60),GBAR(60),
     #          KSTAR,RB,GB,CVAR,TVAR,ITYPE
        REAL*8 KSTAR,KCROBS
C
C   Define the functional subfunctions HVAR and CVARR to calculate the
C   appropriate error variance for HTHETA and C (concentration)
C
        HVAR(XX)=0.0005*XX**2
        CVARR(XXX)=(CVAR*XXX)**2
C
C   If one of the error propogation applications was chosen, then calculate
C   for each data point:
C       - the values of the differential equations
C       - the value of e
C       - the individual error variance contributions
C       - the total error variance
C       - the weighting and the objective function value
C
        IF (ITYPE.EQ.1) THEN
            DO I=1,NOB
               DEDH=-KSTAR*C(I)/(RB/GB*DSIN(THETA(I))*HTHETA(I)**2)
               DEDC=KSTAR/(RB/GB*DSIN(THETA(I))*HTHETA(I))
     #             -2.0*BETA(3)-6.0*BETA(4)*C(I)
               DEDT=-KSTAR*C(I)*DCOS(THETA(I))/(RB/GB*DSIN(THETA(I))**2
     #             *HTHETA(I))-BETA(2)/BETA(1)*DSIN(THETA(I)/2.0D0)
     #             *DCOS(THETA(I)/2.0D0)
               E=KSTAR*C(I)/(RB/GB*DSIN(THETA(I))*HTHETA(I))-
     #           1.0/BETA(1)*(1.0+BETA(2)*DSIN(THETA(I)/2.0)**2)-
     #           2.0*BETA(3)*C(I)-3.0*BETA(4)*C(I)**2
               VARH(I)=DEDH**2*HVAR(GBAR(I))
               VARC(I)=DEDC**2*CVARR(C(I))
               VART(I)=DEDT**2*TVAR**2
               VARE(I)=VARH(I)+VARC(I)+VART(I)
               W(I)=1.0/VARE(I)
               F(I)=E*DSQRT(W(I))
            END DO
        ELSE IF (ITYPE.EQ.2) THEN
            DO I=1,NOB
               DEDH=RB/GB*DSIN(THETA(I))
               DENOM=(1.0+BETA(2)*DSIN(THETA(I)/2.0)**2+
     #             2.0*BETA(3)*C(I)+3.0*BETA(4)*C(I)**2)**2
```

```
            DEDC=KSTAR*BETA(1)*(3.0*BETA(4)*C(I)**2-1.0-
     #          BETA(2)*DSIN(THETA(I)/2.0)**2)/DENOM
            DEDT=RB/GB*DCOS(THETA(I))*HTHETA(I)+
     #          KSTAR*C(I)*BETA(1)*BETA(2)*
     #          (DSIN(THETA(I)/2.0)*DCOS(THETA(I)/2.0))/DENOM
            E=RTHETA(I)-KSTAR*C(I)/(1.0/BETA(1)*(1.0+BETA(2)*DSIN
     #         (THETA(I)/2.0)**2)+2.0*BETA(3)*C(I)
     #          +3.0*BETA(4)*C(I)**2)
            VARH(I)=DEDH**2*HVAR(GBAR(I))
            VARC(I)=DEDC**2*CVARR(C(I))
            VART(I)=DEDT**2*TVAR**2
            VARE(I)=VARH(I)+VARC(I)+VART(I)
            W(I)=1.0/VARE(I)
            F(I)=E*DSQRT(W(I))
         END DO
C
C    If one of the non-linear least squares applications was chosen, then
C    for each data point, calculate the value of the appropriate objective
C    function
C
      ELSE IF (ITYPE.EQ.3) THEN
         DO I=1,NOB
            F(I)=1.0/BETA(1)*(1.0+BETA(2)*DSIN(THETA(I)/2.0)**2)+
     #          2.0*BETA(3)*C(I)+3.0*BETA(4)*C(I)**2
         END DO
      ELSE IF (ITYPE.EQ.4) THEN
         DO I=1,NOB
            F(I)=KSTAR*C(I)/(1.0/BETA(1)*(1.0+BETA(2)*DSIN(THETA(I)
     #          /2.0)**2)+2.0*BETA(3)*C(I)+3.0*BETA(4)*C(I)**2)
         END DO
      END IF
      RETURN
      END
```

```
C
C    This program performs a data analysis on user supplied Low Angle Laser
C    Light Scattering data.  It is currently dimensioned to handle no more
C    than five data points.
C
C    All variables are double precision.
C
      IMPLICIT REAL*8(A-H,O-Z)
      DIMENSION BETA(2),DIFF(2),SIGNS(2),SCRAT(500),Z(5),OBJEC(5),
     #          D(5),DVALUE(5),DCODE(5)
      COMMON/PH/C(5),KCROBS(5),W(5),RSOLN(5),RTHETA(5),
     #          VARG(5),VARG0(5),VARC(5),VARE(60),GSOLN(5),
     #          KSTAR,GVAR,CVAR(5),G0VAR,GSOLN0(5),ITYPE
C
C    The user must define an external MODEL subroutine for the estimation
C    program UWHAUSDD.
C
      EXTERNAL MODEL
      REAL*8  KCROBS,KCRCAL,KSTAR
      INTEGER DCODE
C
C    Only one input data file, LALLSPROP.DAT is required by the program. Inputs
C    are described below.
C
      OPEN(UNIT=1,FILE='LALLSPROP.DAT',STATUS='OLD')
C
C    The following output data files are created by the program:
C
C    KCRVSC.DAT             - stores the absissa and ordinate data required to
C                            construct a Kc/R vs c plot
C    VARPROP.DAT           - contains the relative contributions of each error
C                            variance term accounted for in the error
C                            propogation model to the total error variance
C    STATPROP.DAT          - stores the complete UWHAUSDD screen output for
C                            later viewing if desired
C    RESIDS.DAT            - contains the residuals from the fit
C
      OPEN(UNIT=10,FILE='KCRVSC.DAT',STATUS='UNKNOWN')
      OPEN(UNIT=11,FILE='VARPROP.DAT',STATUS='UNKNOWN')
      OPEN(UNIT=20,FILE='STATPROP.DAT',STATUS='UNKNOWN')
      OPEN(UNIT=50,FILE='RESIDS.DAT',STATUS='UNKNOWN')
      IZERO=0
C
C    Choose a parameter estimation routine
C
      PRINT *, 'ENTER ITYPE - 1,2,3,4:'
      PRINT *, '    1.  Error propogation on Kc/R'
      PRINT *, '    2.  Error propogation on R'
      PRINT *, '    3.  Linear least squares on Kc/R'
      PRINT *, '    4.  Non-linear least squares on R'
      READ *,ITYPE
C
C    Input data file LALLSPROP.DAT, must contain:
C
C    GVAR, G0VAR           - estimates of the standard deviations in G(theta)
C                            and G(zero angle)
C    CVAR                  - estiamtes of the variance in the polymer
C                            concentrations
C    UWHAUSDD parameters NOB, NP, EPS1, EPS2, MIT, FLAM, FNU
C    BETA                  - initial guesses of the model parameters
C    C                     - polymer concentrations at which measurements
C                            were recorded
C    GSOLN, GSOLN0         - measured galvanometer readings of G(theta) and
C                            G(zero angle) at each polymer concentration
C    DCODE                 - a coded integer value between 1 and 5 corresponding
```

```
C                        to a specific attenuation function
C     KSTAR, RSOLV, DIGMA - the values of K, R(solv.), and an optical
C                        constant particular to a set of data
C
      READ (1,*) GVAR,G0VAR
      READ (1,*) (CVAR(I),I=1,5)
      READ (1,*) NPROB,NOB,NP,EPS1,EPS2,MIT,FLAM,FNU
      WRITE (6,*) NPROB,NOB,NP,EPS1,EPS2,MIT,FLAM,FNU
      WRITE (6,*) CVAR
      WRITE (20,*) CVAR
      WRITE (20,*) NPROB,NOB,NP,EPS1,EPS2,MIT,FLAM,FNU
      READ (1,*) (BETA(I),I=1,NP)
      WRITE (6,*) (BETA(I),I=1,NP)
      READ (1,*) (C(I),I=1,5)
      READ (1,*) (GSOLN(I),I=1,5)
      READ (1,*) (GSOLN0(I),I=1,5)
      READ (1,*) (DCODE(I),I=1,5)
      READ (1,*) KSTAR,RSOLV,DSIGMA
C
C     Define the correspondance between DCODE and the attenuating function.
C
      DVALUE(1)=1.0553D-6
      DVALUE(2)=6.6728D-8
      DVALUE(3)=1.6549D-8
      DVALUE(4)=4.3026D-9
      DVALUE(5)=2.6173D-7
C
C     Calculate the absolute values of CVAR; determine the appropriate values
C     for D, the attenuating function; calculate RSOLN, the measured Rayleigh
C     ratio for the solution; RTHETA, the polymer Rayleigh ratio; and KCROBS,
C     the observed values of Kc/R.
C
      DO J=1,NOB
         CVAR(J)=C(J)**2*CVAR(J)
         D(J)=DVALUE(DCODE(J))
         RSOLN(J)=GSOLN(J)/GSOLN0(J)*DSIGMA*D(J)
         RTHETA(J)=RSOLN(J)-RSOLV
         KCROBS(J)=KSTAR*C(J)/RTHETA(J)
         WRITE (10,*) C(J),KCROBS(J)
      END DO
      WRITE (6,*) CVAR
      PRINT 49
      PRINT 50,(C(I),KCROBS(I),I=1,NOB)
C
C     Arbitrarily set the objective vector (used by UWHAUSDD) to zero, which
C     is appropriate for the error propogation applications.
C
      DO I=1,NOB
         OBJEC(I)=0.0
      END DO
C
C     Set the step differential used by UWHAUSDD to evaluate the objective
C     function and set SIGNS equal to 1, thus not allowing negative parameter
C     estimates.
C
      DO I=1,NP
         DIFF(I)=0.0001
         SIGNS(I)=1
      END DO
C
C     If either the linear or non-linear least squares applications has been
C     chosen, set the objective vector to the appropriate function values.
C
      IF (ITYPE.EQ.3) THEN
         DO I=1,NOB
```

```
                OBJEC(I)=KCROBS(I)
            END DO
        ELSE IF (ITYPE.EQ.4) THEN
            DO I=1,NOB
                OBJEC(I)=RTHETA(I)
            END DO
        END IF
C
C    Call the estimation routine UWHAUS.
C
        CALL UWHAUS(NPROB,MODEL,NOB,OBJEC,NP,BETA,DIFF,SIGNS,EPS1,EPS2,MIT,
     #              FLAM,FNU,SCRAT)
C
C    Calculate the predicted values of Kc/R using the final parameter estimates,
C    and the residuals.
C
        DO I=1,NOB
            KCRCAL=1.0/BETA(1)+2.0*BETA(2)*C(I)
            RES=KCROBS(I)-KCRCAL
            WRITE (50,310) I,RES
310         FORMAT(' ',I3,5X,E11.5)
            CVAR(I)=DSQRT(CVAR(I))
        END DO
        WRITE (30,120) ITYPE
        WRITE (30,500) GVAR
        WRITE (30,502) G0VAR
        WRITE (30,505) CVAR
500     FORMAT(///,' ','MEASURED INTENSITY ST. DEV.= ',F6.2)
502     FORMAT(' ','MEASURED INTENSITY AT 0.0 DEG., ST. DEV.= ',F6.2)
505     FORMAT(' ','CONC ST. DEV.= ',5(3X,E11.5),///)
C
C    If the method of error propogation was employed, calculate the relative
C    contribution made by each term in the error propogation formula to the
C    total error variance.
C
        IF (ITYPE.LE.2) THEN
            DO I=1,NOB
                VARG(I)=VARG(I)/VARE(I)
                VARG0(I)=VARG0(I)/VARE(I)
                VARC(I)=VARC(I)/VARE(I)
            END DO
        END IF
        WRITE (11,400) (VARG(I),VARG0(I),VARC(I),VARE(I),I=1,NOB)
        WRITE (30,400) (VARG(I),VARG0(I),VARC(I),VARE(I),I=1,NOB)
400     FORMAT(' ',4(E11.5,3X))
        PRINT 100
        PRINT 110,(C(I),W(I),I=1,NOB)
        WRITE (20,999) (W(I),I=1,NOB)
999     FORMAT (' ',5X,D24.16)
49      FORMAT ('1',8X,'C',11X,'KCROBS',11X,//')
50      FORMAT (5X,F7.5,5X,E11.5)
100     FORMAT ('1',5X,'C',7X,5X,'W'//)
110     FORMAT (3X,F7.5,3X,E11.5)
120     FORMAT (///,' ','ITYPE= ',I2//)
        STOP
        END
C
C
C

        SUBROUTINE MODEL(NPROB,BETA,F,NOB,NP)
        IMPLICIT REAL*8(A-H,O-Z)
        DIMENSION BETA(NP),F(NOB)
        COMMON/PH/C(5),KCROBS(5),W(5),RSOLN(5),RTHETA(5),
     #            VARG(5),VARG0(5),VARC(5),VARE(60),GSOLN(5),
     #            KSTAR,GVAR,CVAR(5),G0VAR,GSOLN0(5),ITYPE
```

```
          REAL*8 KSTAR,KCROBS
          DO I=1,NOB
C
C    If one of the error propogation applications was chosen, then calculate
C    for each data point:
C         - the values of the differential equations
C         - the value of e (the error)
C         - the individual error variance contributions
C         - the total error variance
C         - the weighting and the objective function value
C
              IF (ITYPE.EQ.1) THEN
                  DEDG=-KSTAR*C(I)/(RTHETA(I)**2)*RSOLN(I)/GSOLN(I)
                  DEDG0=-DEDG*GSOLN(I)/GSOLN0(I)
                  DEDC=KSTAR/RTHETA(I)-2*BETA(2)
                  E=KSTAR*C(I)/RTHETA(I)-1.0/BETA(1)-2.0*BETA(2)*C(I)
              ELSE IF (ITYPE.EQ.2) THEN
                  DEDG=RSOLN(I)/GSOLN(I)
                  DEDG0=-RSOLN(I)/GSOLN0(I)
                  DEDC=-(KSTAR/BETA(1))/((1.0/BETA(1)+2.0*BETA(2)*C(I))**2)
                  E=RTHETA(I)-KSTAR*C(I)/(1.0/BETA(1)+2.0*BETA(2)*C(I))
              END IF
              IF ((ITYPE.EQ.1).OR.(ITYPE.EQ.2)) THEN
                  VARG(I)=DEDG**2*GVAR**2
                  VARG0(I)=DEDG0**2*G0VAR**2
                  VARC(I)=DEDC**2*CVAR(I)
                  VARE(I)=VARG(I)+VARG0(I)+VARC(I)
                  W(I)=1.0/VARE(I)
                  F(I)=E*DSQRT(W(I))
              END IF
C
C    If either the linear or non-linear least squares applications was chosen,
C    for each data point, calculate the value of the appropriate objective
C    function.
              IF (ITYPE.EQ.3) THEN
                  F(I)=1.0/BETA(1)+2.0*BETA(2)*C(I)
              ELSE IF (ITYPE.EQ.4) THEN
                  F(I)=KSTAR*C(I)/(1.0/BETA(1)+2.0*BETA(2)*C(I))
              END IF
          END DO
          RETURN
          END
```

```
C
C     This program performs a data analysis of user supplies Dynamic Light
C     Scattering data.  It is currently dimensioned to handle raw
C     autocorrelation data made up of 56 time lag measurements and eight
C     measurements at infinite time delay.
C
C     All variables except those pertaining to the NNLLS routine are double
C     precision.
C
        IMPLICIT REAL*8 (A-H,O-Z)
        INTEGER SHIFTS,SPN
        DIMENSION YY(56),DIFF(20),SIGNS(20),BETA(20),FUN(150,30),
     #            TIME(65),SCRAT(1000),BETAI(20),PRED(56,8),FF(56),
     #            DIAM(4),RES(56,8),PREDT(56,6)
        REAL*4 A(56,20),X(20),B(56),W(20),ZZ(56),TRANMAT(56,56),PHI,
     #            AT(56,20),BT(56)
        INTEGER*2 INDEX(50),MODE
        COMMON/PH/TTIME(56),GAMMA(20),TDC(4),ITYPE,KSQR,COUNTS(64),NEX1,
     #            NEX2
        REAL*8 INTS,INTL,MINCOUNT,KSQR,MAXRES,MINRES,NEX1,NEX2
C
C     The user must define an external MODEL subroutine for the estimation
C     programs UWHAUSDD and NNLLS.
C
        EXTERNAL MODEL
C
C     Only one input data file, DLSIN.DAT is required by the program.  Inputs
C     are described later.
C
        OPEN (UNIT=1,FILE='DLSIN.DAT',STATUS='UNKNOWN')
C
C     The following output data programs are created by the program:
C
C     DLSOUT.DAT          - contains first-order normalized autocorrelation
C                            data as a function of time
C     DIS.DAT             - contains the parameter estimates of the
C                            distribution fit
C     PREDICT.DAT         - contains the predicted values of the first-order
C                            normalized autocorrelation function
C     RESLIM.DAT          - contains the residuals of the fit
C
        OPEN (UNIT=2,FILE='DLSOUT.DAT',STATUS='UNKNOWN')
        OPEN (UNIT=3,FILE='DIS.DAT',STATUS='UNKNOWN')
        OPEN (UNIT=4,FILE='PREDICT.DAT',STATUS='UNKNOWN')
        OPEN (UNIT=5,FILE='RESIDS.DAT',STATUS='UNKNOWN')
        OPEN (UNIT=10,FILE='RESLIM.DAT',STATUS='UNKNOWN')
C
C     Choose a parameter estimation routine.  Note that all estimation problems
C     except ITYPE = 2,3 are linear in the parameters.
C
        PRINT *, 'ENTER ITYPE - 1 to 8:'
        PRINT *, '    1. LAWSON & HANSON NNLS'
        PRINT *, '    2. LAWSON & HANSON NNLS - TRANFORMED DATA'
        PRINT *, '    3. OSTROWSKY SUM OF EXPONENTIALS'
        PRINT *, '    4. ONE EXPONENTIAL, TWO PARAMETERS'
        PRINT *, '    5. TWO EXPONENTIALS, FOUR PARAMETERS'
        PRINT *, '    6. TWO EXPONENTIALS, TWO PARAMETERS'
        PRINT *, '    7. THREE EXPONENTIALS, THREE PARAMETERS'
        PRINT *, '    8. FOUR EXPONENTIALS, FOUR PARAMETERS'
        READ *, ITYPE
C
C     Input data file DLSIN.DAT must contain:
C
C     DELTAT              - channel width (micro-seconds)
C     TCOUNT              - total number of photopulses counted
```

```
C    PCOUNT                 - number of prescaled counts
C    RUNT                   - run time (milli-seconds)
C    PFAC                   - prescale factor
C    COUNTS                 - contents of each individual channel (up to 64), the
C                             second-order un-normalized autocorrelation function
C                             values
C    UWHAUSDD parameters NOB, NP, EPS1, EPS2, MIT, FLAM, FNU
C    SPN                    - determines whether negative parameter estimates will
C                             be allowed or not; YES if SPN = -1; NO if SPN = 1
C    BETAI                  - initial guess of p parameters (only for ITYPE > 0)
C    DL                     - lower diameter value (in nano-metres) at which
C                             parameter estimates start
C    OMEGAMAX               - determines logarithmic spacing between parameter
C                             estimates on diameter scale
C    SHIFTS                 - number of times a set of p parameters are estimated
C                             in each shift; SHIFTS is only equal to 1 unless
C                             Ostrowsky's or Morrison's exponential sampling
C                             methods are used
C    NEX                    - determines whether a weighted NNLLS fit is performed
C                             or not
C
C    Note that some of these input variables are specific to either the
C    UWHAUSDD or NNLLS estimation routines.
C
         READ (1,*) DELTAT,TCOUNT,PCOUNT,RUNT,PFAC
         READ (1,*) (COUNTS(I),I=1,64)
         READ (1,*) NPROB,NOB,NP,EPS1,EPS2,MIT,FLAM,FNU,SPN
         IF (ITYPE.GE.3) READ (1,*) (BETAI(I),I=1,NP)
         READ (1,*) DL,OMEGAMAX,SHIFTS,NEX1,NEX2
C
C    Determine the total number of parameters to be estimated.
C
         NPT=NP*SHIFTS
C
C    Transform the initial parameter estimates from diameter values to
C    translation diffusion coefficient values.
C
         IF ((ITYPE.EQ.4).OR.(ITYPE.EQ.5))
     #       BETAI(2)=214.174/(BETAI(2)/2.0)
         IF (ITYPE.EQ.5) BETAI(4)=214.174/(BETAI(4)/2.0)
         IF (ITYPE.GE.6) THEN
            DO I=1,NP
               READ (1,*) DIAM(I)
               TDC(I)=214.174/(DIAM(I)/2.0)
            END DO
         END IF
C
C    Calculate the initial gamma value where parameter estimation starts.
C
         GAMMA(1)=0.074679/(DL/2.0)
C
C    Calculate the value of the optical constant k(squared) and the constant pi.
C
         KSQR=0.018673**2
         PI=4.0*DATAN(1.D0)
C
C    Determine an average value for the baseline from the eight baseline
C    measurements.
C
         BL=COUNTS(57)
         DO I=58,64
            BL=BL+COUNTS(I)
         END DO
         BL=BL/8.0
C
```

```
C    Let MINCOUNT be the average baseline value and intialize the time.
C
     MINCOUNT=BL*2048.0
     TIME(1)=0.0
C
C    Calculate the first-order, normalized autocorrelation function values from
C    the second-order, un-normalized autocorrelation function values, and
C    increment the time accordingly for each channel.
C
     DO I=1,56
        COUNTS(I)=DSQRT(COUNTS(I)/BL-1.0)
        WRITE (2,*) TIME(I),COUNTS(I)
        TIME(I+1)=TIME(I)+DELTAT
     END DO
C
C    Check :
C
C       1.  the total number of counts
C       2.  the baseline value
C
     CHECK1=PCOUNT*PFAC*2048
     CHECK2=DELTAT*1E-6*TCOUNT*PCOUNT*1000/RUNT/MINCOUNT
     TCOUNT=TCOUNT*2048
     WRITE (6,10) TCOUNT,CHECK1
     WRITE (6,20) CHECK2
10   FORMAT (' ',5X,'TOTAL COUNTS = ',F15.2,5X,F15.2,//)
20   FORMAT (' ',5X,'BASELINE RATIO = ',F15.12)
C
C    If either Ostrowsky's or Morrison's exponential sampling method was chosen,
C    then determine the intervals between each gamma value at which a parameter
C    is estimated and between each shift.
C
     IF (ITYPE.LE.3) THEN
        INTL=DEXP(-PI/OMEGAMAX)
        GAMMA(2)=INTL*GAMMA(1)
        INTS=DLOG(INTL)/SHIFTS
C
C    Define the initial gamma values at which parameter estimation takes place.
C
        DO I=3,NP
           GAMMA(I)=INTL*GAMMA(I-1)
        END DO
     END IF
C
C    If the data is to be transformed to account for autocorrelated errors, then
C    apply the appropriate transformation formula for an AR(1) model.  PHI is
C    fitted AR(1) model parameter.
C
     IF (ITYPE.EQ.2) THEN
        PRINT 65
65      FORMAT (' ',5X,'ENTER PHI')
        READ *, PHI
        TRANMAT(1,1)=SQRT(1.0-PHI**2)
        DO I=2,NOB
           TRANMAT(I,I)=1.0
           TRANMAT(I,I-1)=-PHI
        END DO
     END IF
C
C    Set YY to be the objective function for the UWHAUSDD parameter estimation
C    routine.  If NEX > 1, then the objective function is weighted according
C    to Morrison's forumla.
C
     DO I=1,NOB
        TTIME(I)=TIME(I)
```

```
            YY(I)=COUNTS(I)**NEX1
            PRED(I,1)=TIME(I)
            PRED(I,2)=YY(I)
        END DO
C
C   Set the step differential used by UWHAUSDD to evaluate the objective
C   function and set SIGNS to either allow or disallow negative parameter
C   estimates.
C
        DO I=1,NP
            DIFF(I)=0.0001
            SIGNS(I)=SPN
            BETA(I)=BETAI(I)
        END DO
C
C   For each shift, call the appropriate estimation routine.
C
        DO I=1,SHIFTS
            IF (ITYPE.GE.3) THEN
C
C   For Ostrowsky's exponential sampling method and the special cases where
C   only two to four parameters are estimated, call UWHAUSDD.
C
                CALL UWHAUS(NPROB,MODEL,NOB,YY,NP,BETA,DIFF,SIGNS,EPS1,EPS2,MIT,
     #                     FLAM,FNU,SCRAT)
C
C   For Morrison's exponential sampling approach, using NNLLS, first set up
C   the appropriate matrices and vectors before calling the estimation routine.
C
            ELSE IF (ITYPE.LE.2) THEN
C
C   Initialize the parameter vector, X, to be zero.
C
                DO I1=1,NP
                    X(I1)=0.0
                END DO
C
C   Define the single precision A matrix and the B vector.
C
                DO I1=1,NOB
                    B(I1)=SNGL(YY(I1))
                    DO I2=1,NP
                        A(I1,I2)=SNGL(COUNTS(I1)**(NEX1-NEX2)*
     #                           DEXP(-GAMMA(I2)*TTIME(I1)))
                    END DO
                END DO
C
C   Transform the A matrix and B vector to account for autocorrelated errors
C   according to an AR(1) model if ITYPE = 2 was chosen.
C
                IF (ITYPE.EQ.2) THEN
                    DO I1=1,NOB
                        SUMTB=0.0
                        DO J2=1,NOB
                            SUMTB=SUMTB+TRANMAT(I1,J2)*B(J2)
                        END DO
                        BT(I1)=SUMTB
                        DO J1=1,NP
                            SUMTA=0.0
                            DO K1=1,NOB
                                SUMTA=SUMTA+TRANMAT(I1,K1)*A(K1,J1)
                            END DO
                            AT(I1,J1)=SUMTA
                        END DO
                    END DO
```

```
                  DO I1=1,NOB
                     B(I1)=BT(I1)
                     PRED(I1,2)=B(I1)
                     DO I2=1,NP
                        A(I1,I2)=AT(I1,I2)
                     END DO
                  END DO
               END IF
C
C    Call the NNLLS estimation routine (single precision)
C
               CALL NNLS(A,NOB,NOB,NP,B,X,RNORM,W,ZZ,INDEX,MODE)
               WRITE (6,*) RNORM,MODE
               WRITE (6,*) X
C
C    If the NNLLS routine has destroyed the contents of INTS (the interval
C    between successive shifts), restore it.
C
               IF (INTS.EQ.0) INTS=DLOG(INTL)/SHIFTS
C
C    Transform the final parameter estimates to double precision.
C
               DO I1=1,NP
                  BETA(I1)=DBLE(X(I1))
               END DO
            END IF
C
C    Evaluate the model subroutine at the final values of the parameter
C    estimates.
C
            CALL MODEL(NPROB,BETA,FF,NOB,NP)
            DO J=1,NOB
               PRED(J,I+2)=FF(J)
            END DO
C
C    If Ostrowsky's or Morrison's exponential sampling method was chosen, store
C    final parameter estimates as a function of diameter on both an absolute and
C    a logarithmic scale; increment the starting value of gamma by one shift
C    interval; and re-initialize the initial guesses of the parameters.
C
            IF (ITYPE.LE.3) THEN
               DO J=1,NP
                  FUN(I+(J-1)*SHIFTS,2)=BETA(J)*OMEGAMAX/PI
                  FUN(I+(J-1)*SHIFTS,3)=0.074679*2.0/GAMMA(J)
                  FUN(I+(J-1)*SHIFTS,1)=DLOG(FUN(I+(J-1)*SHIFTS,3))
               END DO
               GAMMA(1)=DEXP(DLOG(GAMMA(1))+INTS)
               BETA(1)=BETAI(1)
               DO J=2,NP
                  GAMMA(J)=INTL*GAMMA(J-1)
                  BETA(J)=BETAI(J)
               END DO
               NPROB=NPROB+1
C
C    If one of the non-linear estimation routines was chosen, then calculate
C    the absolute values of the diameters from the appropriate fitted
C    parameters.
C
            ELSE IF ((ITYPE.EQ.4).OR.(ITYPE.EQ.5)) THEN
               DIAM(1)=214.174*2.0/BETA(2)
               WRITE (3,60) BETA(1),DIAM(1)
               IF (ITYPE.EQ.5) THEN
                  DIAM(2)=214.174*2.0/BETA(4)
                  WRITE (3,60) BETA(3),DIAM(2)
               END IF
```

```
C
C    If one of the linear estimation routines where no more than four parameters
C    have been estimated was chosen, simply output the appropriate number of
C    parameter estimates.
C
          ELSE IF (ITYPE.GE.6) THEN
              DO K=1,2
                  WRITE (3,60) BETA(K),DIAM(K)
              END DO
              IF (ITYPE.GE.7) WRITE (3,60) BETA(3),DIAM(3)
              IF (ITYPE.EQ.8) WRITE (3,60) BETA(4),DIAM(4)
          END IF
      END DO
C
C    Output the parameter estimates.
C
      IF (ITYPE.LE.3) WRITE (3,30) ((FUN(I,J),J=1,3),I=1,NPT)
C
C    Calculate the predicted values of the first-order, normalized
C    autocorrelation function for the case where autocorrelated errors
C    was accounted for.
C
      IF (ITYPE.EQ.2) THEN
          DO I=1,NOB
              DO J=1,SHIFTS
                  SUMC=0.0
                  DO K=1,NOB
                      SUMC=SUMC+TRANMAT(I,K)*PRED(K,J+2)
                  END DO
                  PREDT(I,J)=SUMC
              END DO
          END DO
          DO I=1,NOB
              DO J=3,SHIFTS+2
                  PRED(I,J)=PREDT(I,J-2)
              END DO
          END DO
      END IF
      WRITE (4,40) ((PRED(I,J),J=1,8),I=1,56)
C
C    At each observation, calculate the residuals from each shift, determine
C    the maximum and minimum residual and calculate an average residual.
C
      DO I=1,NOB
          RES(I,1)=PRED(I,1)
          SUMRES=0.0
          MAXRES=PRED(I,2)-PRED(I,3)
          MINRES=PRED(I,2)-PRED(I,3)
          DO J=2,SHIFTS+1
              RES(I,J)=PRED(I,2)-PRED(I,J+1)
              SUMRES=SUMRES+RES(I,J)
              IF (RES(I,J).GT.MAXRES) MAXRES=RES(I,J)
              IF (RES(I,J).LT.MINRES) MINRES=RES(I,J)
          END DO
          RES(I,SHIFTS+2)=SUMRES/SHIFTS
          IF (NEX1.GT.1) THEN
              DIVFAC=COUNTS(I)**(NEX1-NEX2)
              RES(I,SHIFTS+2)=RES(I,SHIFTS+2)/DIVFAC
              MAXRES=MAXRES/DIVFAC
              MINRES=MINRES/DIVFAC
          END IF
C
C    At each observation, output the time lag, the average residual, and the
C    largest and smallest residuals.
C
```

```fortran
            WRITE (10,70) RES(I,1),RES(I,SHIFTS+2),MAXRES,MINRES
         END DO
         WRITE (5,40) ((RES(I,J),J=1,8),I=1,56)
30       FORMAT (' ',F16.12,5X,F16.4,5X,F16.8)
40       FORMAT (' ',1(F8.1,7(5X,F11.7)))
60       FORMAT (' ',F16.4,5X,F16.8)
70       FORMAT (' ',1(F8.1,3(5X,F11.7)))
         STOP
         END
C
C
C

         SUBROUTINE MODEL(NPROB,BETA,F,NOB,NP)
         IMPLICIT REAL*8(A-H,O-Z)
         REAL*8 KSQR,NEX1,NEX2
         DIMENSION BETA(NP),F(NOB)
         COMMON/PH/TTIME(56),GAMMA(20),TDC(4),ITYPE,KSQR,COUNTS(64),NEX1,
     #             NEX2
C
C    If Ostrowsky's or Morrison's exponential sampling method was chosen, then
C    calculate the sum of exponentials according to how many parameters are to
C    be estimated.
C
         IF (ITYPE.LE.3) THEN
            DO II=1,NOB
               SUMING=0.0
               DO JJ=1,NP
                  ADDIT=COUNTS(II)**(NEX1-NEX2)*DEXP(-GAMMA(JJ)*TTIME(II))
                  SUMING=SUMING+BETA(JJ)*ADDIT
               END DO
               F(II)=SUMING
            END DO
C
C    If one of the non-linear estimation problems was chosen, then determine the
C    appropriate objective function with either two or four parameters.
C
         ELSE IF ((ITYPE.EQ.4).OR.(ITYPE.EQ.5)) THEN
            DO II=1,NOB
               SUMING=COUNTS(II)**(NEX1-NEX2)*BETA(1)*
     #                  DEXP(-BETA(2)*KSQR*TTIME(II))
               IF (ITYPE.EQ.5) SUMING=SUMING+COUNTS(II)**(NEX1-NEX2)*
     #                     BETA(3)*DEXP(-BETA(4)*KSQR*TTIME(II))
               F(II)=SUMING
            END DO
C
C    If one of the simpler linear models was chosen, then calculate the
C    appropriate objective function according to how many parameters are to
C    be estimated.
C
         ELSE IF (ITYPE.GE.6) THEN
            DO II=1,NOB
               SUMING=0.0
               DO JJ=1,2
                  SUMING=SUMING+COUNTS(II)**(NEX1-NEX2)*BETA(JJ)*
     #               DEXP(-TDC(JJ)*KSQR*TTIME(II))
               END DO
               IF (ITYPE.GE.7) SUMING=SUMING+COUNTS(II)**(NEX1-NEX2)*
     #                     BETA(3)*DEXP(-TDC(3)*KSQR*TTIME(II))
               IF (ITYPE.EQ.8) SUMING=SUMING+COUNTS(II)**(NEX1-NEX2)*
     #                     BETA(4)*DEXP(-TDC(4)*KSQR*TTIME(II))
               F(II)=SUMING
            END DO
         END IF
         RETURN
         END
```

```
C       SUBROUTINE NNLS (A,MDA,M,N,B,X,RNORM,W,ZZ,INDEX,MODE)
C       C.L. LAWSON AND R.J. HANSON, JET PROPULSON LABORATORY, 1973 JUNE 15
C       APPEARS IN 'SOLVING LEAST SQUARES PROBLEMS', PRENTICE-HALL, 1974
C
C       **********  NON-NEGATIVE LEAST SQUARES  **********
C
C       GIVEN AN M BY N MATRIX, A, AND AN M-VECTOR, B, COMPUTE AN N-VECTOR,
C       X, WHICH SOLVES THE LEAST SQUARES PROBLEM
C
C                       A * X = B     SUBJECT TO X .GE. 0
C
C       A( ),MDA,M,N    MDA IS THE FIRST DIMENSIONING PARAMETER FOR THE ARRAY,
C                       A( ).  ON ENTRY A( ) CONTAINS THE M BY N MATRIX, A.
C                       ON EXIT, A( ) CONTAINS THE PRODUCT MATRIX, Q*A, WHERE
C                       Q IS AN M BY M ORTHOGONAL MATRIX GENERATED IMPLICITLY
C                       BY THIS SUBROUTINE.
C       B( )    ON ENTRY, B( ) CONTAINS THE M-VECTOR, B.  ON EXIT, B( )
C               CONTAINS Q*B.
C       X( )    ON ENTRY, X( ) NEED NOT BE INITIALIZED.  ON EXIT, X( ) WILL
C               CONTAIN THE SOLUTION VECTOR.
C       RNORM   ON EXIT, RNORM CONTAINS THE EUCLIDEAN NORM OF THE RESIDUAL
C               VECTOR.
C       W( )    AN N-ARRAY OF WORKING SPACE.  ON EXIT, W( ) WILL CONTAIN THE
C               DUAL SOLUTION VECTOR.  W WILL SATISFY W(I) = 0 FOR ALL I IN
C               SET P AND W(I) .LE. 0 FOR ALL I IN SET Z.
C       ZZ( )   AN M-ARRAY OF WORKING SPACE.
C       INDEX( )        AN INTEGER WORKING ARRAY OF LENGTH AT LEAST N.
C                       ON EXIT, THE CONTENTS OF THIS ARRAY DEFINE THE SETS
C                       P AND Z AS FOLLOWS...
C
C                       INDEX(1)   THROUGH INDEX(NSTEP) = SET P
C                       INDEX(IZ1) THROUGH INDEX(IZ2)   = SET Z
C                       IZ1 = NSTEP + 1 = NPP1
C                       IZ2=N
C
C       MODE    THIS IS A SUCCESS-FAILURE FLAG WITH THE FOLLOWING MEANINGS.
C               1       THE SOLUTION HAS BEEN COMPUTED SUCCESSFULLY.
C               2       THE DIMENSIONS OF THE PROBLEM ARE BAD.
C                       EITHER M .LE. 0 OR N .LE. 0
C               3       ITERATION COUNT EXCEEDED.  MORE THAN 3*N ITERATIONS.
C
        SUBROUTINE NNLS (A,MDA,M,N,B,X,RNORM,W,ZZ,INDEX,MODE)
        DIMENSION A(MDA,N), B(M), X(N), W(N), ZZ(M)
        INTEGER INDEX(N)
        ZERO=0.
        ONE=1.
        TWO=2.
        FACTOR=0.01
C
        MODE=1
        IF (M.GT.0.AND.N.GT.0) GO TO 10
        MODE=2
        RETURN
10      ITER=0
        ITMAX=3*N
C
C               INITIALIZE THE ARRAYS INDEX( ) AND X( ).
C
        DO 20 I=1,N
           X(I)=ZERO
20         INDEX(I)=I
C
        IZ2=N
        IZ1=1
        NSETP=0
```

```
          NPP1=1
C
C                   *****  MAIN LOOP BEGINS HERE  *****
C
30        CONTINUE
C
C                   QUIT IF ALL COEFFICIENTS ARE ALREADY IN THE SOLUTION
C                   OR IF M COLS OF A HAVE BEEN TRIANGULARIZED.
C
          IF (IZ1.GT.IZ2.OR.NSETP.GE.M) GO TO 350
C
C                   COMPUTE COMPONENTS OF THE DUAL (NEGATIVE GRADIENT) VECTOR W( ).
C
          DO 50 IZ=IZ1,IZ2
             J=INDEX(IZ)
             SM=ZERO
             DO 40 L=NPP1,M
40              SM=SM+A(L,J)*B(L)
50           W(J)=SM
C
C                   FIND LARGEST POSITIVE W(J)
C
60        WMAX=ZERO
          DO 70 IZ=IZ1,IZ2
             J=INDEX(IZ)
             IF (W(J).LE.WMAX) GO TO 70
             WMAX=W(J)
             IZMAX=IZ
70        CONTINUE
C
C                   IF WMAX .LE. 0 GO TO TERMINATION.
C                   THIS INDICATES SATISFACTION OF THE KUHN-TUCKER CONDITIONS.
C
          IF (WMAX) 350,350,80
80        IZ=IZMAX
          J=INDEX(IZ)
C
C                   THE SIGN OF W(J) IS OK FOR J TO BE MOVED TO SET P.
C                   BEGIN THE TRANSFORMATION AND CHECK NEW DIAGONAL ELEMENT TO
C                   AVOIC NEAR LINEAR DEPENDANCE.
C
          ASAVE=A(NPP1,J)
          CALL H12(1,NPP1,NPP1+1,M,A(1,J),1,UP,DUMMY,1,1,0)
          UNORM=ZERO
          IF (SETP.EQ.0) GO TO 100
          DO 90 L=1,NSETP
90           UNORM=UNORM+A(L,J)**2
100       UNORM=SQRT(UNORM)
          IF (DIFF(UNORM+ABS(A(NPP1,J))*FACTOR,UNORM)) 130,130,110
C
C                   COL J IS SUFFICIENTLY INDEPENDENT.  COPY B INTO ZZ, UPDATE
C                   ZZ AND SOLVE FOR ZTEST ( = PROPOSED NEW VALUE FOR X(J) ).
C
110       DO 120 L=1,M
120          ZZ(L)=B(L)
          CALL H12(2,NPP1,NPP1+1,M,A(1,J),1,UP,ZZ,1,1,1)
          ZTEST=ZZ(NPP1)/A(NPP1,J)
C
C                   SEE IF ZTEST IS POSITIVE.
C
          IF (ZTEST) 130,130,140
C
C                   REJECT J AS A CANDIDATE TO BE MOVED FROM SET Z TO SET P.
C                   RESTORE A(NPP1,J), SET W(J)=0, AND LOOP BACK TO TEST DUAL
C                   COEFFS AGAIN.
```

```
C
130       A(NPP1,J)=ASAVE
          W(J)=ZERO
          GO TO 60
C
C                 THE INDEX J=INDEX(IZ) HAS BEEN SELECTED TO BE MOVED FROM
C                 SET Z TO SET P.  UPDATE B.  UPDATE INDICES.  APPLY
C                 HOUSEHOLDER TRANSFORMATIONS TO COLS IN NEW SET Z.  ZERO
C                 SUBDIAGONAL ELTS IN COL J.  SET W(J)=0.
C
140       DO 150 L=1,M
150          B(L)=ZZ(L)
C
          INDEX(IZ)=INDEX(IZ1)
          INDEX(IZ1)=J
          IZ1=IZ1+1
          NSETP=NPP1
          NPP1=NPP1+1
C
          IF (IZ1.GT.IZ2) GO TO 170
          DO 160 JZ=IZ1,IZ2
             JJ=INDEX(JZ)
160          CALL H12(2,NSETP,NPP1,M,A(1,J),1,UP,A(1,JJ),1,MDA,1)
170       CONTINUE
C
          IF (NSETP.EQ.M) GO TO 190
          DO 180 L=NPP1,M
180          A(L,J)=ZERO
190       CONTINUE
C
          W(J)=ZERO
C
C                 SOLVE THE TRIANGULAR SYSTEM.
C                 STORE THE SOLUTION TEMPORARILY IN ZZ( ).
C
          ASSIGN 200 TO NEXT
          GO TO 400
200       CONTINUE
C
C                 *****  SECONDARY LOOP BEGINS HERE  *****
C
C                 ITERATION COUNTER
C
210       ITER=ITER+1
          IF (ITER.LE.ITMAX) GO TO 220
          MODE=3
          WRITE (6,440)
          GO TO 350
220       CONTINUE
C
C                 SEE IF ALL NEW CONSTRAINED COEFFS ARE FEASIBLE.
C                 IF NOT, COMPUTE ALPHA.
C
          ALPHA=TWO
          DO 240 IP=1,NSETP
             L=INDEX(IP)
             IF (ZZ(IP)) 230,230,240
C
230          T=-X(L)/(ZZ(IP)-X(L))
             IF (ALPHA.LE.T) GO TO 240
             ALPHA=T
             JJ=IP
240       CONTINUE
C
C                 IF ALL NEW CONSTRAINED COEFFS ARE FEASIBLE THEN ALPHA WILL
```

```
C                     STILL = 2.  IF SO, EXIT FROM SECONDARY LOOP TO MAIN LOOP.
C
        IF (ALPHA.EQ.TWO) GO TO 330
C
C                     OTHERWISE, USE ALPHA WHICH WILL BE BETWEEN 0 AND 1 TO
C                     INTERPOLATE BETWEEN THE OLD X AND THE NEW ZZ.
C
        DO 250 IP=1,NSETP
           L=INDEX(IP)
250        X(L)=X(L)+ALPHA*(ZZ(IP)-X(L))
C
C                     MODIFY A AND B AND THE INDEX ARRAYS TO MOVE COEFFICIENT I
C                     FROM SET P TO SET Z.
C
        I=INDEX(JJ)
260     X(I)=ZERO
C
        IF (JJ.EQ.NSETP) GO TO 290
        JJ=JJ+1
        DO 280 J=JJ,NSETP
           II=INDEX(J)
           INDEX(J-1)=II
           CALL G1(A(J-1,II),A(J,II),CC,SS,A(J-1,II))
           A(J,II)=ZERO
           DO 270 L=1,N
              IF (L.NE.II) CALL G2(CC,SS,A(J-1,L),A(J,L))
270        CONTINUE
280        CALL G2(CC,SS,B(J-1),B(J))
290     NPP1=NSETP
        NSETP=NSETP-1
        IZ1=IZ1-1
        INDEX(IZ1)=I
C
C                     SEE IF THE REMAINING COEFFS IN SET P ARE FEASIBLE.  THEY SHOULD
C                     BE BECAUSE OF THE WAY ALPHA WAS DETERMINED.
C                     IF ANY ARE INFEASIBLE, IT IS DUE TO ROUND-OFF ERROR.
C                     ANY THAT ARE NONPOSITIVE WILL BE SET TO ZERO AND MOVED
C                     FROM SET P TO SET Z.
C
        DO 300 JJ=1,NSETP
        I=INDEX(JJ)
        IF (X(I)) 260,260,300
300     CONTINUE
C
C                     COPY B( ) INTO ZZ( ).  THEN SOLVE AGAIN AND LOOP BACK.
C
        DO 310 I=1,M
310        ZZ(I)=B(I)
        ASSIGN 320 TO NEXT
        GO TO 400
320     CONTINUE
        GO TO 210
C
C                     ***** END OF SECONDARY LOOP *****
C
330     DO 340 IP=1,NSETP
           I=INDEX(IP)
340        X(I)=ZZ(IP)
C
C                     ALL NEW COEFFS ARE POSITIVE.  LOOP BACK TO BEGINNING.
C
        GO TO 30
C
C                     ***** END OF MAIN LOOP *****
C
```

```
C             COME TO HERE FOR TERMINATION.
C             COMPUTE THE NORM OF THE FINAL RESIDUAL VECTOR.
C
350      SM=ZERO
         IF (NPP1.GT.M) GO TO 370
         DO 360 I=NPP1,M
360         SM=SM+B(I)**2
         GO TO 390
370      DO 380 J=1,N
380         W(J)=ZERO
390      RNORM=SQRT(SM)
         RETURN
C
C             THE FOLLOWING BLOCK OF CODE IS USED AS AN INTERNAL SUBROUTINE
C             TO SOLVE THE TRIANGULAR SYSTEM, PUTTING THE SOLUTION IN ZZ(I).
C
400      DO 430 L=1,NSETP
            IP=NSETP+1-L
            IF (L.EQ.1) GO TO 420
            DO 410 II=1,IP
410            ZZ(II)=ZZ(II)-A(II,JJ)*ZZ(IP+1)
420         JJ=INDEX(IP)
430         ZZ(IP)=ZZ(IP)/A(IP,JJ)
         GO TO NEXT, (200,320)
440      FORMAT (35H0 NNLS QUITTING ON ITERATION COUNT.)
         END
C
C
C
C     SUBROUTINE H12(MODE,LPIVOT,L1,M,U,IUE,,UP,C,ICE,ICV,NCV)
C
C     CONSTRUCTION AND/OR APPLICATION OF A SINGLE HOUSEHOLDER
C     TRANSFORMATION...    Q = I + U*(U**T)/B
C
C     MODE    = 1 OR 2   TO SELECT ALGORITHM H1 OR H2 RESPECTIVELY
C     LPIVOT  IS THE INDEX OF THE PIVOT ELEMENT
C     L1,M    IF L1 .LE. M, THE TRANSFORMATION WILL BE CONSTRUCTED TO
C             ZERO ELEMENTS INDEXED FROML1 THROUGH M.  IF L1 .GT. M, THE
C             SUBROUTINE DOES AN IDENTITY TRANSFORMATION.
C     U( ),IUE,UP     ON ENTRY TO H1, U( ) CONTAINS THE PIVOT VECTOR.
C                     IUE IS THE STORAGE INCREMENT BETWEEN ELEMENTS.
C                     ON EXIT FROM H1, U( ) AND UP CONTAIIN QUANTITIES
C                     DEFINING THE VECTOR U OF THE HOUSEHOLDER
C                     TRANSFORMATION.
C                     ON ENTRY TO H2, U( ) AND UP SHOULD CONTAIN QUANTITIES
C                     PREVIOUSLY COMPUTED BY H1.  THESE WILL NOT BE
C                     MODIFIED BY H2.
C     C( )    ON ENTRY TO H1 OR H2, C( ) CONTAINS A MATRIX WHICH WILL BE
C             REGARDED AS A SET OF VECTORS TO WHICH THE HOUSEHOLDER
C             TRANSFORMATION IS TO BE APPLIED.  ON EXIT, C( ) CONTAINS THE
C             SET OF TRANSFORMED VECTORS.
C     ICE     STORAGE INCREMENT BETWEEN ELEMENTS OF VECTORS IN C( ).
C     ICV     STORAGE INCREMENT BETWEEN VECTORS IN C( ).
C     NCV     NUMBER OF VECTORS IN C( ) TO BE TRANSFORMED.  IF NCV .LE. 0,
C             NO OPERATIONS WILL BE DONE ON C( ).
C
         SUBROUTINE H12(MODE,LPIVOT,L1,M,U,IUE,UP,C,ICE,ICV,NCV)
         DIMENSION U(IUE,M), C(1)
         DOUBLE PRECISION SM, B
         ONE=1.
C
         IF (0.GE.LPIVOT.OR.LPIVOT.GE.L1.OR.L1.GT.M) RETURN
         CL=ABS(U(1,LPIVOT))
         IF (MODE.EQ.2) GO TO 60
C
```

```
C                     *****   CONSTRUCT THE TRANSFORMATION   *****
C
      DO 10 J=L1,M
10        CL=AMAX1(ABS(U(I,J)),CL)
      IF (CL) 130,130,20
20    CLINV=ONE/CL
      SM=(DBLE(U(1,LPIVOT))*CLINV)**2
      DO 30 J=L1,M
30        SM=SM+(DBLE(U(1,J))*CLINV)**2
C
C             CONVERT DBLE. PREC. SM TO SNGL. PREC. SM1
C
      SM1=SM
      CL=CL*SQRT(SM1)
      IF (U(1,LPIVOT))50,50,40
40    CL=-CL
50    UP=U(1,LPIVOT)-CL
      U(1,LPIVOT)=CL
      GO TO 70
C
C             *****   APPLY THE TRANSFORMATION I+U*(U**T)/B TO C
C
60    IF (CL) 130,130,70
70    IF (NCV.LE.0) RETURN
      B=DBLE(UP)*U(1,LPIVOT)
C
C             B MUST BE NONPOSITIVE HERE.  IF B = 0, RETURN.
C
      IF (B) 80,130,130
80    B=ONE/B
      I2=1-ICV+ICE*(LPIVOT-1)
      INCR=ICE*(L1-LPIVOT)
      DO 120 J=1,NCV
         I2=I2+ICV
         I3=I2+INCR
         I4=I3
         SM=C(I2)*DBLE(UP)
         DO 90 I=L1,M
            SM=SM+C(I3)*DBLE(U(1,I))
90          I3=I3+ICE
         IF (SM) 100,120,100
100      SM=SM*B
         C(I2)=C(I2)+SM*DBLE(UP)
         DO 110 I=L1,M
            C(I4)=C(I4)+SM*DBLE(U(1,I))
110         I4=I4+ICE
120   CONTINUE
130   RETURN
      END
C
C
C
      SUBROUTINE G1(A,B,COS,SIN,SIG)
C
C     COMPUTE ORTHOGONAL ROTATION MATRIX.
C     COMPUTE.. MATRIX  (C, S) SO THAT (C, S)(A) = SQRT(A**2+B**2)
C                       (-X,C)          (-S,C)(B) =    0
C     COMPUTE SIG = SQRT(A**2+B**2)
C        SIG IS COMPUTED LAST TO ALLOW FOR THE POSSIBILITY THAT SIG
C        MAY BE IN THE SAME LOCATION AS A OR B.
C
      ZERO=0
      ONE=1
      IF (ABS(A).LE.ABS(B)) GO TO 10
      XR=B/A
```

```fortran
         YR=SQRT(ONE+XR**2)
         COS=SIGN(ONE/YR,A)
         SIN=COS*XR
         SIG=ABS(A)*YR
         RETURN
10       IF (B) 20,30,20
20       XR=A/B
         YR=SQRT(ONE+XR**2)
         SIN=SIGN(ONE/YR,B)
         COS=SIN*XR
         SIG=ABS(B)*YR
         RETURN
30       SIG=ZERO
         COS=ZERO
         SIN=ONE
         RETURN
         END
C
C
C

         SUBROUTINE G2(COS,SIN,X,Y)
         XR=COS*X+SIN*Y
         Y=-SIN*X+COS*Y
         X=XR
         RETURN
         END
C
C
C

         FUNCTION DIFF(X,Y)
         DIFF=X-Y
         RETURN
         END
```

APPENDIX 3

Evaluation of Partial Derivatives

For WALS

Vertically polarized light was used for the data set studied, $1 + \cos^2\theta = 1$ in equation (3.21) and thus,

$$R_\theta = \frac{R_b}{G_b} \sin\theta \, H_\theta$$

Let

$$\beta_1 = \frac{1}{M}$$

$$\beta_2 = \frac{16\pi^2 \langle s^2 \rangle_z}{3\lambda^2}$$

$$\beta_3 = A_2$$

$$\beta_4 = A_3$$

For ITYPE = 1:

$$e = f(R_\theta, c, \theta; \beta_1, \beta_2, \beta_3, \beta_4)$$

$$= \frac{K^* c}{R_b/G_b(\sin\theta \, H_\theta)} - \frac{1}{\beta_1}[1 + \beta_2\sin^2(\theta/2)] - 2\beta_3 c - 3\beta_4 c^2$$

$$\frac{\delta f}{\delta H_\theta} = - \frac{K^* c}{R_b/B_b(\sin\theta \, H_\theta^2)}$$

$$\frac{\delta f}{\delta c} = \frac{K^*}{R_b/G_b(\sin\theta \, H_\theta)} - 2\beta_3 - 6\beta_4 c$$

$$\frac{\delta f}{\delta\theta} = - \frac{K^* c \cos\theta}{R_b/G_b(\sin^2\theta \, H_\theta)} - \frac{\beta_2}{\beta_1}\sin(\theta/2)\cos(\theta/2)$$

For ITYPE = 2:

$$e = f(R_\theta, c, \theta; \beta_1, \beta_2, \beta_3, \beta_4)$$

$$= R_b/G_b \sin\theta \, H_\theta - \frac{K^* c}{1/\beta_1[1 + \beta_2\sin^2(\theta/2)] + 2\beta_3 c + 3\beta_4 c^2}$$

$$\frac{\delta f}{\delta H_\theta} = R_b/G_b \sin\theta$$

$$\frac{\delta f}{\delta c} = \frac{\beta_1 K^*[3\beta_4 c^2 - 1 - \beta_2\sin^2(\theta/2)]}{[1 + \beta_2\sin^2(\theta/2) + 2\beta_3 c + 3\beta_4 c^2]^2}$$

$$\frac{\delta f}{\delta\theta} = R_b/G_b \cos\theta \, H_\theta + \frac{\beta_1\beta_2 K^* c \sin(\theta/2)\cos(\theta/2)}{[1 + \beta_2\sin^2(\theta/2) + 2\beta_3 c + 3\beta_4 c^2]^2}$$

For LALLS

The baseline value (bl) in equation (3.27) was zero for all of data sets used, therefore

$$R_\theta = \frac{G_\theta}{G_o} (\sigma' \lambda' \Gamma^1 D - R_{solv}$$

Let
$$\beta_1 = \frac{1}{\overline{M}_w}$$
$$\beta_2 = A_2$$

For ITYPE = 1:
$$e = f(R_\theta, c; \beta_1, \beta_2)$$
$$= \frac{K^* c}{G_\theta/G_o(\sigma' \lambda' \Gamma^1 D - R_{solv}} - \beta_1 - 2\beta_2 c$$

$$\frac{\delta f}{\delta G_\theta} = - \frac{K^* c}{[G_\theta/G_o(\sigma' \lambda' \Gamma^1 D - R_{solv}]^2} \frac{(\sigma' \lambda' \Gamma^1 D}{G_o}$$

$$\frac{\delta f}{\delta G_o} = - \frac{K^* c}{[G_\theta/G_o(\sigma' \lambda' \Gamma^1 D - R_{solv}]^2} \frac{G_\theta(\sigma' \lambda' \Gamma^1 D}{G_o^2}$$

$$\frac{\delta f}{\delta c} = \frac{K^*}{[G_\theta/G_o(\sigma' \lambda' \Gamma^1 D - R_{solv}]} - 2\beta_2$$

For ITYPE = 2:
$$e = f(R_\theta, c; \beta_1, \beta_2)$$
$$= G_\theta/G_o(\sigma' \lambda' \Gamma^1 D - R_{solv} - \frac{K^* c}{1/\beta_1 + 2\beta_2 c}$$

$$\frac{\delta f}{\delta G_\theta} = \frac{(\sigma' \lambda' \Gamma^1 D}{G_o}$$

$$\frac{\delta f}{\delta G_o} = - \frac{G_\theta(\sigma' \lambda' \Gamma^1 D}{G_o^2}$$

$$\frac{\delta f}{\delta c} = - \frac{K^*/\beta_1}{(1/\beta_1 + 2\beta_2 c)^2}$$

APPENDIX 4

Analysis of Variance on LALLS Polyacrylamide/Water Data

Basis – Three sets of paired replicate experiments given in the tables
below : (R-9E,R-9I), (R-10C,R-10H), (R-11D,R-11G)

Conc.	G_θ		Var (G_θ)	G_0		Var (G_0)
	R-9E	R-9I		R-9E	R-9I	
c	928	915	97.5	465	427	722.0
c	925	922	4.5	552	504	1152.0*
c	930	910	200.0	734	656	3042.0*
c	915	930	112.5	247	923	— ✝
c	910	965	1512.5*	400	383	144.5
pooled variance (degrees of freedom)			385.4 (5) 103.6 (4)			1265.1 (4) 406.3 (3)

Conc.	G_θ		Var (G_θ)	G_0		Var (G_0)
	R-10C	R-10H		R-10C	R-10H	
c	937	925	72.0	229	931	— ✝
c	930	905	312.5	239	965	— ✝
c	910	907	4.5	270	263	24.5
c	920	920	0.0	336	328	32.0
c	930	918	72.0	519	491	392.0*
pooled variance (degrees of freedom)			92.2 (5)			149.5 (3) 28.3 (2)

	G_θ				G_o		
Conc.	R-11D	R-11G	Var (G_θ)		R-11D	R-11G	Var (G_o)
c	908	918	50.0		798	805	24.5
c	913	928	112.5		829	832	4.5
c	920	912	32.0		888	241	– †
c	900	925	312.5		238	267	420.5 *
c	930	920	50.0		366	384	162.0
pooled variance (degrees of freedom)			111.4 (5)				152.9 (4) 63.7 (3)

Overall pooled variance for:

G_θ – var(G_θ) = $\dfrac{385.4 + 92.2 + 111.4}{3}$ = 196.3, 15 degrees of freedom (d.o.f.)

∴ st. dev. (G_θ) ≐ 14

G_o – var(G_o) = $\dfrac{4(1265.1 + 152.9) + 3(149.5)}{4 + 4 + 3}$ = 556.4, 11 d.o.f

∴ st. dev. (G_o) ≐ 24

* – Overall pooled variance, neglecting the noted high values, for:

G_θ – var (G_θ) = $\dfrac{5(92.2 + 111.4) + 4(103.6)}{5 + 5 + 4}$ = 102.3, 14 d.o.f.

∴ st. dev. (G_θ) ≐ 10

G_o – var (G_o) = $\dfrac{2(406.3 + 28.3) + 3(63.7)}{2 + 2 + 3}$ = 151.5, 7 d.o.f.

∴ st. dev. (G_o) ≐ 12

† – Different attenuators were in, ∴ G_o values not comparable.

APPENDIX 5

Calculation of Intensity Ratios from known Mass Concentrations Via the Mie Theory

The number of particles per gram of solution, N may be found from:

$$N = \frac{c}{\rho V}$$

where   c = solution concentration in $\dfrac{\text{grams of particles}}{\text{grams total solution}}$

ρ = particle density in $\dfrac{g}{cm^3}$ = 1.04 for polystyrene latex particles

V = particle volume in cm^3
= $\dfrac{\eta (D \times 10^{-8})^3}{6}$; D = particle diameter in Å

$$N = \frac{6 c}{1.04\, \eta\, (D \times 10^{-8})^3} \qquad (1)$$

The concentrations of the solutions used to prepare the samples were:

c_{98} = 4.347 x 10^{-5}

c_{176} = 1.896 x 10^{-5}

c_{220} = 3.825 x 10^{-5}

c_{275} = 1.931 x 10^{-5}

Inserting the above concentrations and corresponding diameters in (1):

N_{98} = 84.81 x 10^9

N_{176} = 6.39 x 10^9

N_{220} = 6.60 x 10^9

N_{275} = 1.71 x 10^9

From the Mie theory, the relative intensity contributions per particle size was found to be[*]:

i_{98} = 0.00113

i_{176} = 0.02680

i_{220} = 0.07157

i_{275} = 0.13792

Therefore, the theoretical intensity ratio for sample B98/D176, relative to 98 nm particles, is:

$$R = \frac{[6.39(0.02680) + 6.60(0.07157) + 1.71(0.13792)] \times 10^9}{84.81(0.00113) \times 10^9}$$
$$= 9.17$$

Similarly, for sample B98/275:

$$R = \frac{1.71(0.13792) \times 10^9}{84.81(0.00113) \times 10^9}$$
$$= 2.45$$

[*] - The i-values were determined from "Angular Scattering Functions for Spherical Particles" by W.J. Pangonis and W. Heller (1960) for the intensity of a wave scattered by a single sphere from an incident polarized beam of unit intensity whose electric vector is perpindicular to the plane of observation. For these samples, the angle of observation, Υ , was 90° and the m-value was 1.2.